SINTEF

OC2017 A-087- Unrestricted

FINAL Report

Subsea Dispersant Injection – Large-scale experiments to improve algorithms for initial droplet formation (modified Weber scaling)

An approach using the Ohmsett facility, NJ, USA and SINTEF Tower Basin in Norway

Author(s)
Per Johan Brandvik, Emlyn Davies, Øistein Johansen, Frode Leirvik (all SINTEF) and Randy Belore (SL Ross)

Images from SINTEF Tower Basin experiments with the 32 mm nozzle and 120 L/min of Oseberg blend (left) and with injection of 1% Corexit 9500 (right).

SINTEF Ocean AS
Environmental Technology
2017-03-20

SINTEF Ocean AS
Address:
Postboks 4762 Sluppen
NO-7465 Trondheim
NORWAY
Switchboard: +47 464 15 000
ocean@sintef.no
www.sintef.no/ocean
Enterprise /VAT No:
NO 937 357 370 MVA

KEYWORDS:
Sub sea
Oil release
Droplet formation
Weber scaling
Monitoring
Dispersant
Effectiveness

FINAL Report

Subsea Dispersant Injection – Large-scale experiments to improve algorithms for initial droplet formation (modified Weber scaling)

VERSION
Final

DATE
2017-03-20

AUTHOR(S)
Per Johan Brandvik, Emlyn Davies, Øistein Johansen, Frode Leirvik (all SINTEF) and Randy Belore (SL Ross)

CLIENT(S)
The American Petroleum Institute – API JITF D3

CLIENT'S REF.
Colin M. Frazier

PROJECT NO.
Project 1020 9018

NUMBER OF PAGES/APPENDICES:
68 + Appendices

TENTATIVE ABSTRACT
The main objective of performing these up-scaled tests was to generate experimental oil droplet size data representative of significantly larger release conditions than earlier laboratory testing. This new data set was used to test the modified Weber Equation's ability to predict initial droplet sizes on a more realistic scale (0.05 - 12 mm).

Up-scaled experiments have been performed at the SINTEF Tower Basin, in Norway and at the large outdoor test basin at the Ohmsett facility in NJ, USA.

The main conclusions are:

1. The generated experimental data show a very high correlation with predicted values (d_{50}) from the modified Weber algorithm.
2. A comprehensive data set, including replicate measurements, spanning a wide range of droplets sizes, nozzle sizes and flow rates have been generated.
3. New release arrangement for large-scale laboratory subsea releases have been developed and tested (nozzles, dispersant injection systems and flow monitoring & control system).
4. Novel sensors for quantifying oil droplets and gas bubbles (SINTEF Silhouette camera) over a wide size range (0.05 - 12 mm) have been developed and verified.

PREPARED BY
Per Johan Brandvik, Senior Research Scientist/Professor
SIGNATURE

CHECKED BY
Per Snorre Daling, Senior Research Scientist
SIGNATURE

APPROVED BY
Mimmi Throne-Holst, Research Manager
SIGNATURE

REPORT NO.	ISBN	CLASSIFICATION	CLASSIFICATION THIS PAGE
OC2017 A-087	978-82-7174-280-5	Unrestricted	Unrestricted

Document history

VERSION	DATE	VERSION DESCRIPTION
FINAL	2017-03-20	Final version incorporating final comments from API

Recommended reference:
Brandvik, P.J., Johansen, Ø., Davies, E. Leirvik, F., and Belore, R.. 2015: Subsea Dispersant Injection – large-scale experiments to verify algorithms for initial droplet formation (modified Weber scaling). An approach using the Ohmsett facility, NJ, USA and SINTEF Tower Basin in Norway.
SINTEF report no: OC2017 A-087 (Unrestricted). Trondheim Norway 2017. ISBN: 978-82-7174-280-5

SINTEF

Table of contents

1 Background

The size distribution of oil droplets formed in deep water oil and gas blowouts is known to have strong impact on the subsequent fate of the oil in the environment (Johansen, 2003).

In blowouts from moderate to shallow depths, the large buoyancy generated by the expanding gas will in general bring the plume of entrained water to the sea surface together with dispersed oil droplets and gas bubbles. The gas will leave the plume on surfacing, but the large volumes of entrained water will set up an outward horizontal flow of water at the surface. This might form a relatively homogeneous, thin surface oil slick as the dispersed oil droplets settle out from the horizontal flow of surfacing entrained water. Experimental field releases have shown that if the resulting surface oil slick is too thin to emulsify it tends to naturally disperse, resulting in a very short lifetime at the sea surface, see Figure 1.1 (Rye et al., 1996, and Rye et al., 1997).

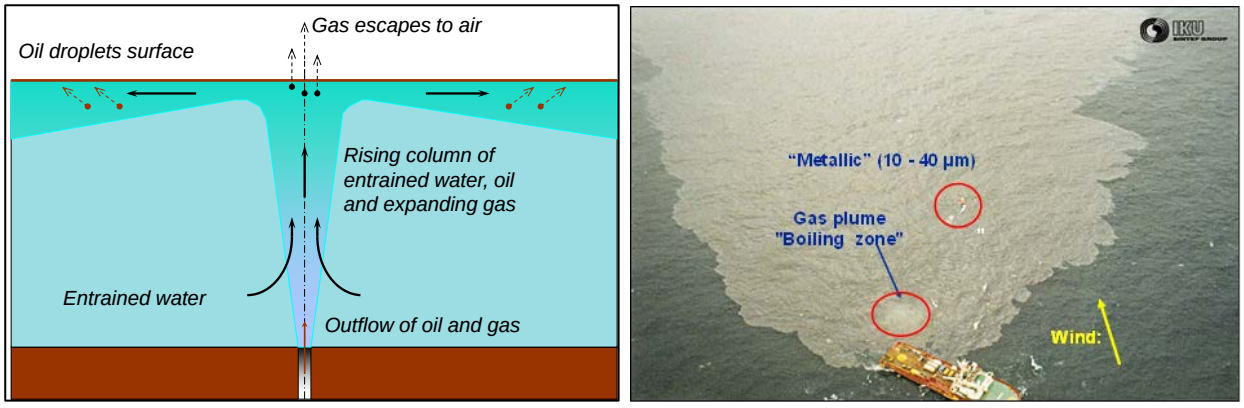

Figure 1.1: From the experimental oil-gas releases at the Frigg field in 1996 from 106 meters depth (Rye et al., 1996). Principles for the surfacing plume and the outflow of entrained water (left) and an aerial image from the release (right) are shown. The gas is penetrating the sea surface resulting in a thin initial oil film thickness

Deep water blowouts are more sensitive to cross-flow and ambient density stratifications than blowouts in moderate to shallow water. This is due to reduced buoyancy caused by the strong compression of gas in deep water, together with other factors such as non-ideal gas behavior, the potential for a substantial fraction of gas dissolved in the oil phase and gas being dissolved in the sea water. Such a deep water plume (with low buoyancy) is more likely to be trapped by the ambient density stratification or bend over by cross-flow. In both cases, gas bubbles and oil droplets will separate from the plume and rise to the surface with their own terminal velocities. Large droplets will rise relatively rapidly and come to the surface close to the discharge location, while small droplets will rise more slowly and can be transported long distances from the discharge location by ambient currents before reaching the sea surface. The smallest droplets may even be kept suspended in the water column for prolonged time periods by vertical oceanic turbulent mixing, subject to enhanced dissolution and natural biodegradation. The surfacing large droplets usually form a thick surface oil slick which, dependent on oil properties, may emulsify and form a persistent surface oil slick as experienced during the DeepSpill experiment in 2000 and the Macondo release in the Gulf of Mexico 2010 (Johansen et al. 2003 and Daling et al., 2014), see also example from the DeepSpill experiment in Figure 1.2.

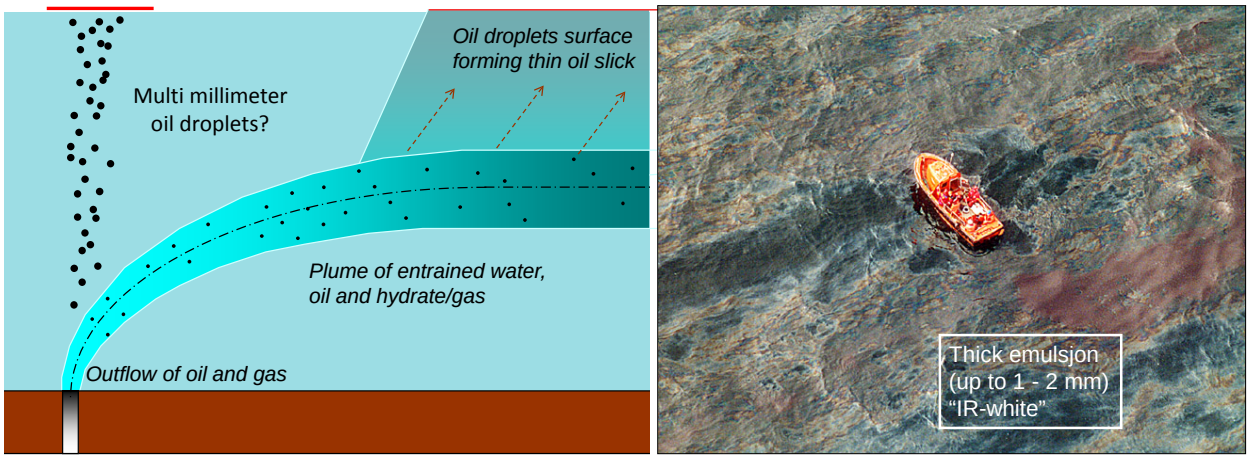

Figure 1.2: From a experimental deep water oil and gas release in 2000 from 840 meters depth (Johansen 2003).Simplified drawing of the entrained plume and surfacing of large (multi millimetre) oil droplets (Left) and the thick surface oil slick formed (right).

Reliable predictions of the droplet sizes from a subsea well blowout (including subsea dispersant injection) will thus improve our ability to forecast the fate of oil in the environment, provide guidance for oil spill response operations and relevant information to the public. Presently, the only available experimental droplet size data at near full scale was obtained in the DeepSpill experiment conducted at 844 m in the Norwegian Sea (Johansen et al. 2003). These limited observations have formed the basis for a prediction method for droplet size, based on the Weber number, which is used in many deep water blowout models today (Chen and Yapa 2007). More recently, however, SINTEF has performed laboratory studies of oil droplet breakup in their Tower Basin leading up to new algorithm for droplet formation (modified Weber scaling), see Brandvik et al., 2013 and Johansen et al., 2013.

The studies performed earlier for API in SINTEF Tower Basin are with release diameters in the 0.5-3 mm range with a flow rate of 0.1 to 10 L/min (Brandvik et al., 2014 and Brandvik et al., 2015). These results together with the data from the DeepSpill experiment (120 mm) form the basis for the new algorithm (modified Weber scaling). To extend the existing data set and strengthen the validity of the new algorithm, laboratory experiments should be performed on a larger scale. The strategy of this study is to increase the release rate of oil, to increase our understanding of subsurface blowouts and dispersant effectiveness on more realistic scales. Experiments on a scale ten to hundred times larger than the earlier experiments (release diameter and flow rate) to fill this gap are described in this report.

Both SL Ross Environmental Research, Ottawa, Canada and SINTEF, Trondheim, Norway delivered project proposals to API regarding performing up-scaling experiments (autumn 2013). API later asked the two institutions to join forces regarding this demanding project (May 2014) and to utilized earlier experience and expertise at both companies.

A description of the current design and operation of the SINTEF Tower Basin are given in several earlier API reports (Brandvik et al., 2014) and publications (Brandvik et al., 2013). The experiments performed as a part of API Phase I and II are within the red area in Figure 1.3. In this study we

performed experiments (green region) that supplement earlier experiments to fill the gap between prior experiments and the DeepSpill 2000 experiment.

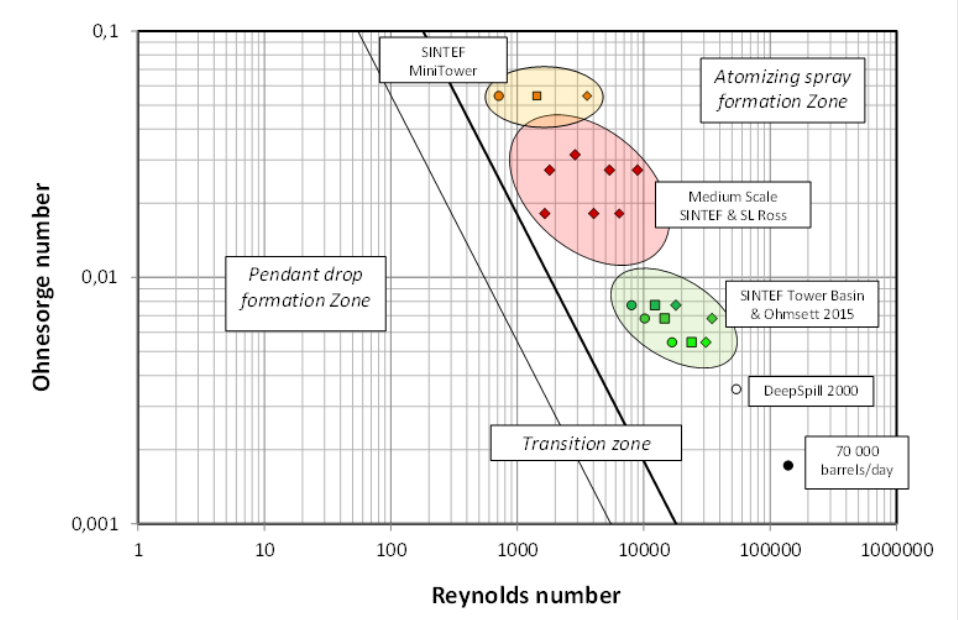

Figure 1.3: Earlier experiments plotted in an Ohnesorge vs. Reynolds number diagram (yellow and red green rings). Injection rate varied from 0.1 to 8 L/min, with nozzle diameters from 0.5 to 4.5 mm. Green shaded area give conditions for up-scaled experiments. Approximate location of a 25-50 mm & 50-400 L/min, the DeepSpill 2000 experiment and a hypothetical 70 000 barrel/day incident are shown for comparison.

Discussions with the API JITS D3 management group during IOSC in Savanah May 2014 and later discussions between SL Ross and SINTEF resulted in the criteria for up-scaled experiments summarized in Table 1.1.

Table 1.1: Initial criteria for up-scaled experiments

Criterion	**Requirement**
Increased oil release rate	80 – 600 L/min
Increased nozzle diameter	10 – 40 mm
Increased water depth	12 m (double current Tower Basin height)
Increased droplet sizes	Multi millimeter range
Increase basin volume	Multiple times larger than existing SINTEF Tower Basin
Fast experimental turnaround time	2-3 days between experiments
Experiment run time	Min 5 minutes at stable release rate
Continuous monitoring	Droplet size and oil concentration in the plume

API, SL Ross and SINTEF discussed several options for doing such up-scaled subsea releases of oil and injection of dispersants. As seen in Figure 1.3, it is necessary for any up-scaling to handle oil fluxes that are substantially higher than the capabilities of the existing facilities at SINTEF and SL Ross.

Increasing oil fluxes are obtained by using larger nozzle diameters. However, the oil flow rates (or release velocities) have to be very high to obtain droplet sizes within the size range for existing instrumentation used to characterise oil droplets (LISST < 500 µm). See Table 1.2 below for estimates of droplet sizes versus release diameters and flow rates.

Table 1.2: Estimated oil flow rates needed to obtain three different d_{50} (300, 1000 and 5000 µm using different release diameters (D: 0.5 – 50 mm) using the modified Weber algorithm (Johansen et al., 2013) and assuming oil properties similar to Oseberg blend.

D (mm)	**Oil flux (L/min)**		
	d_{50}=300 µm	**d_{50}=1000 µm**	**d_{50}=5000 µm**
0,5	0,1		
1,5	1,2		
3	3		
5	10		
8	29		
10	65	15	
15	130	38	
20	245	75	
25	550	120	45
32	1000	345	80
50	2800	615	225

As seen in the Table 1.2 above larger nozzle diameters produces larger droplets, so to generate droplets suitable for traditional instrumentation (LISST-100X, d_{50} < 300 um) with large nozzles, very high flow rates (or release velocities) are needed. Such high flow rates create challenges in experimental operations, especially oil concentrations exceeding the upper limit for instrumentation and increased time & resources needed for water treatment and waste handling.

To continue using traditional monitoring equipment (LISSTs) for up-scaled experiments would necessitate both high release velocities (10-30 m/s) and small droplets (< 300 µm), both are very unrealistic for most large-scale subsea oil & gas scenarios.

New measurement capabilities are needed to perform up-scaled experiments with more realistic release velocities (1-2 m/s) and realistic droplet sizes (multiple millimetres). A suitable size range for untreated and treated oil would be;

1. 2 - 12 mm for untreated oil and
2. 0.05 – 1 mm for oil treated with dispersants.

These challenges require development and modifications of monitoring equipment, release arrangements and the facility to perform the experiments.

SINTEF has developed a new system for subsea monitoring of oil droplets and gas particles (Silhouette camera, see Appendix D for further details) which was further improved and tested as a part of this project, see Davies et al., 2017 for further details. The version used in this study was rated down to a depth of 200 meters, but a later version was used at high pressure experiments down to 172 atm (2500 PSI) or 1720 meters depth (Brandvik et al., 2016 and Brandvik et al., 2017a).

Two facilities or locations for performing such up-scaled experiments have earlier been identified; the Tower Basin at SINTEF and the Ohmsett facility in New Jersey, USA. Descriptions of both facilities can be found in the experimental section of this report.

The main part of the experimental work in this project was performed at Ohmsett, while the SINTEF facilities were mainly used to develop and test monitoring and release equipment. However, valuable replicate data, comparable to those generated at Ohmsett, were also generated at SINTEF.

2 Objectives

The main objectives of this study were to;

1. Generate data that fill the existing gap between earlier laboratory experiments at SINTEF and SL Ross and the DeepSpill 2000 experiment.
2. Describe the relationship between initial droplet formation, release conditions and dispersant injection for release diameters and rates in the 20 - 30 mm and 200-600 L/min range, respectively.
3. Use the new data to test the modified Weber Equation's ability to predict initial droplet sizes at significantly larger scales that are closer to real releases.

3 Feasibility study – Optimization of design and parameters for large-scale experiments

The initial task in this project was a feasibility study to test and optimise the suggested experimental approach. The main objective was to:

- identify suitable nozzle sizes and flow rates
- verify plume dilution to obtain suitable oil concentrations for the instrumentation
- verify instrumentation for quantification of oil droplet sizes (50 – 12 000 microns).

3.1 Modelling and experiments in SINTEF Tower Basin

This initial testing was performed in the SINTEF Tower Basin and included nozzle sizes and oil flow rates shown in Table 3.1.

Table 3.1: Nozzle sizes and flow rates used for the initial testing in the SINTEF Tower Basin

Nozzle (mm)	Oil flow rate (L/min)		
25	50	80	120
32	80	120	200
50	200	300	400

Each experiment in this initial testing lasted for 90 seconds and the droplet size distribution were quantified using different silhouette camera configurations (mainly varying resolution, lenses and flow cell gap). Two cameras with different resolution were used in all experiments.

Dispersants were injected for one of the flow rates for each nozzle size (50, 120 and 300 L/min). These experiments were used to verify and improve;

1. Design of oil release and dispersant injection systems.
2. Oil plume behaviour and dilution and prediction of oil concentrations and droplet sizes (oil alone and after dispersant treatment).
3. Configuration and design of Silhouette cameras (SilCams).

Plume modelling (SINTEF Plume 3D) was used to explore how different nozzle and flow rates influenced droplet sizes and plume concentrations as a function of distance from the nozzle. This was important for identifying an optimal position (distance from nozzle) in the oil plume for the instrumentation (SilCams). Some of these predictions are presented in Figure 3.1 and Figure 3.5 on the next pages.

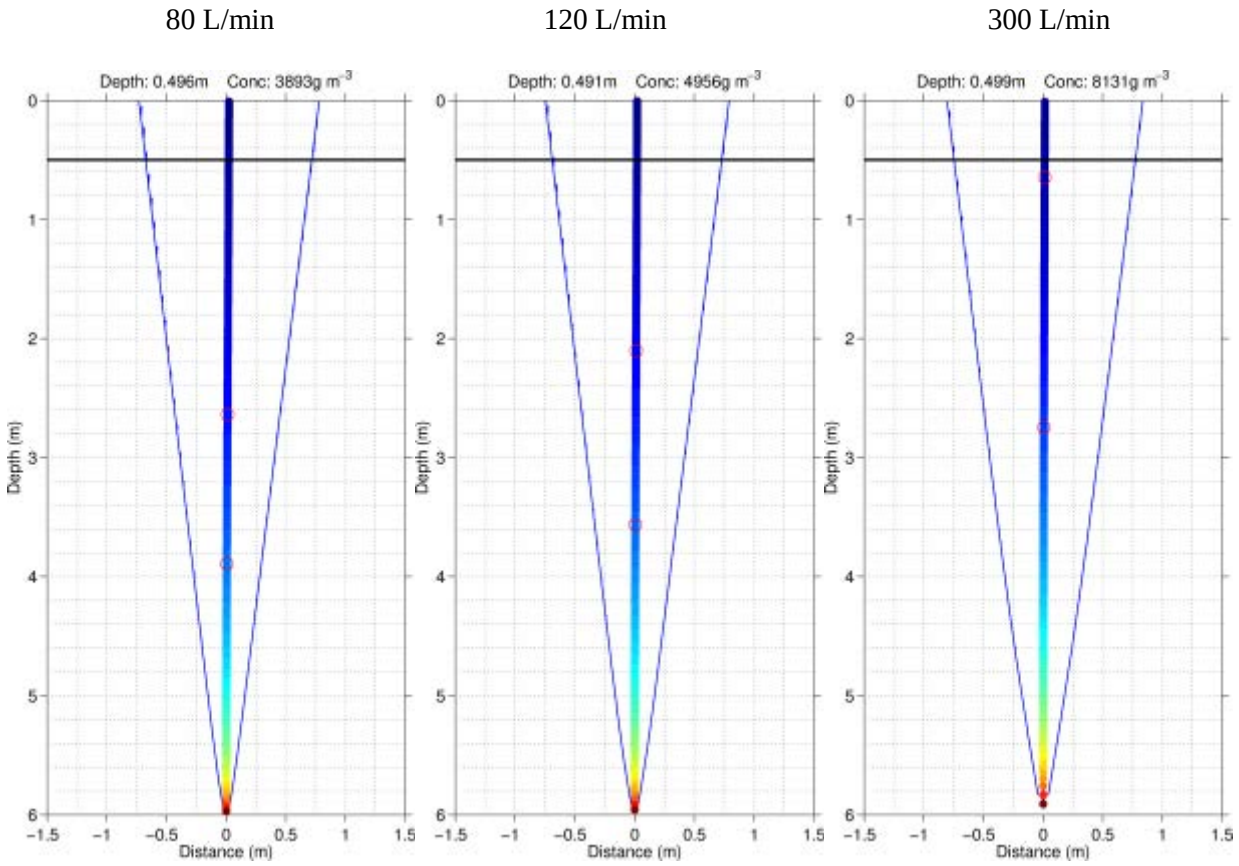

Figure 3.1: Simulation of plume behaviour in the Tower Basin at different flow rates for release from 32 mm nozzle (SINTEF Plume 3D). Location of Silhouette cameras (twin configurations) are indicated with the black line. Colour of centre line indicate oil concentration, the two circles indicate 50 and 100 times dilution. Concentrations at camera positions are indicated at top of figures.

3.2 Modelling oil releases in the Ohmsett facility

The Ohmsett facility offers a versatile and flexible basin with its large horizontal dimensions (200 m x 20 m), two moving bridges and extensive water filtration/oil removal capability. The main challenge using the Ohmsett facility is the limited water depth (2.4 m), which limits the possible dilution of the subsea oil plume. However, modelling work from the feasibility study indicated that performing the release while moving the release point horizontally (simulating a horizontal cross current) increases the dilution of the oil plume sufficiently for monitoring the oil droplets. This was achieved by mounting both the release and monitoring arrangements on two coordinated moving bridges.

Figure 3.2 and Figure 3.3 show results from simulations from the feasibility study with SINTEF's Plume3D model for an oil flow rate of 300 L/min (18 m^3/h) through a 30 mm orifice with different discharge arrangements (vertical and horizontal) and different towing speeds (0, 0.25 and 0.5 m/s). Figure 3.2 shows the plume geometry in terms of the trajectory of the plume centerline (thick line) and the plume width (thin lines). Open markers on the trajectories show the location where the dilution ratio exceeds 50:1, while filled markers refer to a dilution ration of 100:1. Figure 3.3 shows the dilution ratio as a function of depth for the different cases.

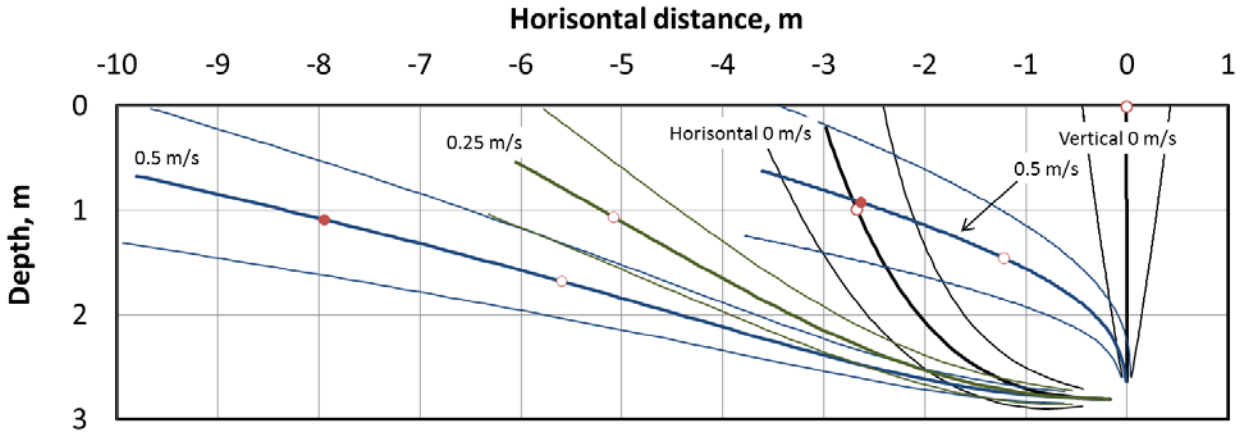

Figure 3.2: Plume geometry computed with Plume3D for different discharge arrangements (vertical and horizontal) and towing speeds (0, 0.25 and 0.5 m/s from left to right). Open (filled) markers on the trajectories show the location where the dilution ratio exceeds 50:1 (100:1). The discharge rate is 300 L/min through an orifice diameter of 30 mm. N.B.! Later info has revealed that the operational depth is 2.5 m.

The results indicate that both horizontal and vertical discharge arrangement towed at a speed of 0.5 m/s may assure sufficient dilution (n > 100) at depths of about 1 m. However, the vertical discharge arrangement may be preferable due to the shorter distance from the discharge point to the location where the dilution ratio exceeds 100:1 (less than 3 m, compared to 8 m for the horizontal discharge). Closer inspection of the results (not shown) also reveals that the droplet separation is minimal for the vertical discharge – 99% of the oil remains in the plume at the distance where n exceeds 100:1, while 30% of the oil has separated from the plume at the corresponding location for the horizontal discharge.

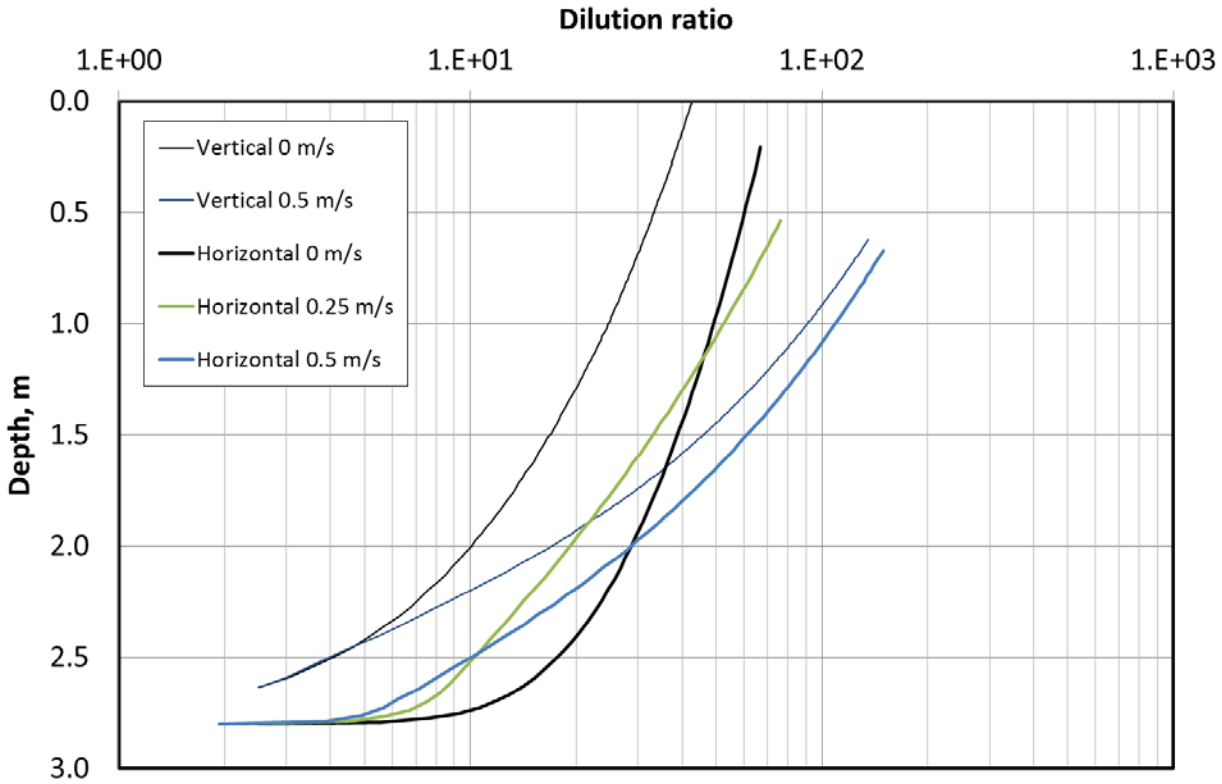

Figure 3.3: Dilution ratio as a function of depth computed with Plume3D for different discharge arrangements and towing speeds. Same discharge conditions as in Figure 3.2.

Two vertical discharge arrangements were mounted on the same tow bridge (Figure 3.4). One of these contained a twin nozzle system with both 32 and 50 mm nozzles. More details are given in the experimental section; see Figure 4.7 and Figure 4.10.

With equal oil discharge rates and orifice diameters, the plumes are expected to behave similarly, independent of the DOR within these limited distances. The optical imaging instruments (SilCam) was mounted on an auxiliary instrumentation bridge positioned downstream of the discharge points at a distance and elevation adjusted to the trajectories of the plumes. After release of 1000 - 2000 liters of oil, two days were needed for surfacing of oil droplets and skimming before a new experiment could be initiated.

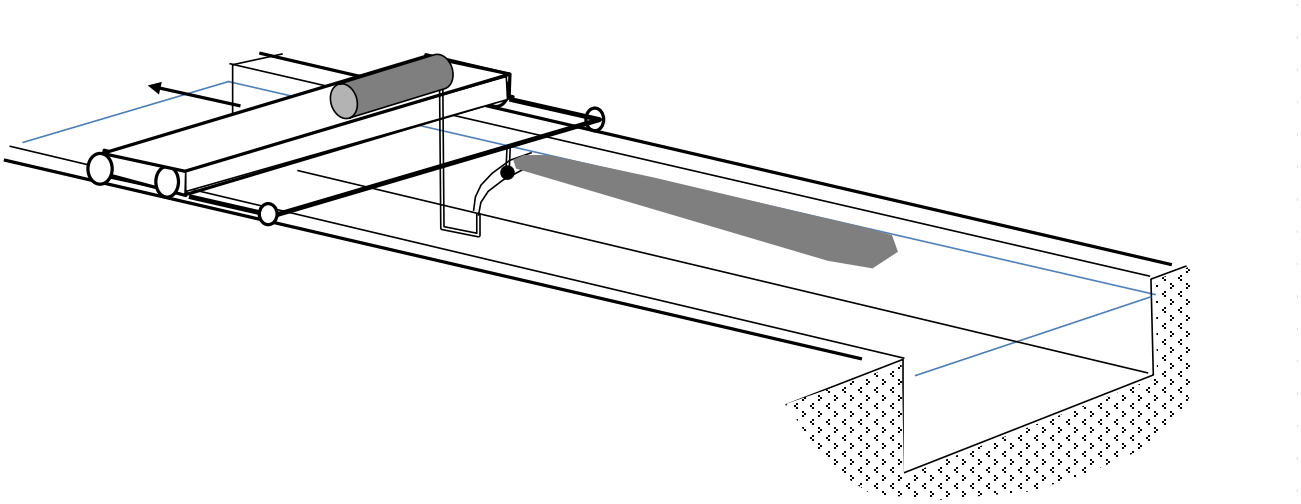

Figure 3.4: Principal sketch of towing bridge with discharge arrangement. The arrow indicates the towing direction.

The experiments with oil alone (untreated oil) generated very large droplets (multiple millimeters) which would make it possible to perform two experiments a day, due to rapid rise and surfacing of the large droplets. One experiment with untreated oil could be conducted early in the day and then after 3-4 hours (surfacing of droplets and oil skimming), a second experiment with dispersant injection could be performed.

Since 200-500 microns droplets were expected for the oil treated with dispersant (similar to experiments at SINTEF), the effort needed for settling & cleaning was not expected to be proportional to the large volumes used (see example of settled droplets in Figure 4.6). The volume of oil droplets smaller than 30 microns was expected to be less than five litres for each experiment.

A large difference in plume behaviour between the low and high release rates, due to different droplet sizes and buoyancy, could be a challenge for correctly positioning the instruments. They should be positioned in the middle of the oil plume. Simulations of plume behaviour with three different flow rates (80, 120 and 300 L/min) with a 32 mm nozzle (Figure 3.5) show that the low flow rate produces a lower and more concentrated plume compared to the high flow rate experiment.

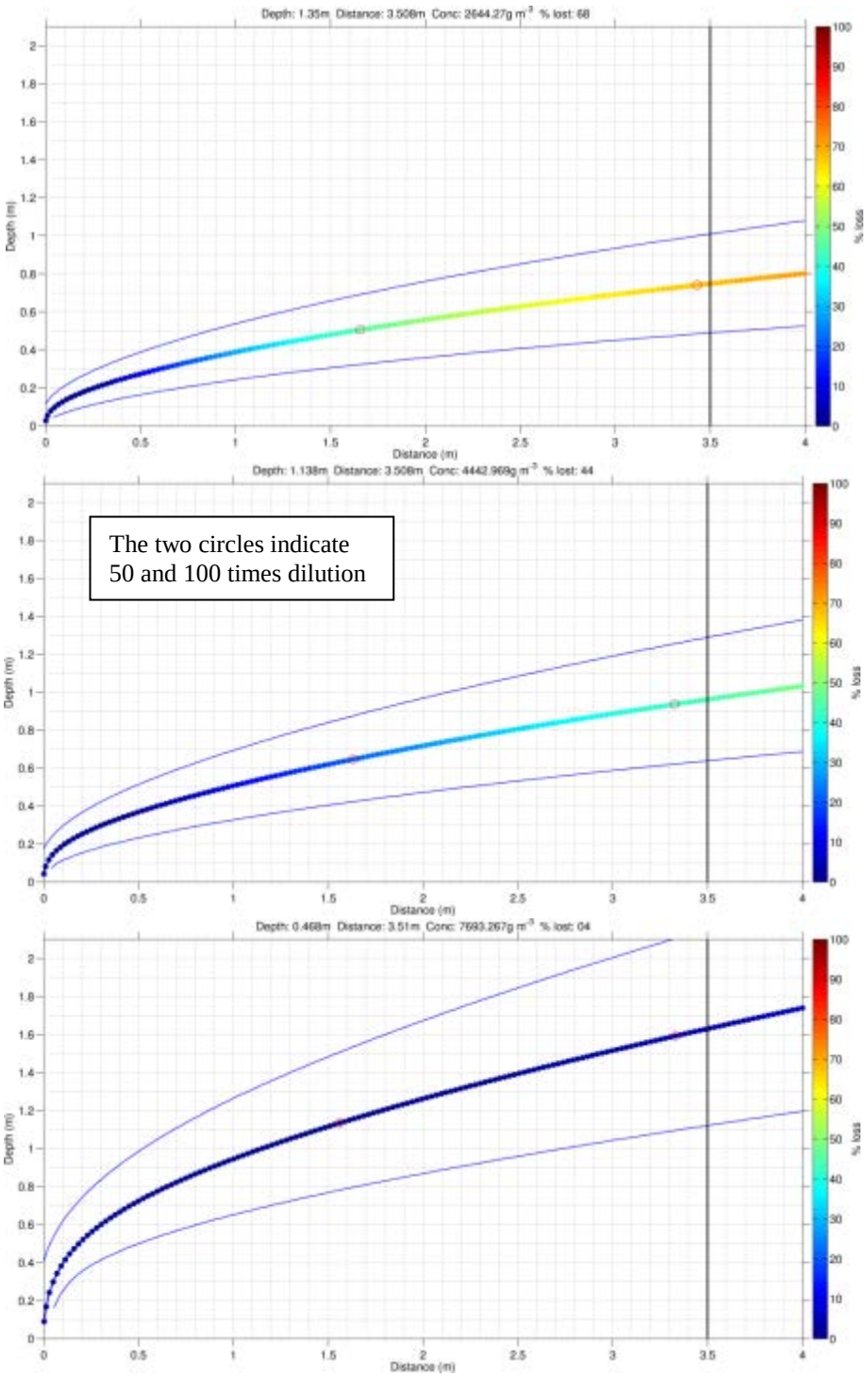

Figure 3.5: Simulation of plume behaviour in the Ohmsett basin (SINTEF Plume 3D) for flow rates of (A) 80 L/min, (B) 120 L/min and (C) 300 L/min using a 32 mm nozzle with a towing speed of 0.5 m/sec. Location of Silhouette cameras are indicated by the black line, with information on the depth of plume centre-line, oil concentration, and percentage of oil lost from the plume shown above each plot. N.B.! When comparing with Figure 3.1, note that colours of centreline in this figure indicate percentage of oil lost from plume due to separation of large droplets.

The plume modeling of the different nozzle sizes and release rates strongly indicate (Figure 3.5) that two different silhouette cameras are needed to both;

1. Monitor a larger plume area (centre & middle of plume) and
2. Target a larger span in droplet sizes (oil alone and dispersed oil)

To cover the range of nozzles and flow rates described in Table 3.1, experiments with different towing speed are needed. The low flow rate experiments (Figure 3.5A) required a low towing speed to let the deep plume rise to the instrumentation, while in the high flow rate experiments (Figure 3.5C) at higher speed is needed to keep the plume in the water for a prolonged period.

To perform the low flow rate experiments together in one run a release system with multiple nozzles was constructed (see Figure 4.9). This made it possible to perform low flow rate experiments for all nozzle sizes (25, 32 and 50 mm) in the same run (low towing speed).

Low flow rate releases:
The modelling of the plume behaviour in the Ohmsett basin (Figure 3.5), shows that the smallest flow rates form a very concentrated plume which stays too deep in the basin at a towing speed of 0.5 m/sec. The downstream distance needed for dilution is large (>5 meters) which enables the larger droplets to leave the plume (> 50 vol. %) before the plume is sufficiently diluted. As a result, these experiments need to be performed at a lower towing speed (0.25 m/sec).

Medium flow rate releases:
These releases show sufficient dilution at the instrument position (1.5 meter) and very little loss of large droplets (<10 vol. %).

High flow rate releases:
Some of these releases show rapid surfacing of the plume with very high concentrations at the instrument position. These experiments need to be performed at a higher towing speed (0.65 m/sec) to keep the plume submerged for a longer period to obtain the necessary dilution.

4 Experimental description

Two possible facilities were identified for these large-scale experiments; The Ohmsett facility in New Jersey, USA and SINTEFs Tower Basin in Trondheim Norway. An experimental plan to utilize the potential of these facilities was worked out as a part of the feasibility study (see Chapter 3).

The Ohmsett facility is located at the Navy weapon base Earle in New Jersey and is owned by the U.S Department of the Interior's Bureau of Safety and Environmental Enforcement (BSEE), the facility is operated & maintained by MAR Inc. The Tower Basin is located in Trondheim and is an integrated part of SINTEFs laboratory facilities to study subsea oil releases, see Figure 4.1.

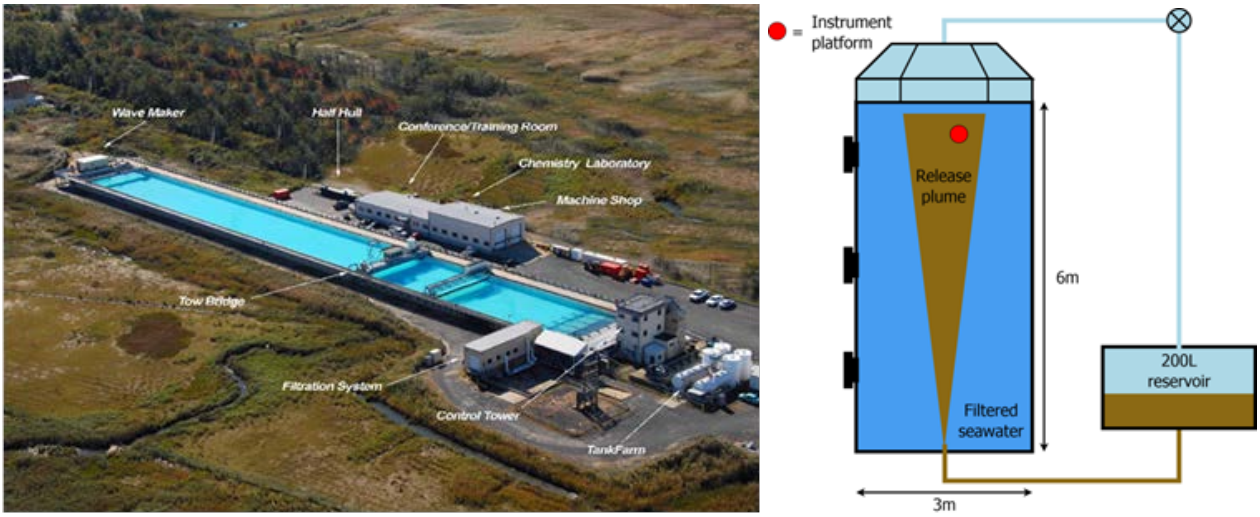

Figure 4.1: Left: Layout of the Ohmsett test tank: Length 200 m, width 20 m and depth 2.4 m. Holding 9 500 m^3 of sea water. Right: layout of the SINTEF Tower Basin: 6 m height and 3 m diam. Holding 42 m^3 of sea water.

4.1 SINTEF Tower Basin

The Tower Basin was used for initial feasibility studies to;

1. Test and verify the performance of suggested up-scaled release nozzles & dispersant injection system
2. Verify modelling of plume dilution
3. Verify performance of the new silhouette cameras (droplet sized and dilution)

Before using the SINTEF Tower Basin for up scaled experiments some minor modifications were performed (oil & dispersant supply and flow monitoring system), but it was mainly used as in previous studies. The consequence of the limited water volume in the Tower Basin is that the durations of the experiments are relatively short (60-90 minutes). However, this was sufficient to fulfil the objectives with the feasibility study. Further details regarding the SINTEF Tower Basin are given in Brandvik et al., 2013 and in Appendix A.

The arrangement at SINTEF for transferring the oil from the 1 m^3 IBC tank using the high capacity pump through the flow meter to the nozzle in the Tower Basin is shown in Figure 4.2.

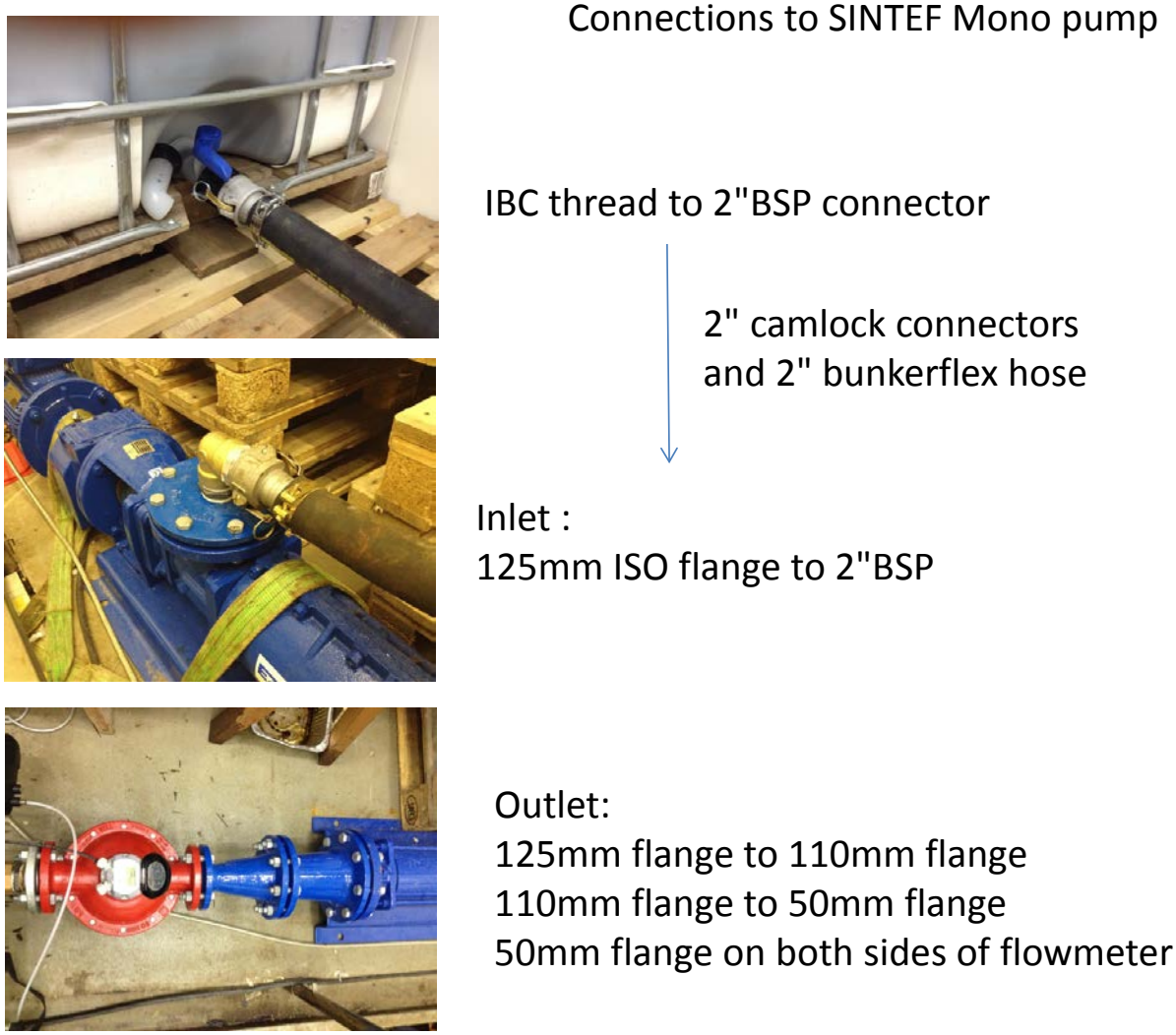

Figure 4.2: Details showing how the large capacity pumps was connected directly to the 1 m^3 pallet (IBC) tank and through the flow meter directly to the Tower Basin.

From the high capacity pump and flow meter arrangement (Figure 4.2 the oil flux is directed to the release nozzle inside the Tower Basin. An example from an experiment with the 32 mm nozzle and the 120 L/min experiment is shown in Figure 4.3. Oil alone to the left and with 1% C9500 (Simulated Insertion Tool) to the right. The dispersant was injected into the oil stream 6 release diameters before the release opening, see Brandvik et al., 2014 and Brandvik et al., 2017c.

After the initial droplet formation immediate above the nozzle (10-15 release diameters) the plume of droplets rise towards the SilCams at the top of the Tower basin (5 meter above the release nozzle), see Figure 4.4. Two different SilCams with different resolution and designed for different ranges of droplet sizes (see Table 4.2) were used.

A water sample taken from the rising oil plume, with dispersed oil droplets (200-500 µm), after 24 hours is shown in Figure 4.6.

Figure 4.3: Images from TowerBasin experiments with the 32 mm nozzle and 120 L/min of Oseberg blend (left) and with simulated insertion tool (SIT) injection of 1% C9500 (right). See Brandvik et al., 2017c for further details regarding injection techniques.

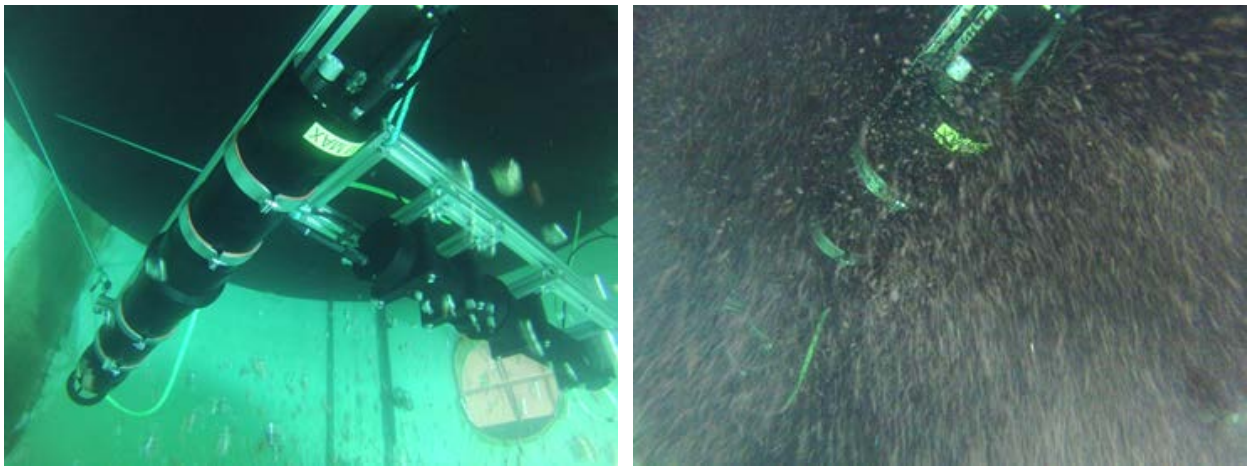

Figure 4.4: Images from TowerBasin experiments showing two silhouette cameras in the top section of the tank (1 meter depth, five meter above the release nozzle), before (left) and under release of oil (right).

A key element of the experimental setup are the automated measurement and data acquisition systems deployed to monitor the flow rates of the released oil and dispersant.

Figure 4.5 shows set points and obtained flow rates for both oil and dispersants during an experiment in the Tower Basin. This is a part of SINTEF laboratory control and QA system. This documentation is vital when analysing the data. Usually the last 30 seconds of each period (after stable conditions are obtained) are used in the data analysis. This documentation of flow rate settings and obtained rates are available for all experiments at both SINTEF and Ohmsett.

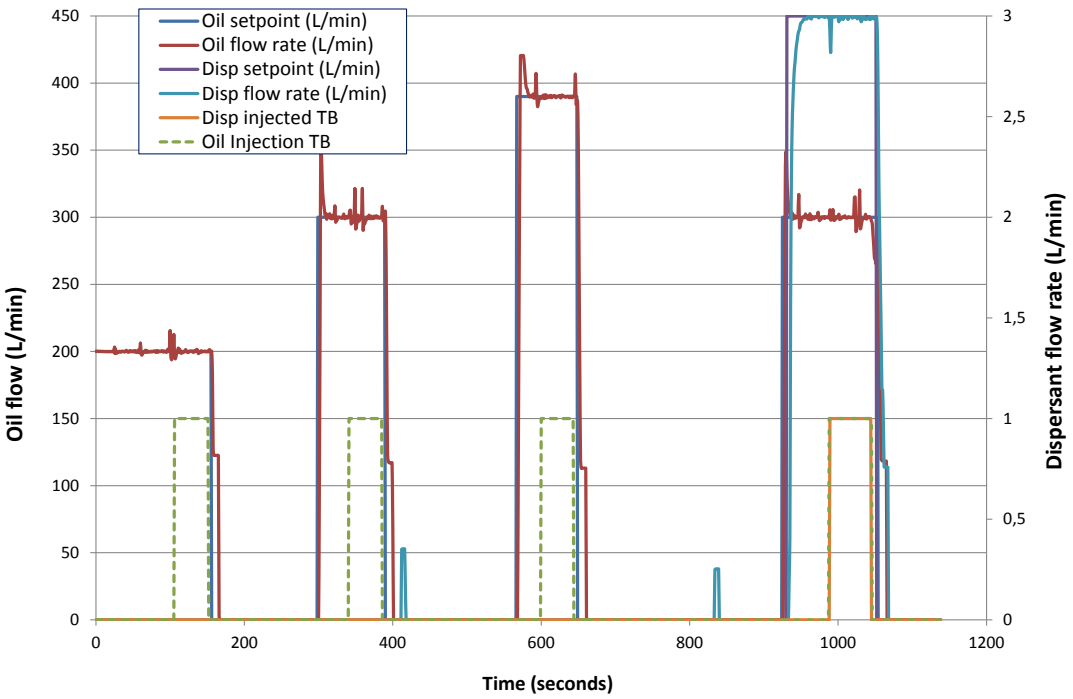

Figure 4.5: Documentation of flow rates for the 50 mm nozzle experiment in the Tower Basin (TB). Both set point and measured values for oil (left axis) and dispersant (right axis) are shown. Both oil and dispersant are pumped through the oil/dispersant lines and returned to their tanks using tri-way valves. When stable flows are obtained oils is directed to the nozzle inside the Tower Basin (green dotted line indicates oil flow to nozzle). For the last experiment both oil and dispersant are directed to the Tower Basin nozzle after stable flows are obtained (green and yellow line).

Figure 4.6: Water sample from large scale dispersant experiment (25 mm nozzle, 50 L/min and 1% C9500) in the Tower Basin after 24 hours. All the dispersed droplets (200-500 microns) rise to the surface during 24 hours.

The experiments in the Tower Basin were performed in January and February 2015. The nozzles, flow rates and instrument (Silhouette cams) conditions used are given the Table 4.1and Table 4.2 below.

Table 4.1: Experimental conditions for the Tower Basin experiments

Experiment no	Date	Nozzle diam (mm)	Flow rates (L/min)	Dispersant (1% C9500)
1-4	22-23 January 2015	25	50, 80 and 120	50 l/min
5	28. January 2015	32	120, 200 and 300	200 L/min
6	2. February 2015	50	200, 300 and 400	300 L/min

All experiments in the SINTEF Tower Basin were performed with natural sea water with a salinity of 3.5 % and a water temperature of 8 °C. The oil was stored at room temperature and injected with a temperature of
22 °C. Since the oil is cooling during droplet formation, an average between the water and the oil temperature (15 °C) is used for calculating a theoretical initial droplet distribution with modified Weber scaling (Johansen et al., 2013).

The gap between the two parts of the SilCams forms the measuring cell and together with the optics/CCD determines the resolution of the camera. The gap is also important for the maximum droplets sizes that will penetrate through the measuring cell. The gaps for the two instruments used in all experiments in the Tower Basin are given in Table 4.2.

Table 4.2: Gaps or path length (mm) in Silhouette cameras for Tower Basin experiments

Experiment no	Low resolution SilCam (mm)	Med resolution SilCam (mm)
1-4	12 10 (dispersant)	10 8 (dispersant)
5	10	6
6	10	5

4.2 Ohmsett facility

The facility has proven to be ideal for testing oil spill technology, evaluating acquisition options, and validating research findings because of its large outdoor above ground test tank which is capable of handling full-scale equipment. Two movable bridges span the 667 feet long (213 m), 65 feet (21 m) wide and 11 feet deep (3.5 m) tank filled with 2.5 million gallons (9500 m^3) of salt water that are used to tow full-size response equipment though the water at speeds up to 6.5 knots to simulate actual deployment at sea. The tank's wave generator creates realistic sea environments by producing different wave types of up to 3-feet high (1 m) while state-of-the-art data collection and video systems record test results.

Additional details regarding the Ohmsett facility are given in Appendix B.

Some of the unique equipment and experimental setup used at Ohmsett for this project are highlighted in the following figures.

Oil releases were made from two locations during each run. The oil release points were at the bottom of the tank at positions that divided the width of the tank as shown in Figure 4.7. Various nozzle diameters, oil and dispersant flow rates, bridge speeds and bridge separations were used during the test program.

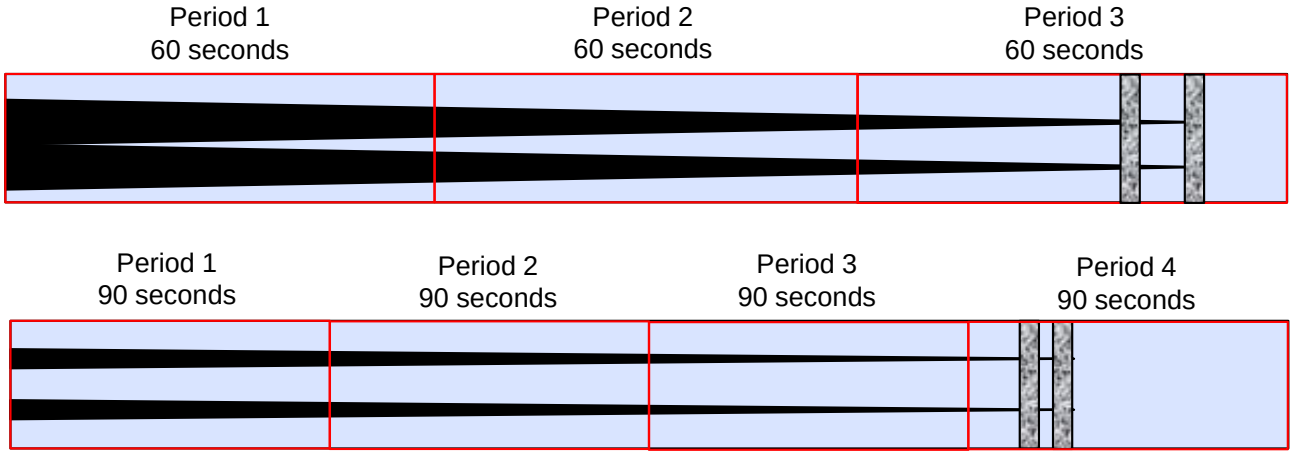

Figure 4.7: Principle sketch of how the Ohmsett basin was divided into sections with different parameters (nozzle/flow rates) during one run or experiment. The moving release- and monitoring bridge are indicated together with the resulting oil plume. Upper part shows an example from a dispersant experiment (high towing speed and three different measuring sections or periods). Lower part shows an example from oil alone experiment (low towing speed and four different measuring periods).

The oil and dispersant flow rates were monitored with inline flow meters and data acquisition systems developed and tested at SINTEF in the Tower Basin tests. Figure 4.8 shows a typical example of the flow data collected during one of the test runs.

Figure 4.9 provides photos of the oil release and dispersant injection lines used at Ohmsett both prior to deployment and in operation during one of the tests. Photos of the SilCam deployment are also shown in Figure 4.8.

Example photos of the oil plumes generated during the Ohmsett testing are shown in Figure 4.10

The orientations of the two towing bridges during a dispersant applied run in the top photo and for an oil only test are shown in Figure 4.11.

Example images from a SilCam used to measure the oil drop size distribution and an action camera deployed to document an overview of the oil plume during an oil only release are shown in Figure 4.12. Example images for a dispersant applied test are shown in Figure 4.13.

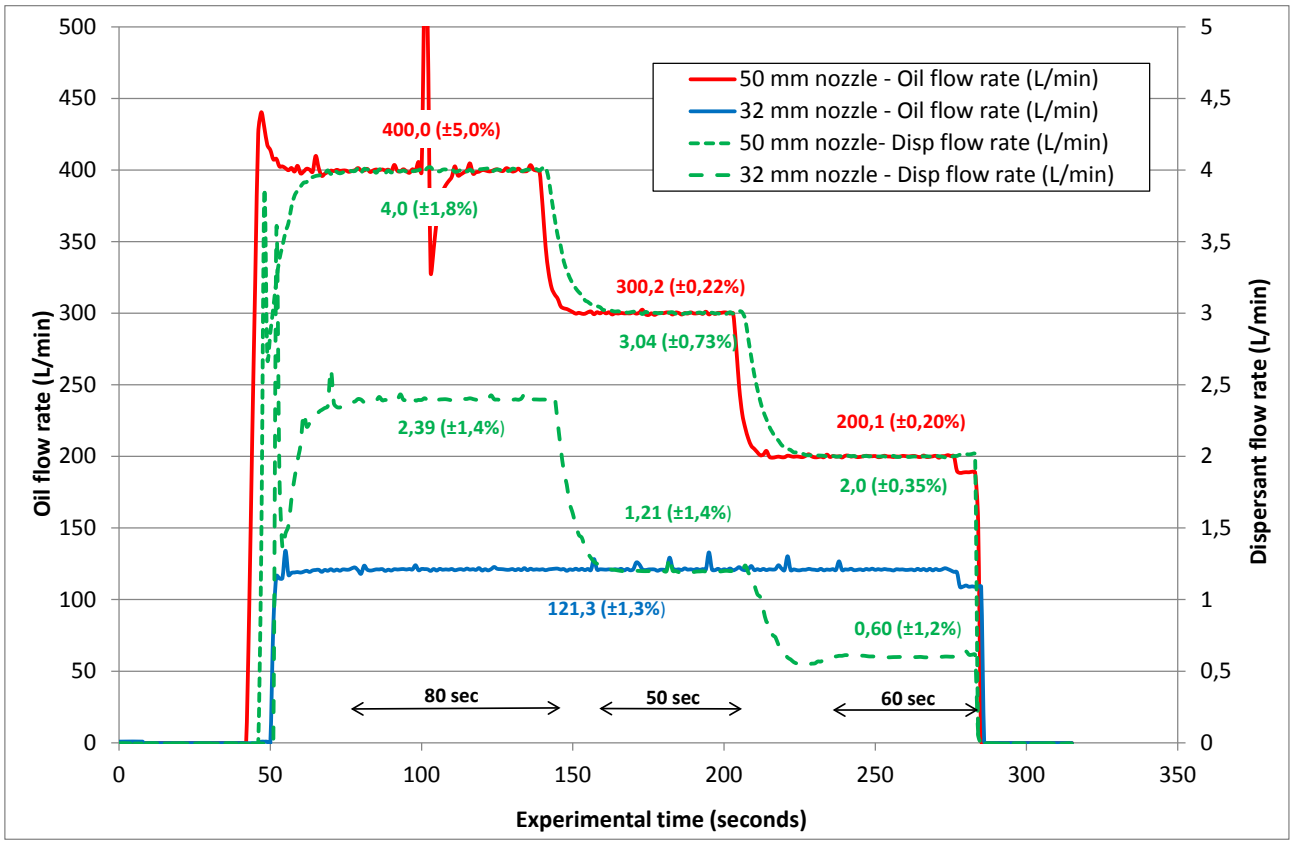

Figure 4.8: Flow rates during experiment 9, oil from 50 mm (red) and 32 mm (blue) nozzles. Dispersant flowrates are given as green dotted lines. Average flow rates (after target flow rate is obtained) and standard deviation (%) are indicated for each experimental period (80, 50 and 60 seconds). Data from the last 30 seconds of each period are usually used to establish the droplet size distributions.

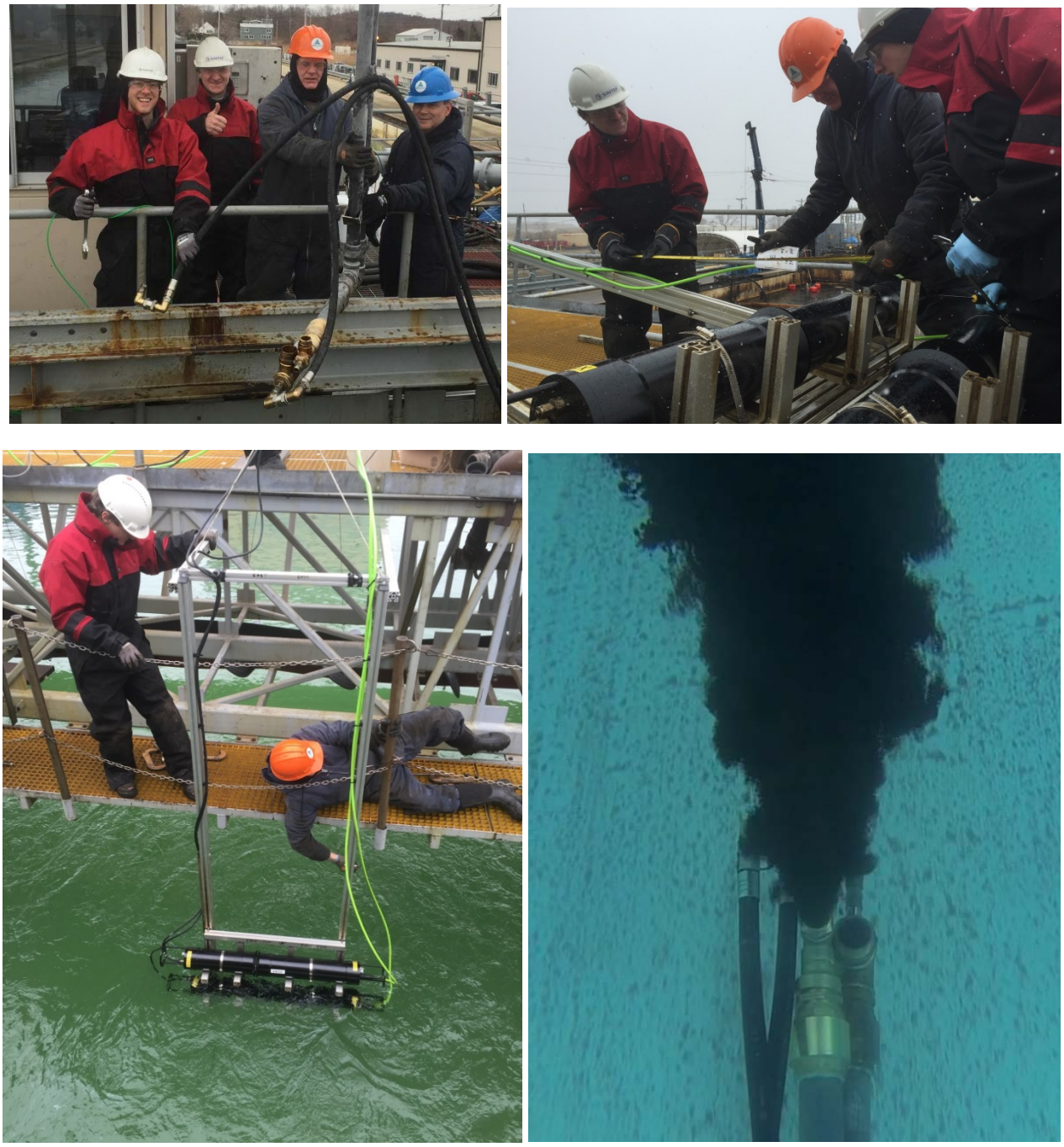

Figure 4.9: Images showing SL Ross, MAR and SINTEF personnel during the preparations. Upper left shows the mounting of the twin nozzle and lower right shows the twin nozzle in operation (32 & 50 mm). The two smaller black tubes are for dispersant injection directly into the nozzles (Simulated insertion tool) The other two images show mounting and lowering the Silhouette Cameras.

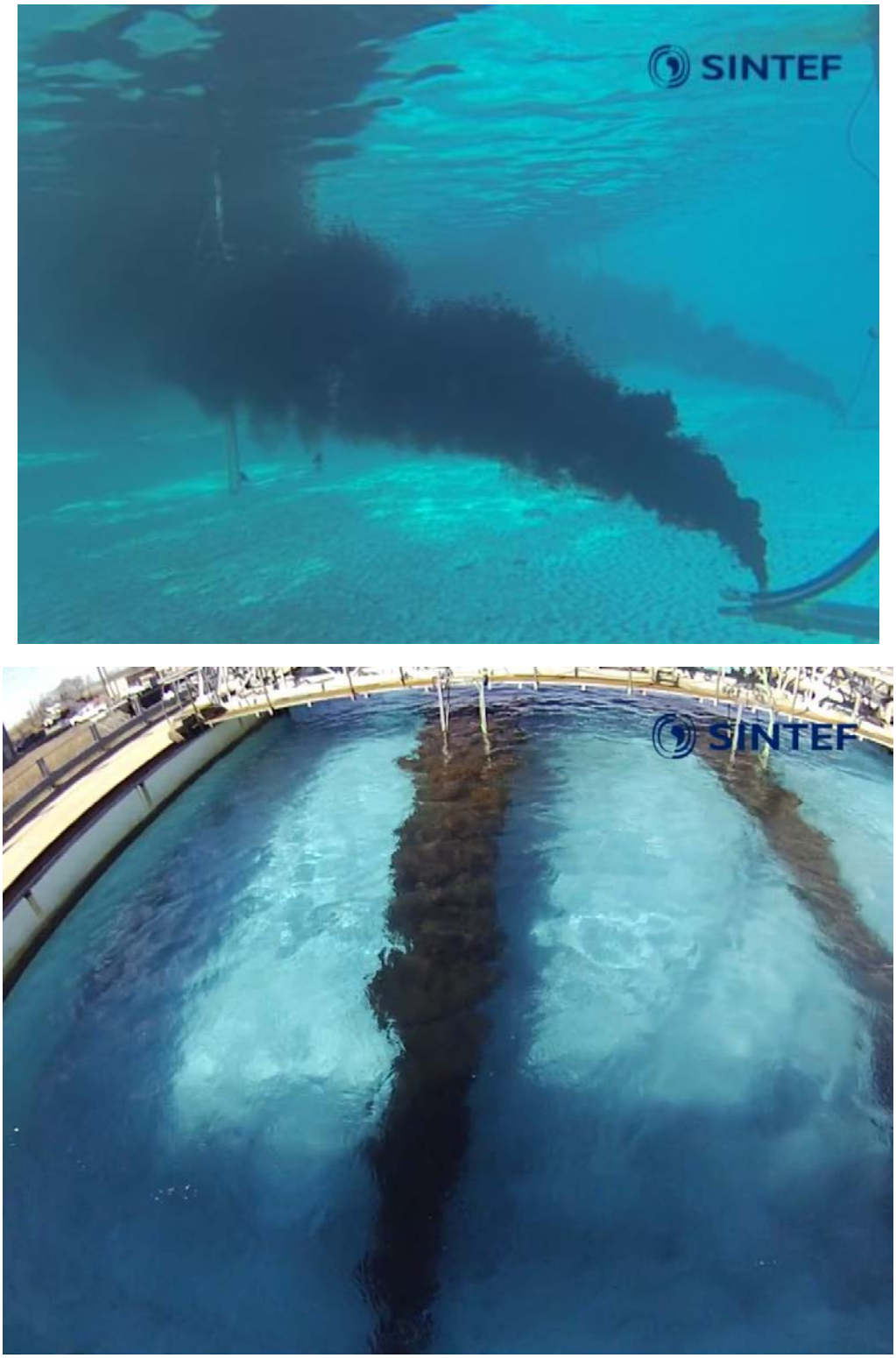

Figure 4.10: Twin releases of oil from the two different nozzle configurations. Oil alone (upper) and experiments with dispersants in lower picture (longer distance for better dilution of concentrated plumes).

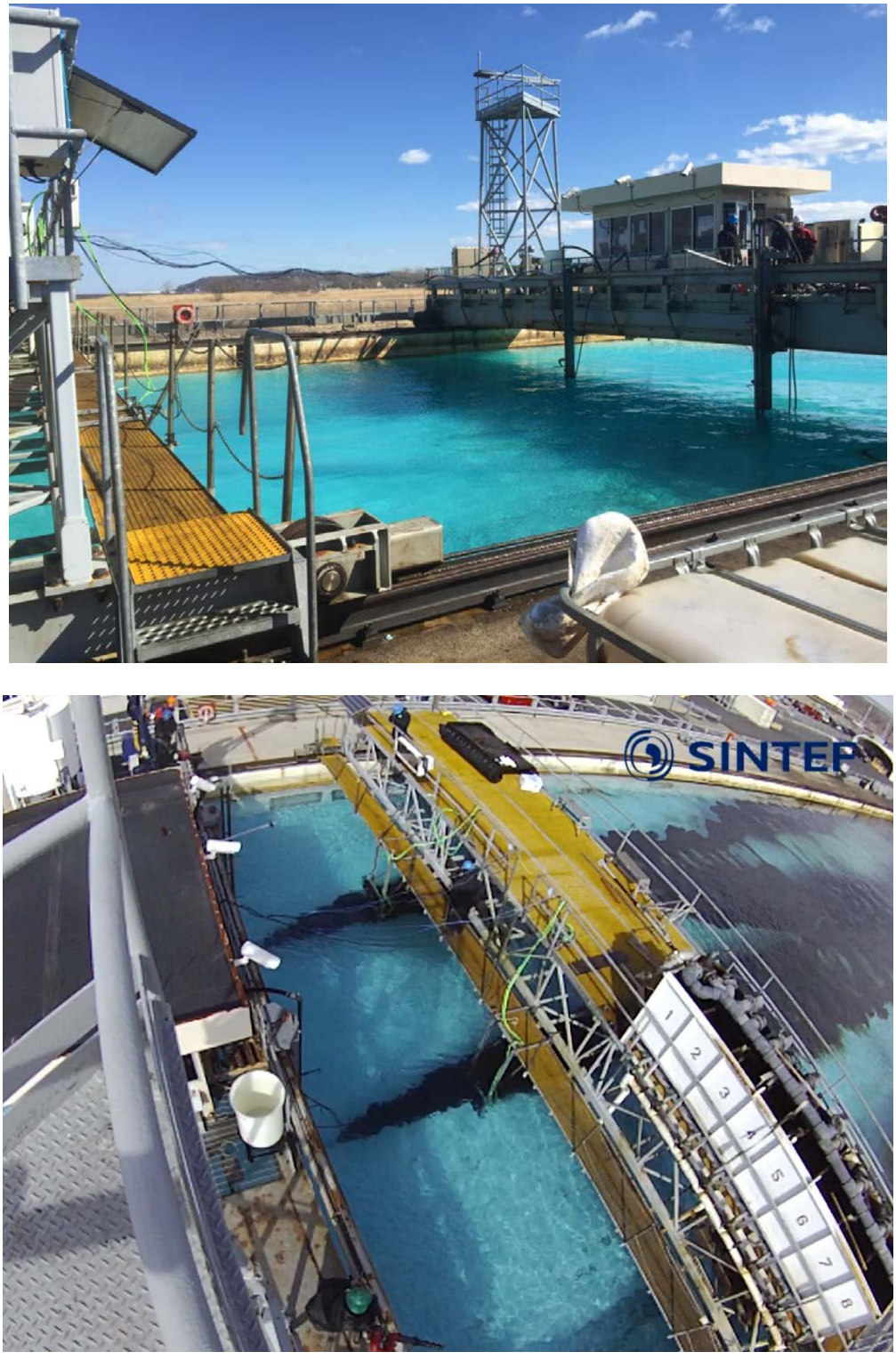

Figure 4.11: Images showing the two bridges being towed. The first bridge is holding the nozzles for the releases (1 x 25 mm and 1 x 32 or 50 mm) and the second bridge is holding the instrumentation (4 x SilCams). Lower image is showing the short distance used for oil alone experiments, while the upper image the longer distance for the dispersant testing.

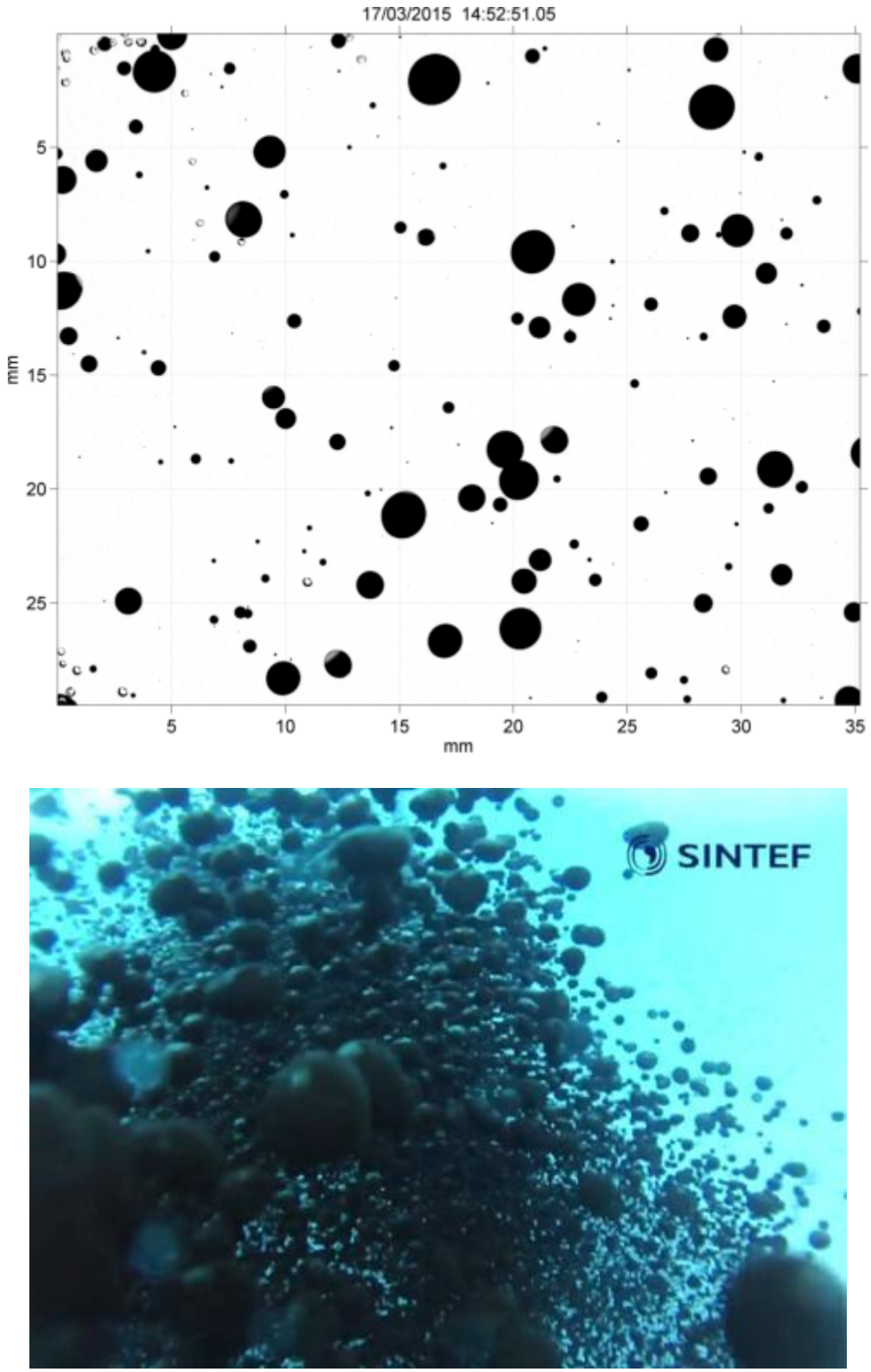

Figure 4.12: Image of Oil alone plume with large droplets, 3-5 mm (lower) from experiment 1 and example of image from Silhouette camera taken inside this plume (upper). The lower image is taken with an action-camera located in between the two SilCams.

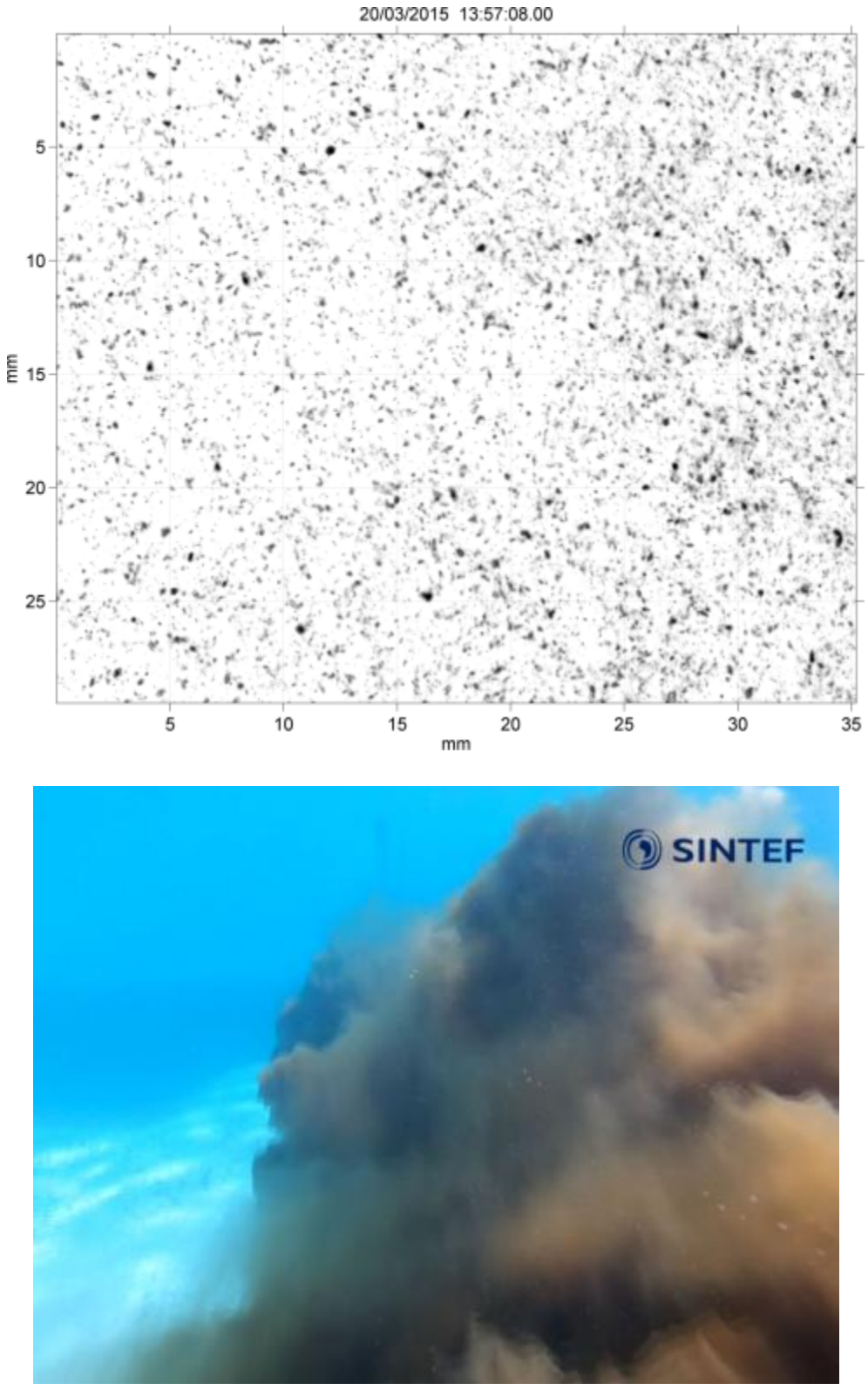

Figure 4.13: Image of dispersed plume (lower) showing the smaller droplets (from experiment 3) and example of image from Silhouette camera taken inside this plume (upper). The lower image is taken with an action-camera located below the SilCams.

A summary of the experiments that were completed during the Ohmsett test program is presented in Table 4.3 and Table 4.4. Three nozzle exit diameters were tested (25, 32 and 50 mm). Oil released alone and oil treated with dispersant injected into the flow stream near the exit were studied. The oil and dispersant flow rates were adjusted during each run to achieve three different flow combinations or periods during a given test from each of the two nozzles. The predicted d_{50} for each of the test is also provided in Table 4.3.

Table 4.3: Summary of experimental design of large-scale experiments at Ohmsett in March 2015. Two parallel releases were performed to utilise the width of the Ohmsett basin and each release is divided into three or four periods (see Figure 4.7). See Table 4.5 for details (only three periods shown in table).

	Periode 1		Periode 2		Periode 3		Estimated d_{50} µm (modified Weber)		
Nozzle	oil (L/min)	Disp dosage	oil (L/min)	Disp dosage	oil (L/min)	Disp dosage	1	2	3
25 mm	50	0 %	80	0 %	120	0 %	4500	2700	1700
32 mm	80	0 %	120	0 %	200	0 %	5000	3200	1200
50 mm	200	0 %	300	0 %	400	0 %	5600	3700	2700
25 mm	50	1 %	80	1 %	120	1 %	400	260	180
32 mm	80	1 %	120	1 %	300	1 %	430	300	130
50 mm	200	1 %	300	1 %	400	1 %	480	330	260

Table 4.4: Overview of large-scale experiments performed at Ohmsett March 2015. See Table 4.5 for details.

Exp#	Date	Nozzles	Flow rates	Type of experiment
	(mm)	(L/min)		
1	17.03.2015	25/32/50	50-200	Oil alone - Low flow rate I
2	18.03.2015	25/32/50	120-400	Oil alone - High flow rate I
3	18.03.2015	25/32/50	50-200	Dispersant (C9500-1%) - Low flow rate I
4	20.03.2015	25/32/50	50-300	Oil alone – Low flow rate II
5	20.03.2015	25/32/50	120-300	Dispersant (C9500-1%) – High flow rate I
6	23.03.2015	25/32/50	200-400	Oil alone – High flow rate II
7	23.03.2015	25/32/50	50-200	Dispersant (C9500-1%) - Low flow rate II
8	25.03.2015	32/32/50	50-400	Oil alone – All flow rates
9	25.03.2015	32/32/50	120-400	Dispersant (C9500-0.5/1/2%) – High flow rate II

Each experiment consisted of two parallel releases, one with the 25 mm nozzle and the other with either the 32 or the 50 mm nozzles (except for experiment 8 and 9 where only the 32 & 50 mm nozzles were used. The oil alone experiments (1, 2, 4, 6 and 8) were performed with a low towing speed (0.25-0.5 m/sec), while the experiments with dispersant injection (3, 5, 7 and 9) were performed with a high towing speed (0.75 – 1 m/sec). The towing speed, distance between bridges and instrument heights were adjusted to match the predicted trajectory of the oil plumes (oil release velocity, droplet sizes), see illustrations in Figure 3.5, Figure 4.7, Figure 4.10 and Figure 4.14. Positions of SilCams and towing speeds are presented in Table 4.5.

Table 4.5: Positions of the SilCams as vertical height over nozzle (VHON) and bridge-to-bridge distance together with the towing speed (m/s) for the two parallel releases divided into three periods (dispersant experiments) and four periods (oil alone experiments), see also Figure 4.7 and Table 4.4.

				Period 1		Period 2		Period 3		Period 4	
				m/sec - kts	sec	m/sec - kts	sec	m/sec - kts	sec	m/sec - kts	sec
	Experiment no:		1								
	Bridge-to-bridge distance:		1.9 m	0,25	90	0,25	90	0,30	90	0,30	90
	SilCam VHON (m)			0,49		0,49		0,58		0,58	
	Top Cam	Bottom Cam	Nozzle (mm)	oil (L/min)	disp	oil (L/min)	disp	oil (L/min)	disp	oil (L/min)	disp
1a	1,40	1,10	**25**	50		80		120		80	
2a	1,90	1,30	**32**	80		0		0		120	
2b			**50**	0		200		300		0	
	Experiment no:		2								
	Bridge-to-bridge distance:		3.0 m	0,5	70	0,5	70	0,55	70	0,30	70
	SilCam VHON (m)			0,97		0,97		1,07		0,58	
	Top Cam	Bottom Cam	Nozzle (mm)	oil (L/min)	disp	oil (L/min)	disp	oil (L/min)	disp	oil (L/min)	disp
1a	1,10	0,80	**25**	80	0 %	120	0 %	120	0 %	80	
2a	1,80	1,45	**32**	300		0		0		120	
2b			**50**	0		300		400		0	
	Experiment no:		3								
	Bridge-to-bridge distance:		10 m	0,8	60	0,8	60	0,85	60		
	SilCam VHON (m)			1,56		1,56		1,65			
	Top Cam	Bottom Cam	Nozzle (mm)	oil (L/min)	disp	oil (L/min)	disp	oil (L/min)	disp		
1a	1,50	1,10	**25**	50	1 %	80	1 %	120	1 %		
2a	1,80	1,45	**32**	0	1 %	120	1 %	0	1 %		
2b			**50**	200	1 %	0	1 %	300	1 %		
	Experiment no:		4								
	Bridge-to-bridge distance:		1.4 m	0,25	90	0,25	90	0,30	90	0,30	90
	SilCam VHON (m)			0,49		0,49		0,58		0,58	
	Top Cam	Bottom Cam	Nozzle (mm)	oil (L/min)	disp	oil (L/min)	disp	oil (L/min)	disp	oil (L/min)	disp
1a	1,20	0,90	**25**	50		80		120		80	
2a	1,70	1,10	**32**	80		0		0		120	
2b			**50**	0		200		300		0	
	Experiment no:		5								
	Bridge-to-bridge distance:		10 m	0,6	60	0,8	60	0,85	60		
	SilCam VHON (m)			1,17		1,56		1,65			
	Top Cam	Bottom Cam	Nozzle (mm)	oil (L/min)	disp	oil (L/min)	disp	oil (L/min)	disp		
1a	1,50	1,10	**25**	50	1 %	80	1 %	120	1 %		
2a	2,20	1,45	**32**	80	1 %	300	1 %	0			
2b			**50**	0		0		400	1 %		
	Experiment no:		6								
	Bridge-to-bridge distance:		3.0 m	0,5	90	0,3	90	0,30	90	0,30	90
	SilCam VHON (m)			0,97		0,58		0,58		0,58	
	Top Cam	Bottom Cam	Nozzle (mm)	oil (L/min)	disp	oil (L/min)	disp	oil (L/min)	disp	oil (L/min)	disp
1a	1,50	1,10	**25**	80		120		120		80	
2a	1,80	1,40	**32**	300		0		0		120	
2b			**50**	0		300		400		0	
	Experiment no:		7								
	Bridge-to-bridge distance:		10 m	0,8	60	0,8	60	1,0	60	NB! Towing speed accelerated from	
	SilCam VHON (m)			1,56		1,56		2,00		0.85 to 1 m/s during periode 3	
	Top Cam	Bottom Cam	Nozzle (mm)	oil (L/min)	disp	oil (L/min)	disp	oil (L/min)	disp		
1a	1,50	1,10	**25**	50	1 %	80	1 %	120	1 %		
2a	1,90	1,40	**32**	0		120	1 %	0			
2b			**50**	200	1 %	0		300	1 %		
	Experiment no:		8								
	Bridge-to-bridge distance:		3.0 m	0,55	90	0,4	90	0,35	90	0,25	90
	SilCam VHON (m)			1,07		0,78		0,68		0,49	
	Top Cam	Bottom Cam	Nozzle (mm)	oil (L/min)	disp	oil (L/min)	disp	oil (L/min)	disp	oil (L/min)	disp
1a	1,80	1,40	**32**	300		120		0		80	
2a	1,80	1,40	**32**	0		0					
2b			**50**	400		300		200		0	
	Experiment no:		9								
	Bridge-to-bridge distance:		10 m	0,8	60	0,8	60	0,80	60		
	SilCam VHON (m)			1,56		1,56		1,56			
	Top Cam	Bottom Cam	Nozzle (mm)	oil (L/min)	disp	oil (L/min)	disp	oil (L/min)	disp		
1a	1,70	1,40	**32**	120	2 %	120	1 %	120	0,5 %		
2a	1,90	1,60	**32**	0		0		0			
2b			**50**	400	1 %	300	1 %	200	1 %		

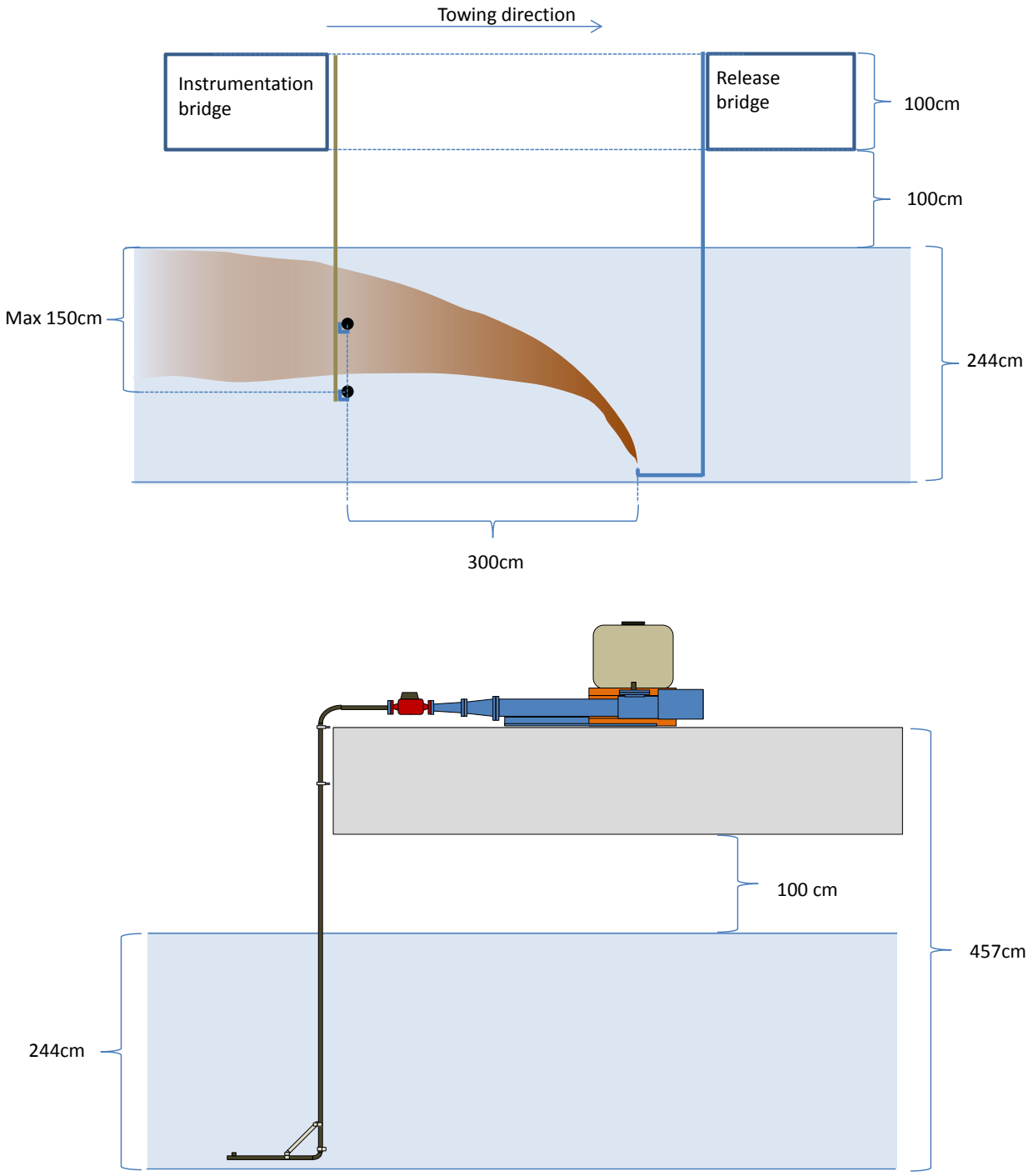

Figure 4.14: **Upper part:** Side view of the release nozzles, resulting plume and the two silhouette cameras used to monitor droplet size distributions. Distance between release and Silhouette cameras were varied as a function of release rates, nozzles & towing speeds. **Lower part**: Side view of the release arrangements, showing release pump, flow meter and the oil tank. See next figure for more details.

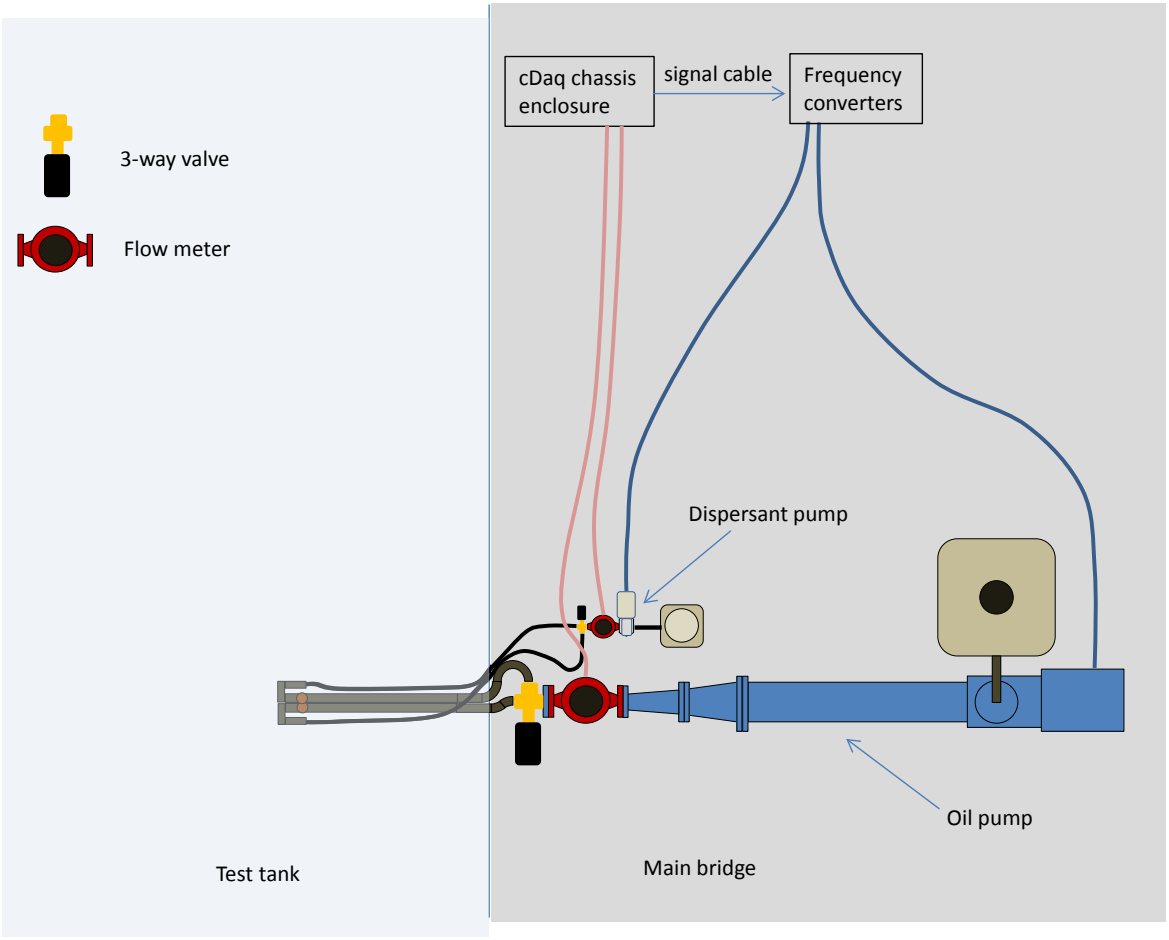

Figure 4.15: Top view showing the release point (interchangeable nozzle; 32 or 50 mm), dispersant & oil pump with remote operated 3-way valves, flow meters and pump controllers.

The experiments at Ohmsett were performed in March 2015 and description of experiments (type, nozzles, flow rates and temperatures) used are given the Table 4.6 and Table 4.7.

Table 4.6: Environmental conditions for Ohmsett experiments

Exper no	Type of experiments	Date	Oil temp (°C)	Air temp (°C)	Water temp (°C)
1	Oil alone, low flow rates	17. March 2015	13.0	14.7	5.1
2	Oil alone, high flow rates	18. March 2015	3.8	5.2	4.5
3	Dispersant, low flow rates	18. March 2015	3.2	4.8	5.7
4	Oil alone, low flow rates	20. March 2015	4.7	3.8	5.7
5	Dispersant, high flow rates	20. March 2015	4.6	0.5	5.7
6	Oil alone, high flow rates	23. March 2015	6.0	0.8	5.6
7	Dispersant, low flow rates	23. March 2015	5.8	1.0	5.6
8	Oil alone, high flow rates	25. March 2015	7.0	4.1	5.3
9	Dispersants, dosage exper.	25. March 2015	7.0	3.8	5.6

All experiments were performed with a water salinity of 2.75 % (measured at 4 °C). The reduced salinity is caused by fresh water input from precipitation. The water salinity is adjusted regularly by adding salt to the basin. No salt was added during this experimental period.

The gap of the SilCams is forming the measuring cell and the gaps for the two instruments used in all experiments at Ohmsett are given in Table 4.7.

Table 4.7: Gaps or path length (mm) in Silhouette cameras for Tower Basin experiments. Experiment 3, 5, 7 and 9 was performed with dispersant injection.

Exper no	Low resolution SilCam (mm)	Med resolution SilCam (mm)
1	12	10
2	12	10
3	12	8
4	12	10
5	12	8
6	12	10
7	8	5
8	12	10
9	8	5

To create similar underwater plumes that could be monitored with the instrumentation in the same position (height above nozzle), Experiments with high and low flow rates and dispersant injection had to be performed separately. Plume modelling (SINTEF Plume 3D) was used to determine how nozzle sizes and flow rates influenced plume positions and concentrations. These predictions (see examples in Figure 3.5) were used to determine the operational parameters (flow rates, towing speeds), so the instrumentation could be kept in the same position during one experiment usually performed with three different flow rates (see Table 4.4 and Table 4.5).

4.3 Oil type and Dispersant

Correct viscosity is of major importance using modified Weber scaling for predicting oil droplet sizes since the viscosity now is included as opposed to ordinary Weber scaling which does not include this term. Measuring viscosity at high shear rate and as a function of relevant temperatures is also needed to discover and correct for non-Newtonian behaviour of the oil, especially if it is due to high wax and/or asphaltene content. High viscosities are often measured on this type of oils at low shear rate (10-100 s^{-1}). Using these viscosities, only compensating for temperature, could give high viscosity and corresponding over estimation of droplet sizes with modified Weber scaling. In this study oil viscosity is measured at a high shear rate (1000 s^{-1}), more representative for such subsea experiments, as a function of temperature and presented in Figure 4.16.

4.3.1 Oil type

The oil was delivered by Statoil at the Sture oil terminal (20 m^3) outside Bergen, Norway in January 2015. The oil was shipped to Ohmsett in separate 1 m^3 tanks in a 40 foot shipping container. The oil was received at Ohmsett in mid-February 2015. One 1 m^3 container was also shipped to SINTEF in

Trondheim. Oseberg blend is a light paraffinic North Sea crude and the properties are presented in the table below. A total of 18 m^3 of oil was used in this project, 2 m^3 at SINTEF and 16 m^3 at Ohmsett. For the experiments with the largest nozzle at SINTEF, a mix of reused Oseberg and a light gas oil had to be used, due to lack of oil. This mix had a similar viscosity and IFT as Oseberg blend (5.2 mPas/15°C and 18 mN/m).

Table 4.8: Properties of MC252 oil and Oseberg blend.

	Macondo MC252	**Oseberg blend 2015 (2015-0014)**
Specific gravity (kg/l)	0.833	0.826
Pour Point (°C)	-27	-36
Viscosity (mPas at 40°C)	4	2.7
Asphaltene (wt%)	0.2	0.2
Waxes (wt%)	1.6	2.3
150°C – Evaporative loss (vol%)	27	22
200°C – Evaporative loss (vol%)	39	34
250°C – Evaporative loss (vol%)	50	45

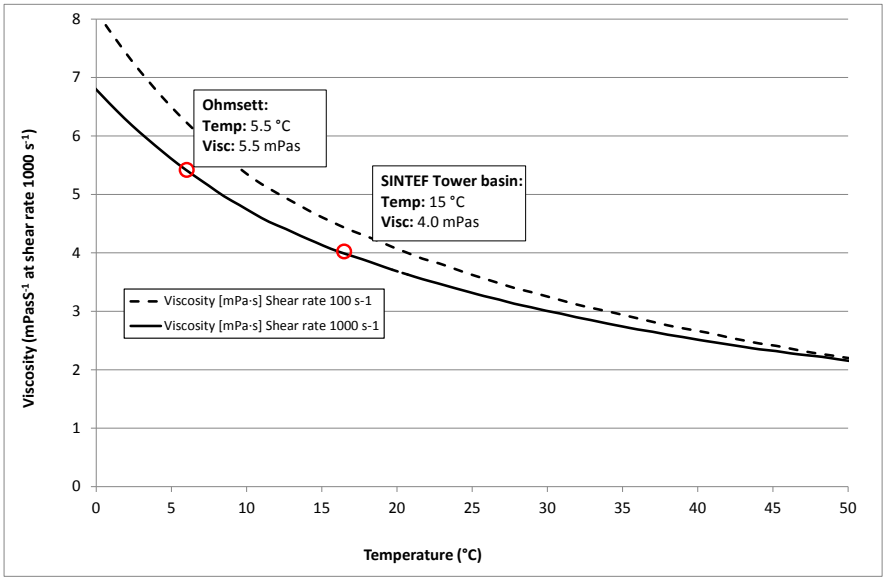

Figure 4.16: Viscosity of Oseberg blend as a function of temperature at shear rate of 1000. The oil temperature during the experiments at Ohmsett and SINTEF is marked in the figure.

4.3.2 Dispersant

Corexit 9500A was the main dispersant used in this project. Due to the large quantities needed the supplier (Nalco) was approach for a new 200 litre batch. However, Nalco required a signed Non-disclosure agreement with SINTEF to deliver the dispersant. This NDA conflicted with SINTEFs contract with API and would limit SINTEF further use of the dispersant in other projects.

SINTEF has a close cooperation with several European contingency organisations and the dispersant was supplied from one of them. SINTEF bought a sealed tank of C9500A and 200 litres were transferred to a new plastic lined barrel and shipped to Ohmsett. A few litres of dispersant were used at SINTEF, while almost 40 litres was used during the Ohmsett experiments.

4.4 SINTEF Silhouette camera

The silhouette cameras operate using the principle of backlighting to create silhouettes of particles suspended between the light and the camera. Further details are given in Appendix D and Davies et al., 2017.

Two systems with different magnifications have been used to optimize droplet sizing over the very large range of diameters created during the experiments. Fifteen images are taken per second (approximately 4.5 GB of data generated per minute) and the number of droplets per image varies from 15 to several hundred, depending on droplet size and resolution of the camera. Particle dimensions are quantified and used to determine droplet sizes and size distribution (see below). The number of droplets processed per distribution can vary between around 20 000 for large untreated droplets to over 1-million for small droplets after dispersant treatment (see Figure 5.1).

Droplet equivalent circular diameters (ECD) are quantified and counted into log-spaced volume size classes, which are divided (and extended) in an identical manner to the LISST-100 size classes. This enables a seamless transition in size distributions when comparing multiple magnifications and earlier results from the LISST-100.

5 Results

This section presents the results from the experiments performed both at SINTEF and at Ohmsett. The droplet size data are also given in Appendix C.

5.1 SINTEF Tower Basin

The experiments in the Tower Basin were performed in January and February 2015. The nozzles, flow rates and instrument (Silhouette cams) conditions used are given the Table 4.1and Table 4.2.

The experiments at SINTEF were a part of the feasibility study and the main objectives were to design and test the release arrangement and optimize the Silhouette cameras.

Representative SilCam images and oil droplet size distribution results, with and without dispersion injection, for the three nozzle sizes from the Tower Basin experiments are presented in Figure 5.1 and Figure 5.2 (25 mm nozzle), Figure 5.3 and Figure 5.4 (32 mm nozzle) and Figure 5.5 and Figure 5.6 (50 mm nozzle).

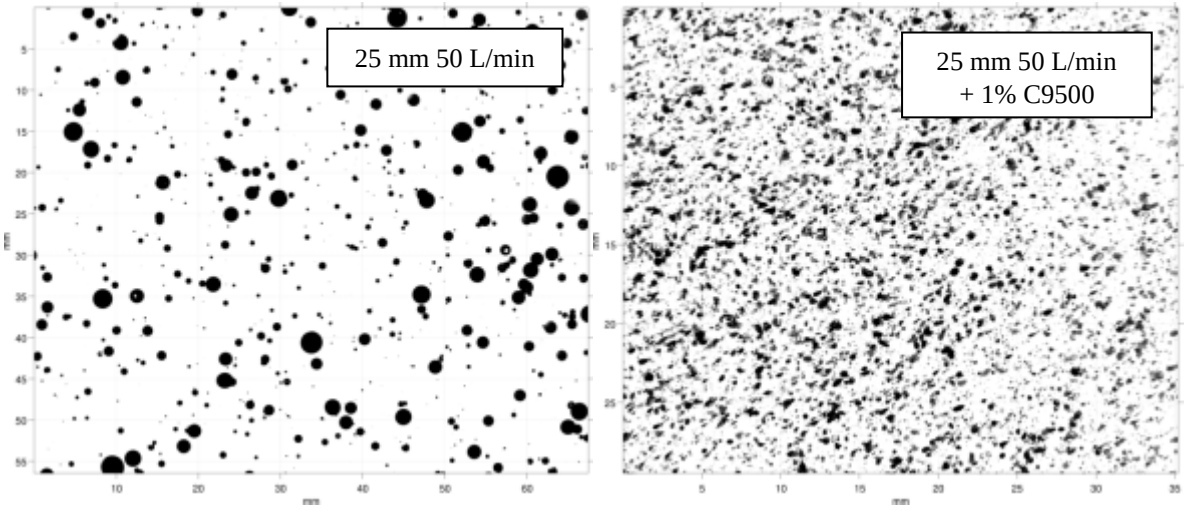

Figure 5.1: Images from Silhouette cameras showing individual droplets (25 mm nozzle, 50 L/min and 50 L/min with 1% C9500. NB! Note the different scaling!

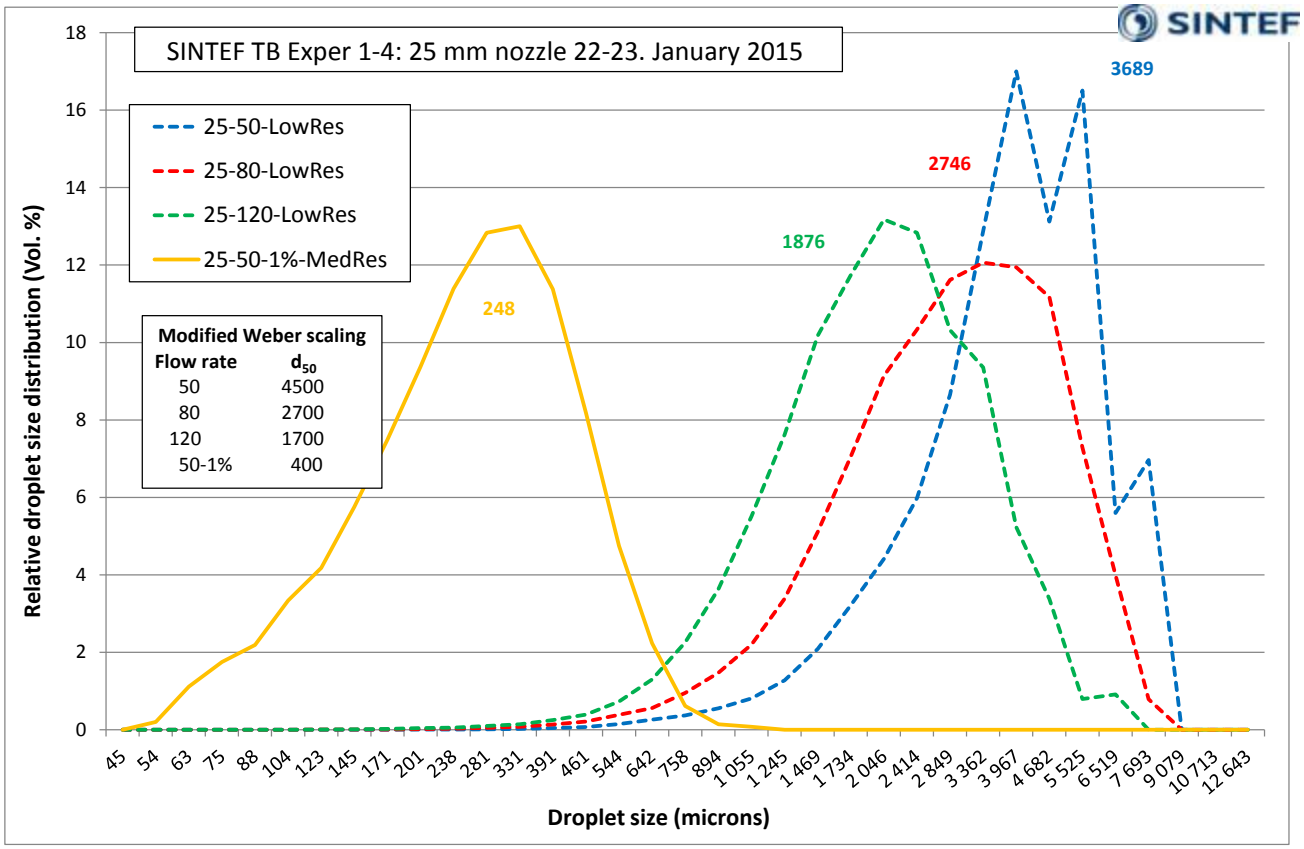

Figure 5.2: Droplet size distribution (45 - 12 000 µm) from the experiments with the 25 mm nozzle at 50, 80 and 120 L/min and at 50 l/min with 1% Corexit 9500 (simulated injection tool – SIT). Numbers beside graphs are estimated d_{50} from cumulative distribution function (not peak maximum as used previously). Dotted lines are low resolution SilCam and solid lines medium resolution SilCam.

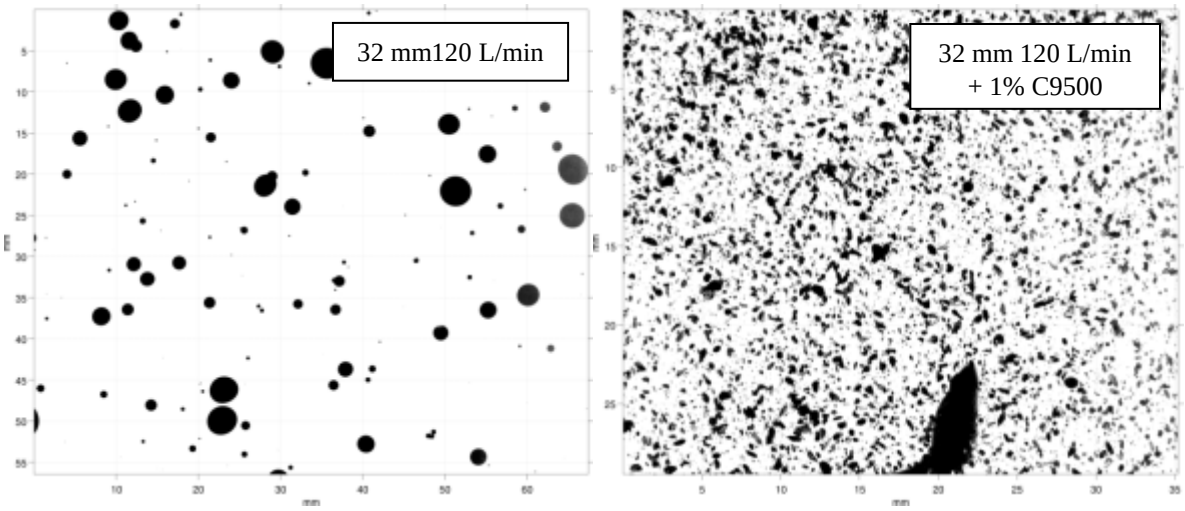

Figure 5.3: Images from Silhouette cameras showing individual droplets (32 mm nozzle, 120 L/min and 200 L/min with 1% C9500. NB! Note the different scaling!

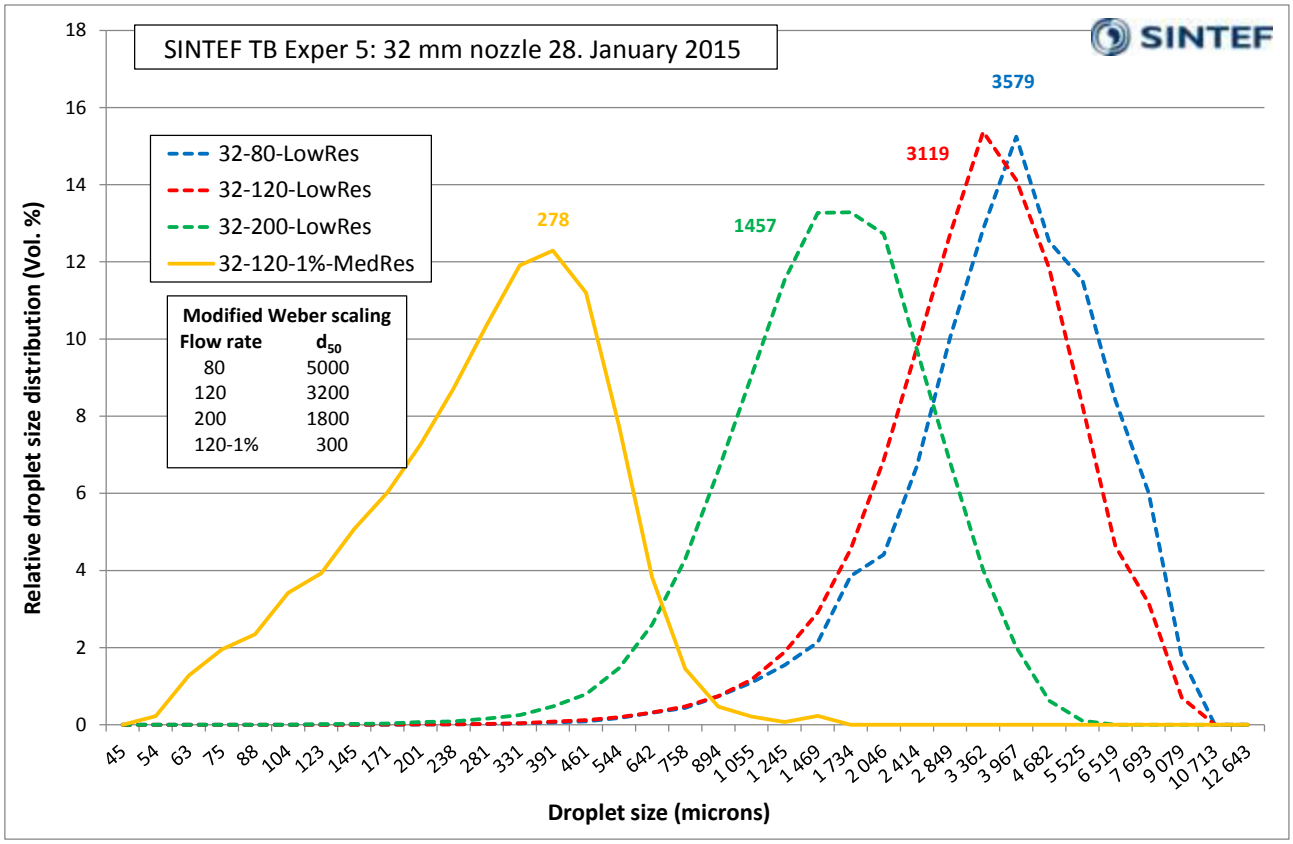

Figure 5.4: Droplet size distribution (45 - 12 000 µm) from the experiments with the 32 mm nozzle at 80, 120 and 200 L/min and at 120 l/min with 1% Corexit 9500 (simulated injection tool – SIT). Numbers beside graphs are estimated d_{50} from cumulative distribution function (not peak maximum as used previously). Dotted lines are low resolution SilCam and solid lines medium resolution SilCam.

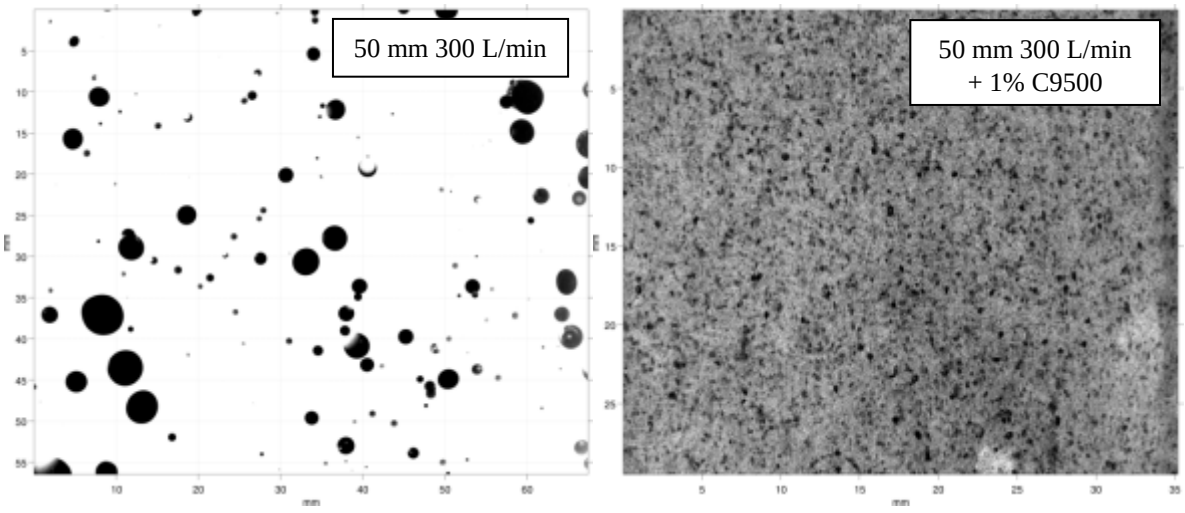

Figure 5.5: Images from Silhouette cameras showing individual droplets (50 mm nozzle, 300 L/min and 300 L/min with 1% C9500. NB! Note the different scaling!

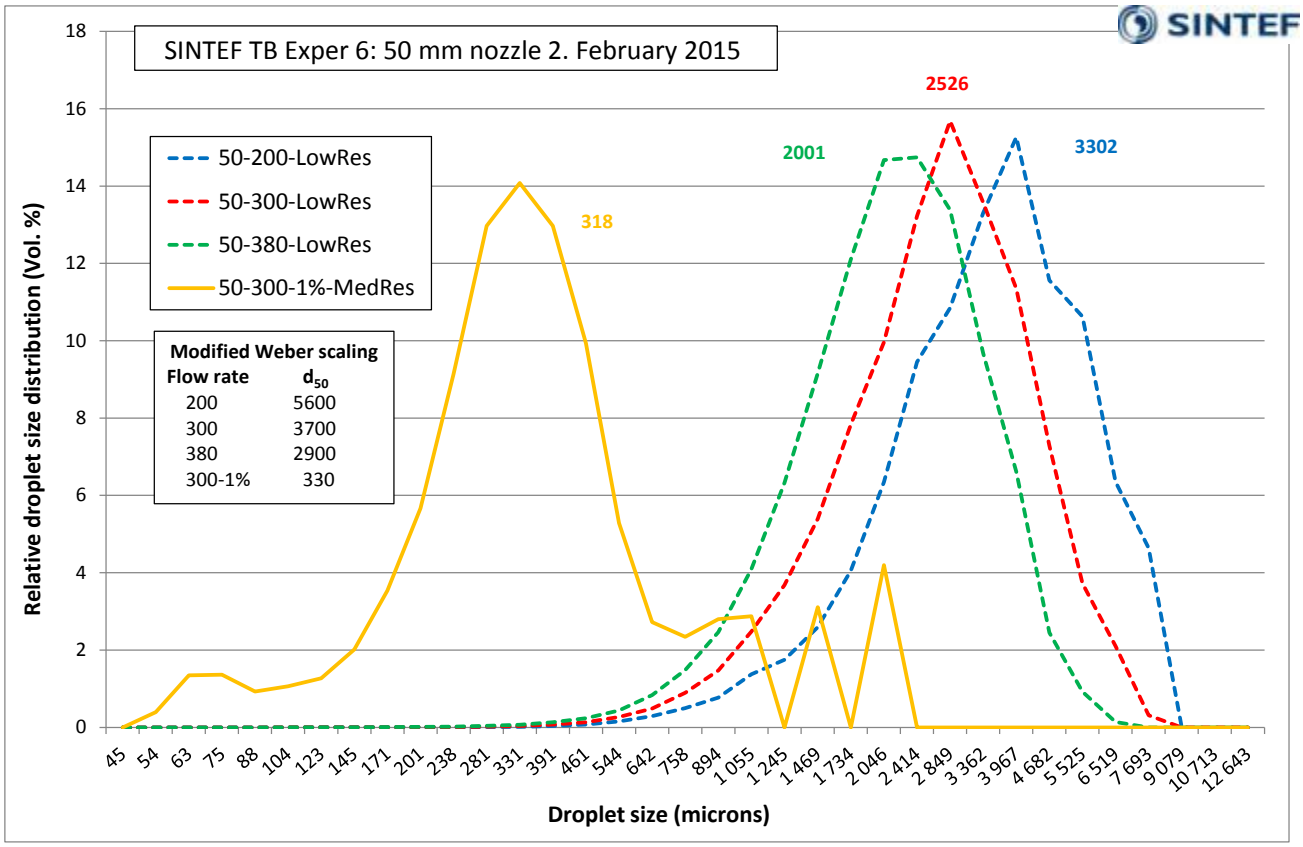

Figure 5.6: Droplet size distribution (45 - 12 000 µm) from the experiments with the 50 mm nozzle at 200, 300 and 400 L/min and at 50 l/min with 1% Corexit 9500 (simulated injection tool – SIT). Numbers beside graphs are estimated d_{50} from cumulative distribution function (not peak maximum as used previously). Dotted lines are low resolution SilCam and solid lines medium resolution SilCam. NB! Experiments were performed with a blend of Oseberg and a light gas oil (partly transparent). SilCam underestimate sizes of transparent droplets.

5.2 Ohmsett Facilitiy

The experiments at Ohmsett were performed in March 2015 and description of experiments (type, nozzles, flow rates and temperatures) used are given the Table 4.6 and Table 4.7.

A summary of all the experiments, including replicates, are presented in the next section, but a selection of representative droplet size distributions for the three different nozzles (25, 32 and 50 mm) is presented on the next pages. To present combined figures with multiple flowrates for each nozzle, measurements from multiple experiments have to be combined.

Representative SilCam images and oil drop size distributiond from selected Ohmsett experiments are shown in Figure 5.7 and Figure 5.8 (25 mm nozzle), Figure 5.9 and Figure 5.10 (32 mm nozzle) and Figure 5.11 and Figure 5.12 (50 mm nozzle). The ID of the individual experiments (experiment number, see Table 4.4) are given in the legend of the figures.

Cumulative droplet size distributions from the same Ohmsett experiments as discussed above Figure 5.8 (25 mm nozzle), Figure 5.10 (32 mm nozzle) and Figure 5.12 (50 mm nozzle) are compared to both log linear and Rosin Rambler distributions in Figure 5.13.

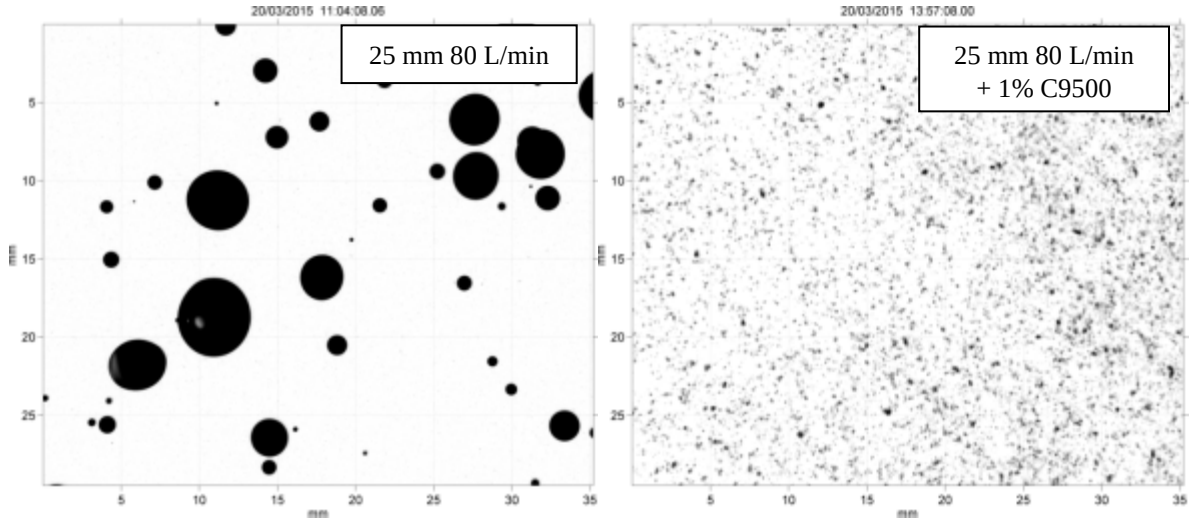

Figure 5.7: Images from Silhouette cameras showing individual droplets (25 mm nozzle, 80 L/min and 80 L/min with 1% C9500.

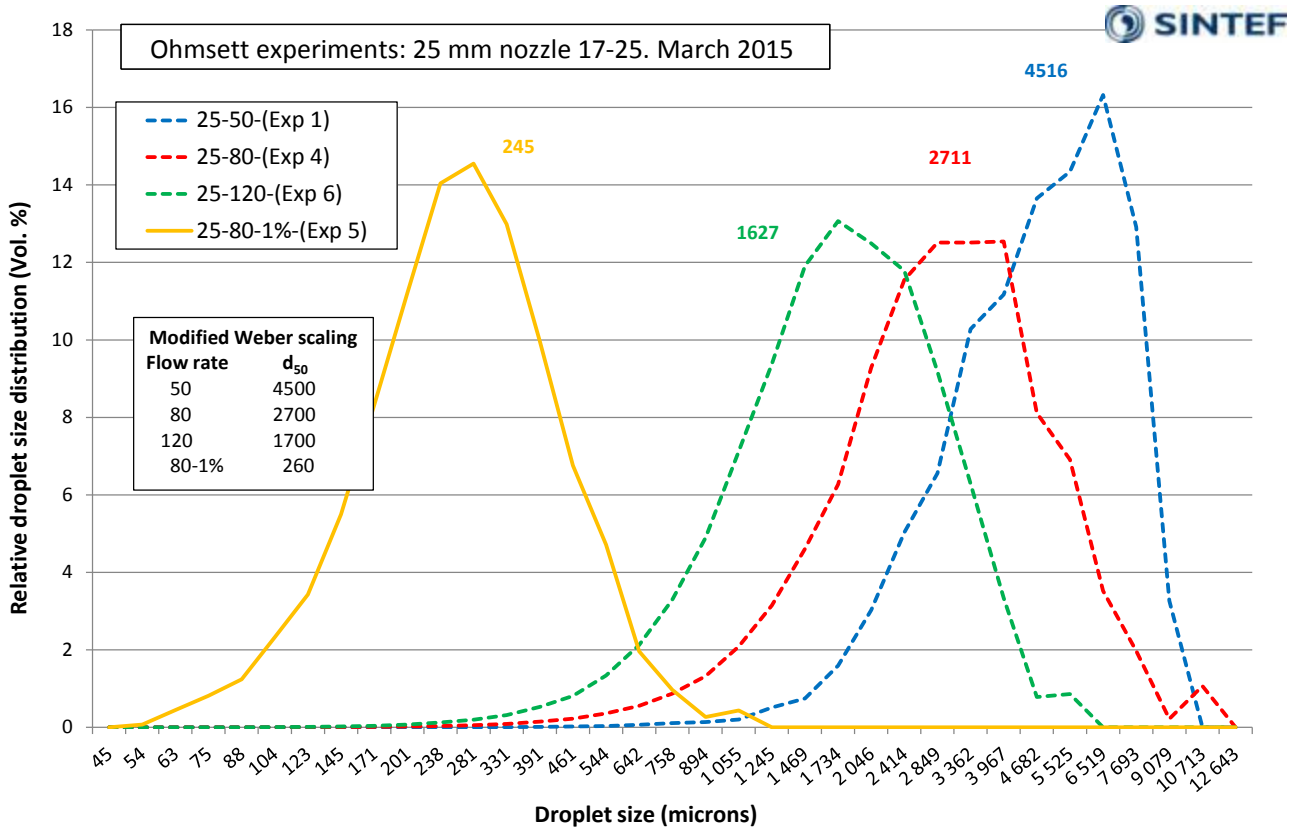

Figure 5.8: Droplet size distribution (45 - 12 000 µm) from the experiments with the 25 mm nozzle at 50, 80 and 120 L/min and at 50 l/min with 1% Corexit 9500 (simulated injection tool – SIT). Numbers beside graphs are estimated d_{50} from cumulative distribution function (not peak maximum as used previously). Dotted lines are low resolution SilCam and solid lines medium resolution SilCam.

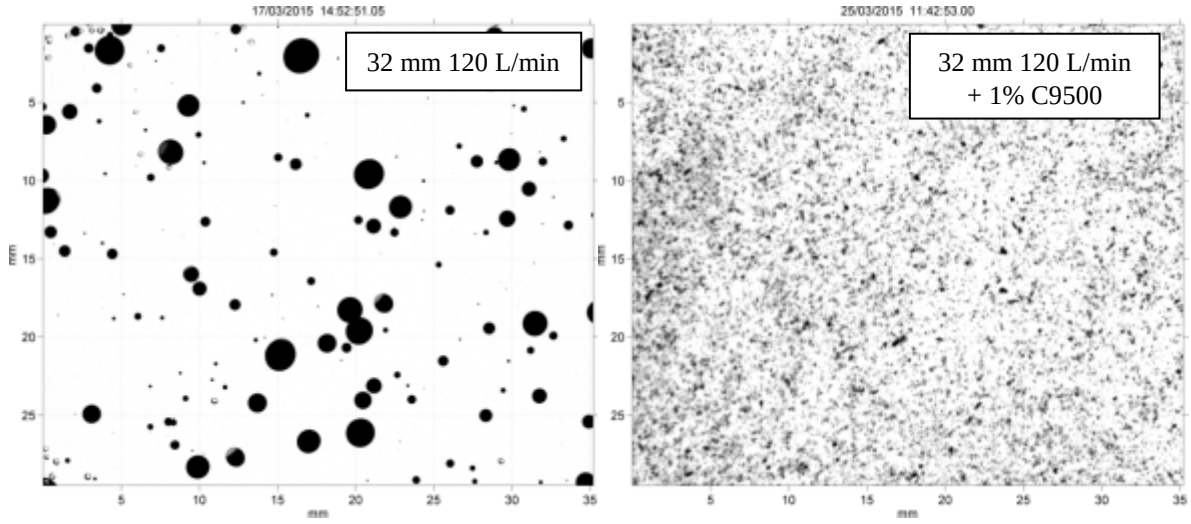

Figure 5.9: Images from Silhouette cameras showing individual droplets (32 mm nozzle, 120 L/min and 120 L/min with 1% C9500.

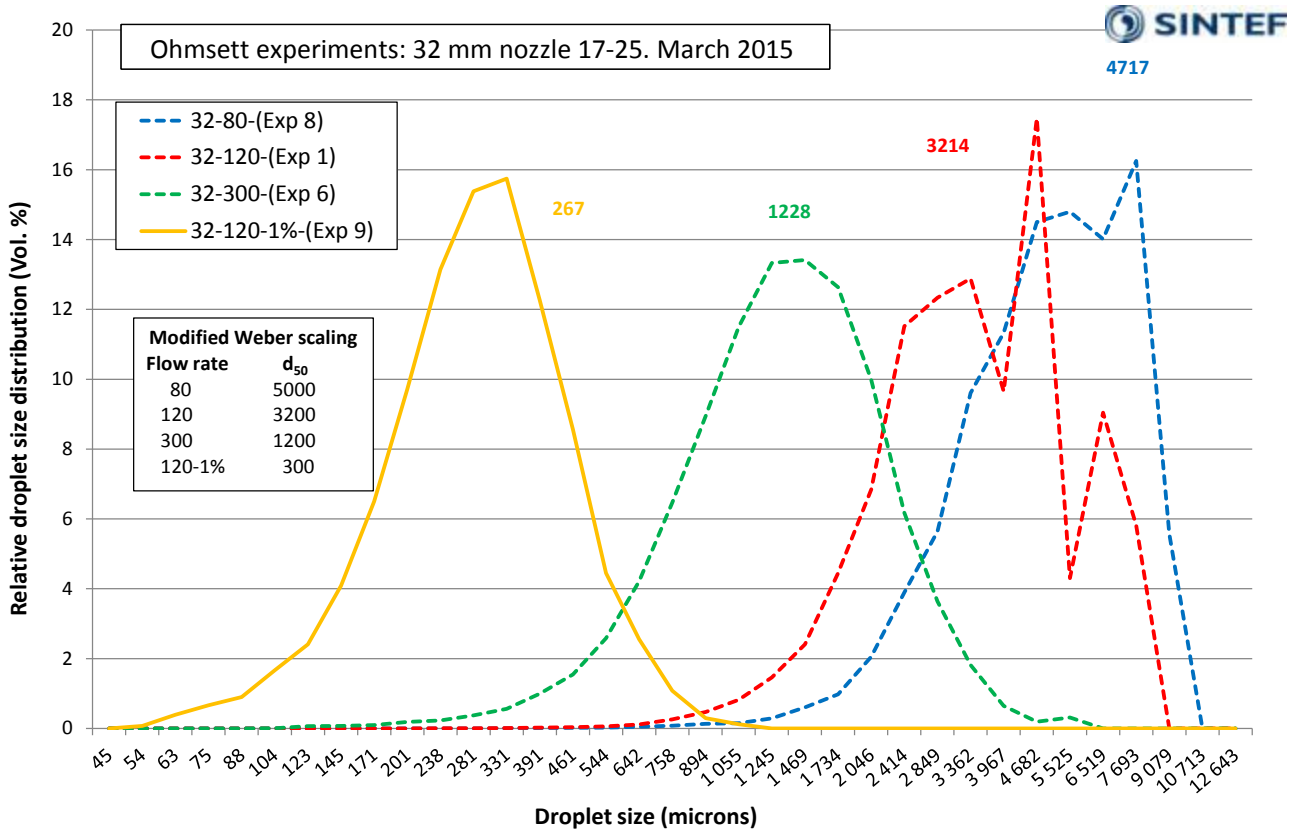

Figure 5.10: Droplet size distribution (45 - 12 000 µm) from the experiments with the 32 mm nozzle at 80, 120 and 300 L/min and at 50 l/min with 1% Corexit 9500 (simulated injection tool – SIT). Numbers beside graphs are estimated d_{50} from cumulative distribution function (not peak maximum as used previously). Dotted lines are low resolution SilCam and solid lines medium resolution SilCam.

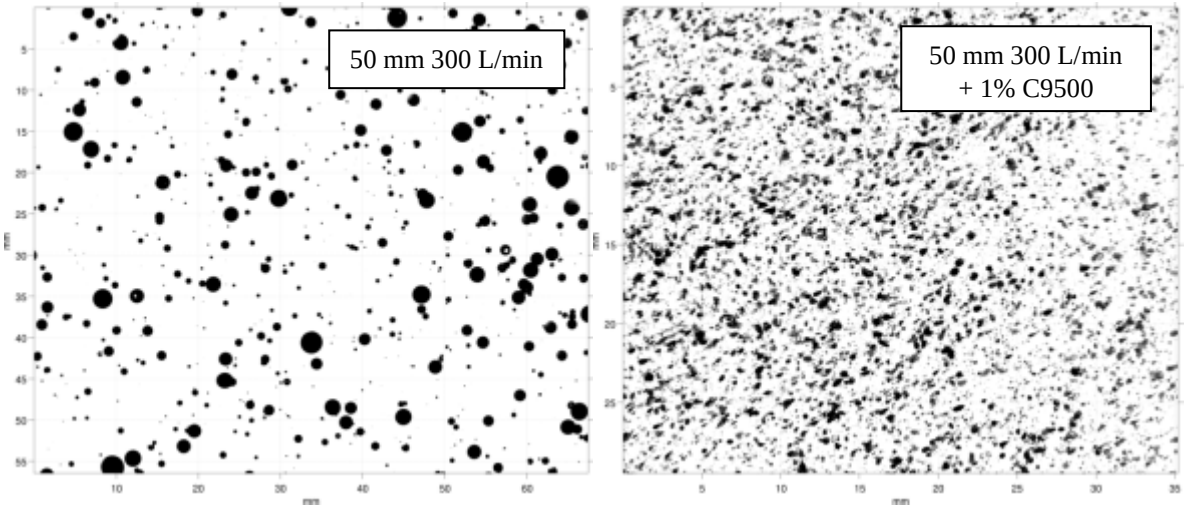

Figure 5.11: Images from Silhouette cameras showing individual droplets (50 mm nozzle, 300 L/min and 300 L/min with 1% C9500. NB! Note the different scaling!

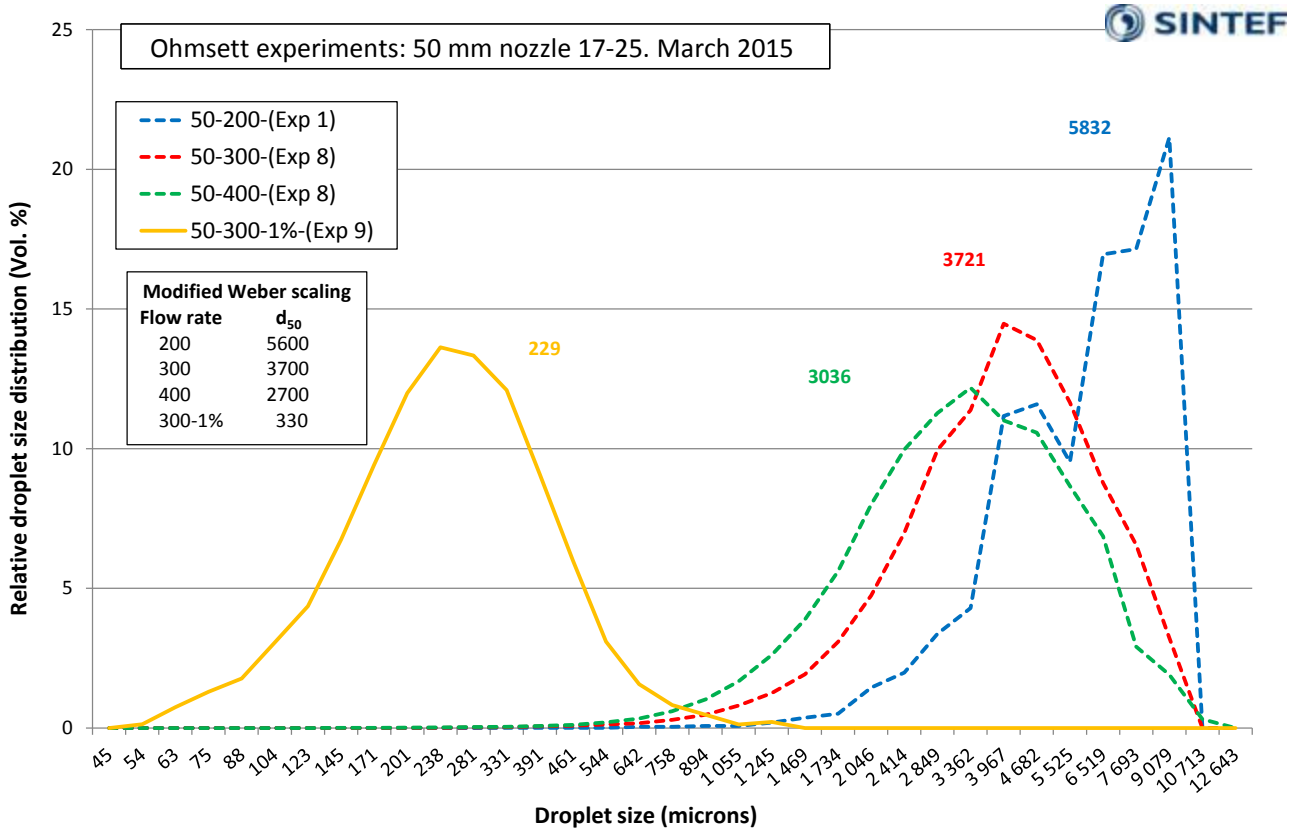

Figure 5.12: Droplet size distribution (45 - 12 000 µm) from the experiments with the 50 mm nozzle at 200, 300 and 400 L/min and at 300 l/min with 1% Corexit 9500 (simulated injection tool – SIT). Numbers beside graphs are estimated d_{50} from cumulative distribution function (not peak maximum as used previously). Dotted lines are low resolution SilCam and solid lines medium resolution SilCam.

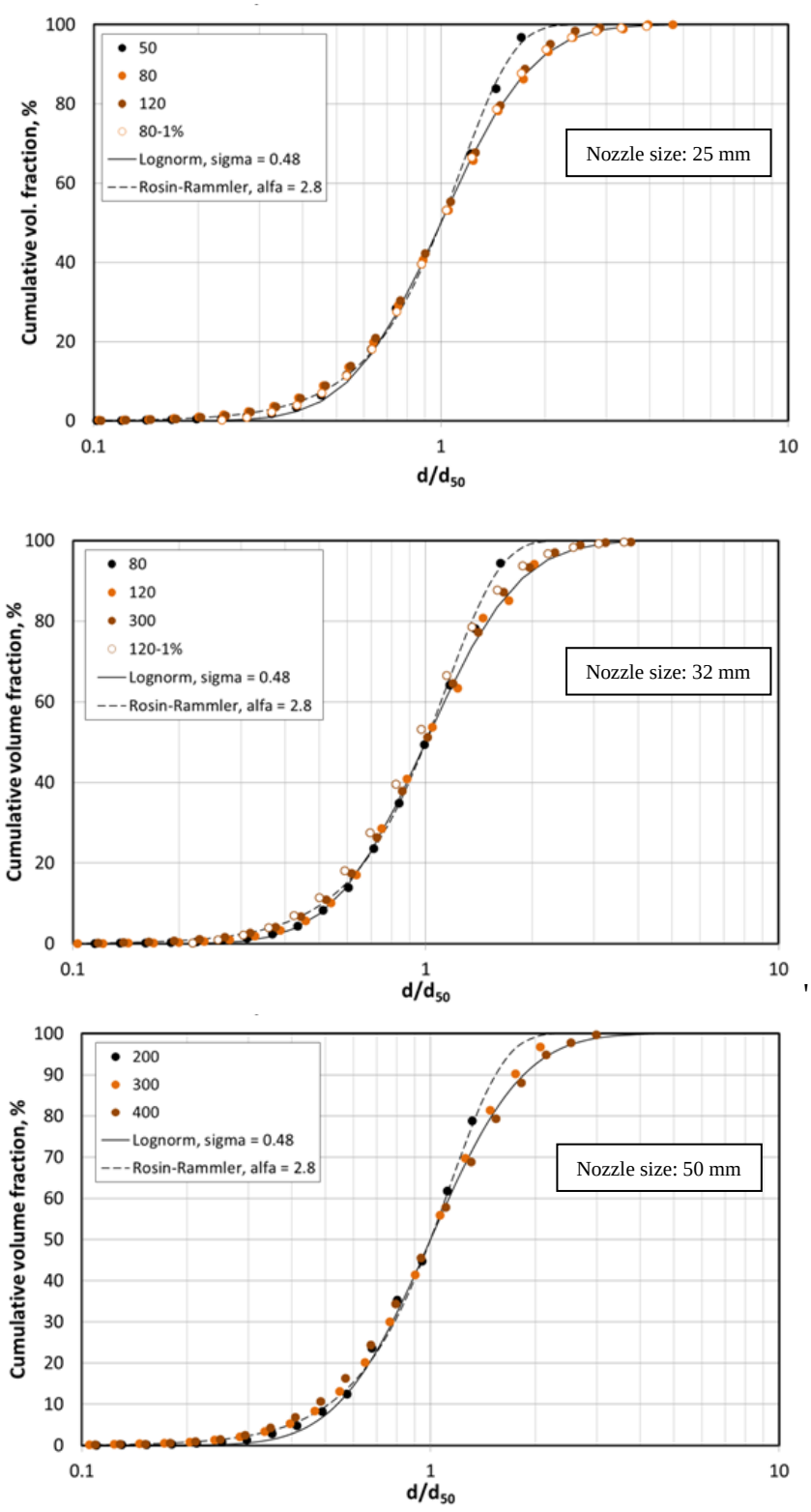

Figure 5.13: Cumulative droplet size distributions for the three nozzle sizes 25, 32 and 50 mm (SINTEF Tower basin experiments) compared to both log linear and a Rosin Rambler distributions.

5.3 Summary of Ohmset results

Since oil during the Ohmsett experiments was released from two parallel nozzles and each run was divided into three periods (Oil alone experiments, low towing speed, 90 seconds each) and four periods (high towing speed, dispersant experiments, 60 seconds each), an extensive dataset was generated during the nine experiments. The number of replicates for most combinations of nozzles and flow rates varied between 3 and 5. Representative oil drop size distributions are shown in Figure 5.8 (25 mm nozzle), Figure 5.10 (32 mm nozzle) and Figure 5.12 (50 mm nozzle). The oil drop size distribution volume median diameters (d_{50}) from each of the replicates are presented in tables for each nozzle size (Table 5.1 - 25 mm, Table 5.2 - 32 mm and Table 5.3- 50 mm Table 5.4 - 25 mm with dispersant, Table 5.5 - 32 mm with dispersant and Table 5.6 - 50 mm with dispersant). These d_{50} data are also plotted alongside predicted values in Figure 5.14 - 25 mm nozzle, Figure 5.15 - 32 mm nozzle, Figure 5.16 - 50 mm nozzle, Figure 5.17 - 25 mm nozzle with dispersant, Figure 5.18 - 32 mm nozzle with dispersant, Figure 5.19 - 50 mm nozzle with dispersant. A complete table of all measured droplet sizes (d_{50}) is provided in Appendix C.

A standalone version of the near field model used in SINTEFs OSCAR model (DeepBlow or Plume 3D) was used to position the SilCam instruments in the plume (see examples in Figure 3.2). The objective was to position both SilCams within the oil plume. The Silcam with the medium resolution was always the upper instrument, while the low resolution version was used as the lower instrument. In most cases, one or both SilCams were in the plume for a sufficient length of time to generate representative data and stable distributions were measured over a period of 30 seconds or more. The upper SilCam usually measured slightly larger droplets than the lower Silcam. If both instruments were in the plume an average of the two measured distributions were used to estimate the d_{50} for the actual experimental setting. The positions of the SilCams were adjusted according to the Plume 3D predictions by changing; (1) the vertical eight over the nozzle (VON), (2) distance between the release- and instrument bridge and (3) the towing speed. See Experimental section 3 and Table 4.5 for further details.

The evaluation of data quality of this dataset was based on several factors. The most significant were;

1. Instrument position in the plume: In some cases, we observed or experienced from the data that one or both of the instruments were not positioned correctly in the plume.
2. Smearing of optics: Especially for the releases with low release velocity (low flow rates), smearing of the optics could occur due to high concentration of large droplets.
3. High droplet concentration: In some cases were the plumes too concentrated and reliable data could not be obtained.
4. Pump irregularities: All flow rates were monitored and documented with in-line flow meters (see examples in Figure 4.5 and Figure 4.8). Oil flow rates were generally very stable with standard deviations around 1%. However, larger deviations occurred (human errors and system malfunction) and were documented in the log-files.
5. Transparent oil: Due to lack of oil during the initial experiment in Trondheim, a mix of reused, slightly weathered Oseberg and a light gas oil was used for the 50 mm experiments at SINTEF. The SilCam underestimate sizes of the (large untreated) transparent oil droplets in this experiment due to the transparent nature of the oil.

Evaluation of data quality:
Based on an evaluation of the factors discussed above (1-5), the quality of the individual replicate measurements were evaluated and sorted into three categories. The following colour coding was used in to indicate three categories of data quality;

1. Red indicates that the data quality is unacceptable (17%) due to known & documented conditions during the experiments. Data should not be used for further analysis and is not reported in Table C.1
2. Yellow indicates acceptable data quality (41%), will, however, cause scatter and should be interpreted with caution
3. Green indicates excellent data quality (45%).

Table 5.1: 25 mm nozzle - Untreated: Droplet sizes from all experiments at both SINTEF Tower Basin and Ohmsett. Colour coding indicate quality of results (red is unacceptable, yellow is acceptable and green is excellent.

25 mm Nozzle - Oil alone experiments

	Low		Medium		High	
	50 L/min		80 L/min		120 L/min	
	Exp#	d_{50}	Exp#	d_{50}	Exp#	d_{50}
Ohmsett	1	4500	1	3450	1	2000
			1	2900		
			2	2750	2	2300
			2	2100	2	2400
	4	4200	4	3100	4	2100
			4	3150		
			6	3000	6	1450
			6	2200	6	1700
SINTEF TB	1	3700	1	2800	1	1900

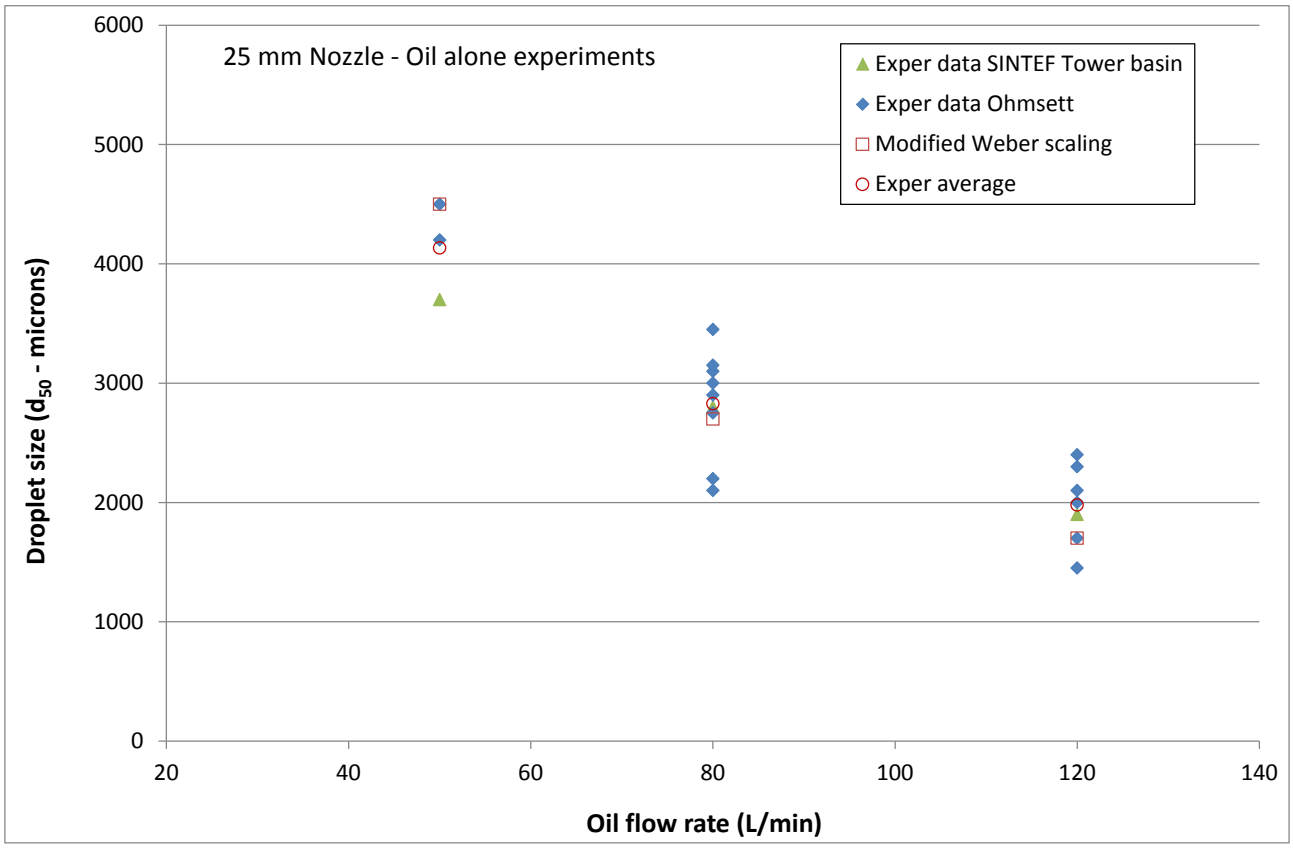

Figure 5.14: 25 mm Nozzle: Droplet sizes (d_{50}) as a function of flow rates for all experiments (Ohmsett/Tower Basin). Predicted values (Modified Weber scaling- open squares) and average values for experimental data (open circles) are also included in the figure.

Table 5.2: 32 mm nozzle – Untreated: Droplet sizes from all experiments at both SINTEF Tower Basin and Ohmsett. Colour coding indicate quality of results (red is unacceptable, yellow is acceptable and green is excellent.

32 mm Nozzle - Oil alone experiments

	Low		Medium		High	
	80 L/min		120 L/min		300 L/min	
	Exp#	d_{50}	Exp#	d_{50}	Exp#	d_{50}
Ohmsett	1	4650	1	3200		
			2	3400	2	2300
	4	3600	4	2800		
			6	2500	6	1350
	8	4150	8	3550	8	1700
SINTEF TB	0	3600	0	3100	0	1500

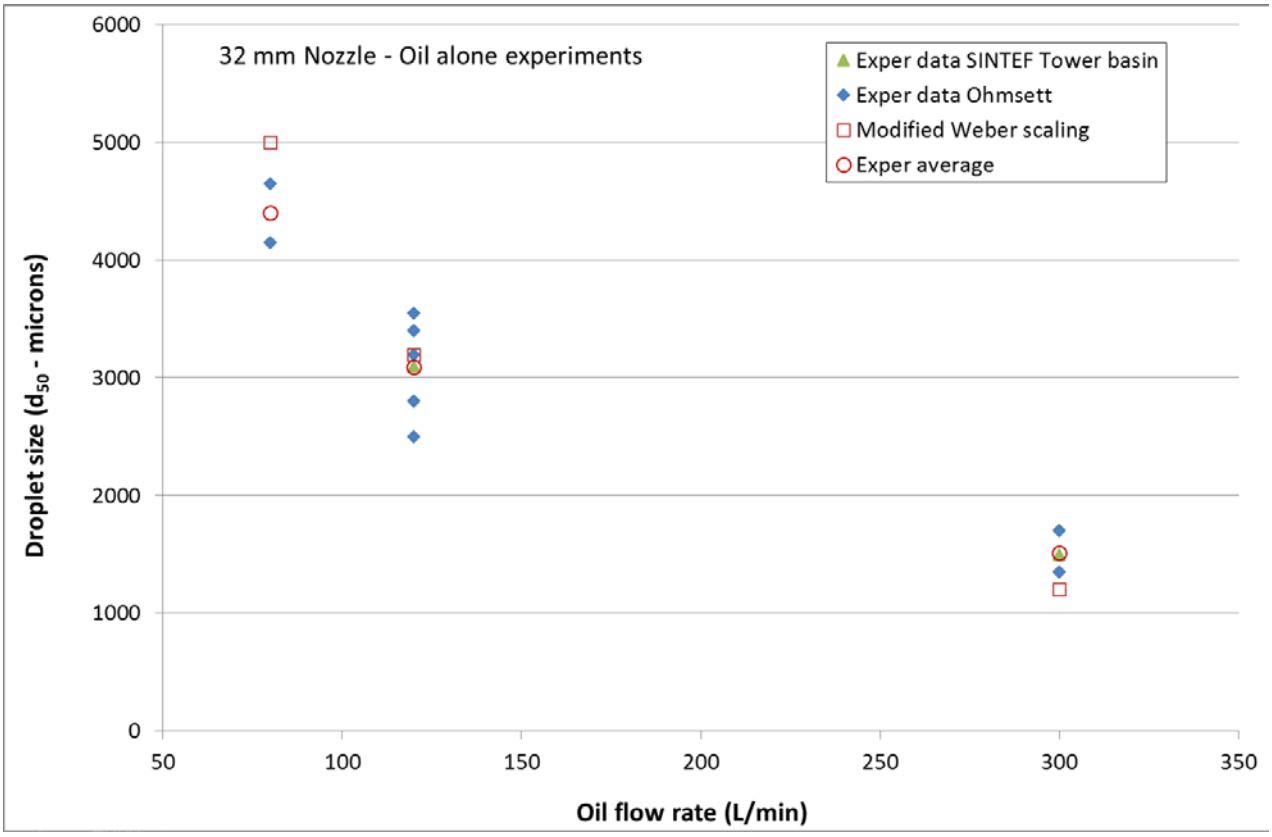

Figure 5.15: 32 mm Nozzle: Droplet sizes (d_{50}) as a function of flow rates for all experiments (Ohmsett/Tower Basin). Predicted values (Modified Weber scaling- open squares) and average values for experimental data (open circles) are also included in the figure.

Table 5.3: 50 mm nozzle - Untreated: Droplet sizes from all experiments at both SINTEF Tower Basin and Ohmsett. Colour coding indicate quality of results (red is unacceptable, yellow is acceptable and green is excellent.

50 mm Nozzle - Oil alone experiments

	Low		Medium		High	
	200 L/min		300 L/min		400 L/min	
	Exp#	d_{50}	Exp#	d_{50}	Exp#	d_{50}
Ohmsett	1	5200	1	3700		
			2	5700	2	4300
	4	4500	4	3000		
			6	2100	6	2100
	8	4500	8	3700	8	3000
SINTEF TB	1	3300	1	2500	1	2000

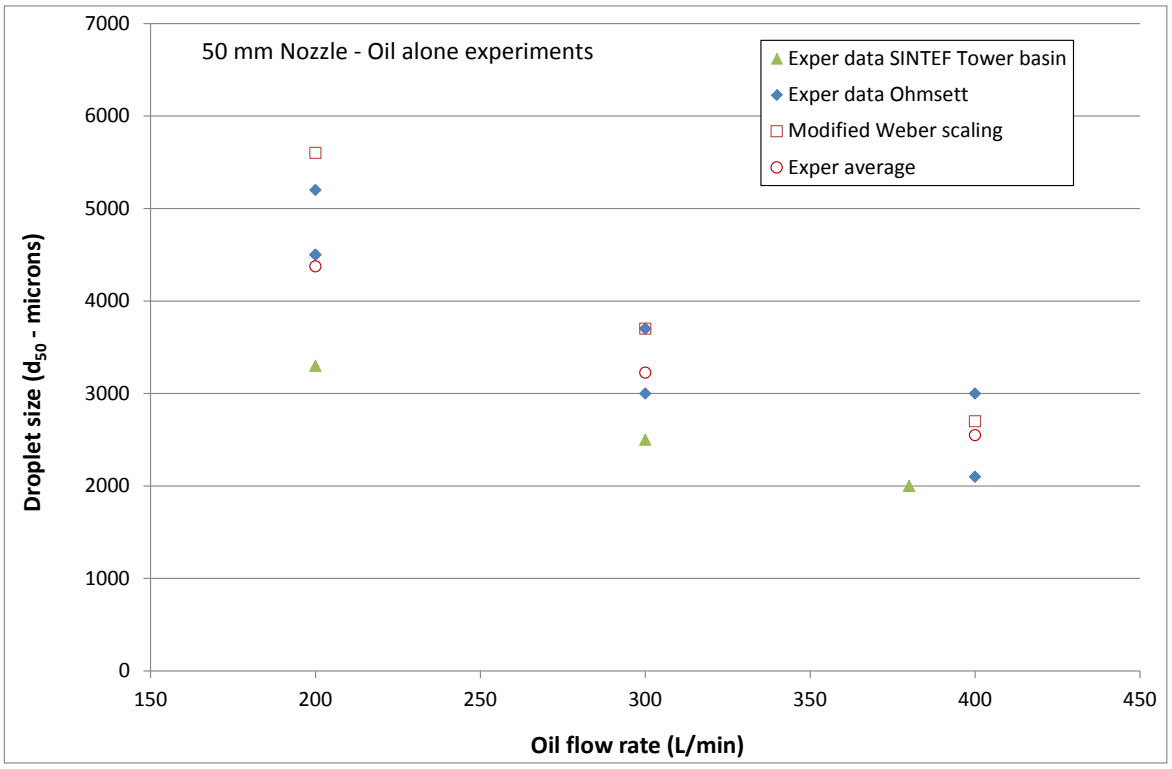

Figure 5.16: 50 mm Nozzle: Droplet sizes (d_{50}) as a function of flow rates for all experiments (Ohmsett/Tower Basin). Predicted values (Modified Weber scaling- open squares) and average values for experimental data (open circles) are also included in the figure. Results from Tower Basin experiments are included, even though the results are marked as red due to probable systematic under-representation of droplet sizes (transparent oil).

Table 5.4: 25 mm nozzle dispersant experiments (all 1%): Droplet sizes from all experiments at both SINTEF Tower Basin and Ohmsett. Colour coding indicate quality of results (red is unacceptable, yellow is acceptable and green is excellent).

25 mm Nozzle - Dispersant experiments

	Low		Medium		High	
	50 L/min		80 L/min		120 L/min	
	Exp#	d_{50}	Exp#	d_{50}	Exp#	d_{50}
Ohmsett	3	900	3	345	3	220
	5	480	5	250	5	240
	7	360	7	250	7	240
SINTEF TB		250				

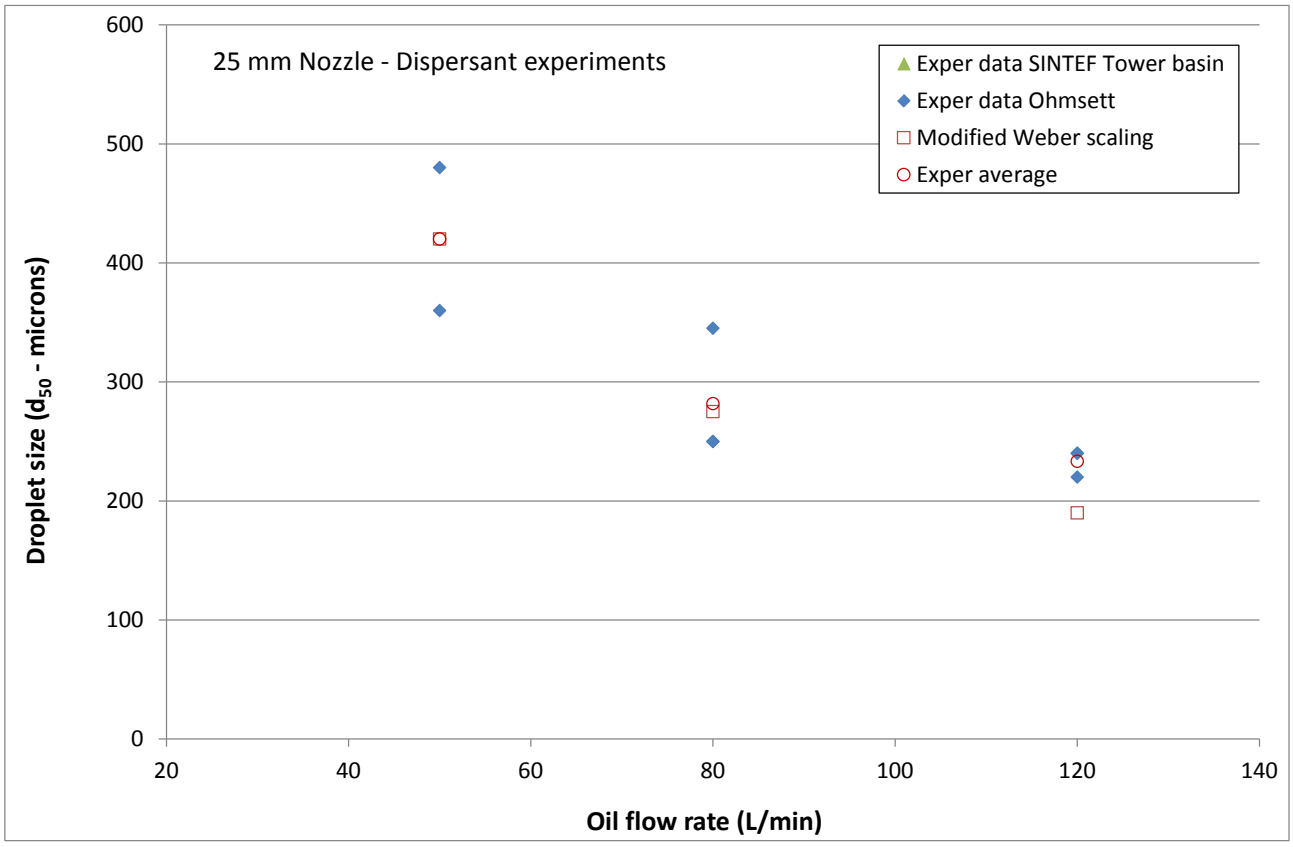

Figure 5.17: 25 mm Nozzle and dispersants: Droplet sizes (d_{50}) as a function of flow rates for all experiments (Ohmsett/Tower Basin). Predicted values (Modified Weber scaling- open squares) and average values for experimental data (open circles) are also included in the figure.

Table 5.5: 32 mm nozzle dispersant experiments (all 1%, except for experiment 9 (2-0.5%)): Droplet sizes from all experiments at both SINTEF Tower Basin and Ohmsett. Colour coding indicate quality of results (red is unacceptable, yellow is acceptable and green is excellent).

32 mm Nozzle - Dispersant experiments

	Low		Medium		High	
	80 L/min		120 L/min		300 L/min	
	Exp#	d_{50}	Exp#	d_{50}	Exp#	d_{50}
Ohmsett			3	290		
	5	550			5	220
	7	220				
			9-2%	190		
			9-1%	260		
			9-0.5%	320		
SINTEF TB			1	280		

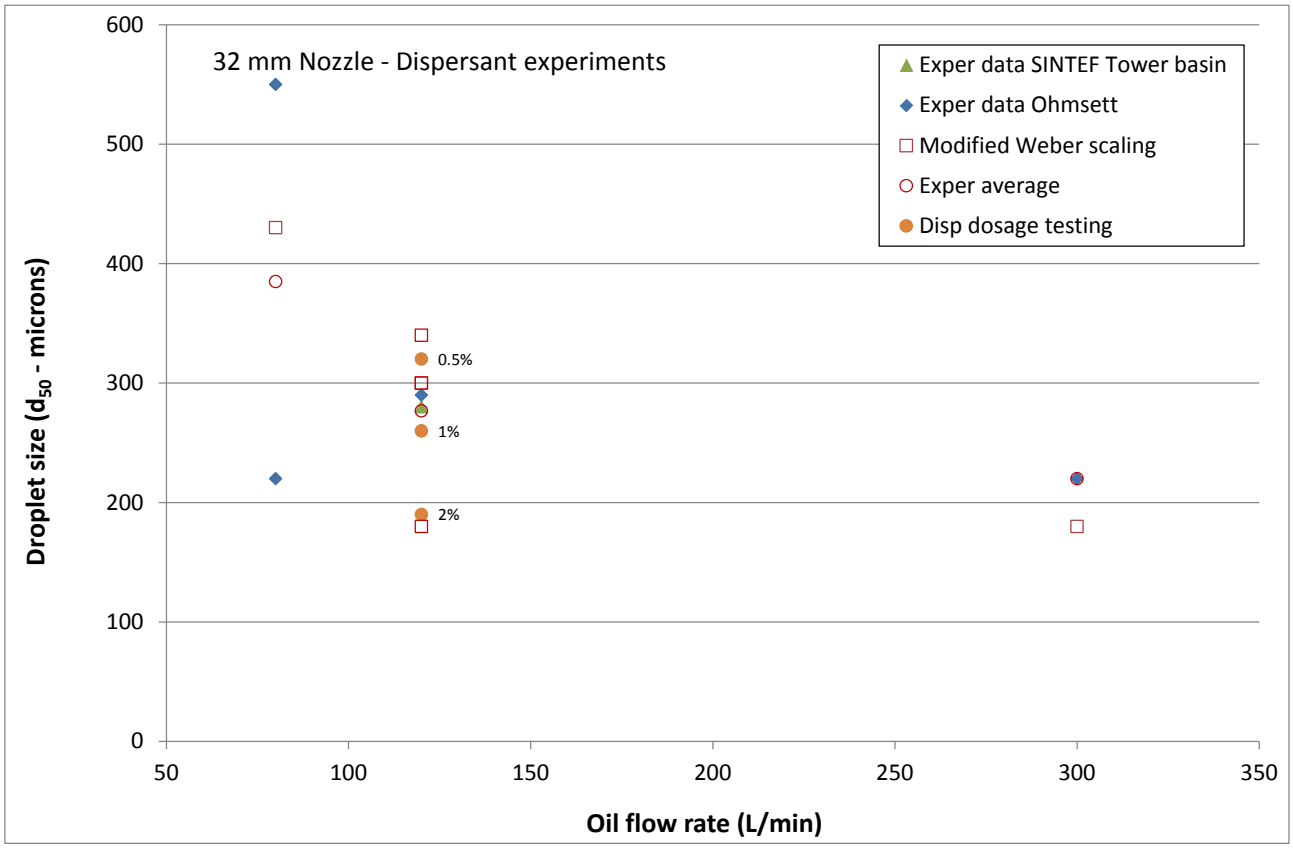

Figure 5.18: 32 mm Nozzle and dispersants: Droplet sizes (d_{50}) as a function of flow rates for all experiments (Ohmsett/Tower Basin). Dosage experiments (2, 1 and 0.5% dispersants) are also included. Predicted values (Modified Weber scaling- open squares) and average values for experimental data (open circles) are also included in the figure.

Table 5.6: 50 mm nozzle dispersant experiments (all 1%): Droplet sizes from all experiments at both SINTEF Tower Basin and Ohmsett. Colour coding indicate quality of results (red is unacceptable, yellow is acceptable and green is excellent).

50 mm Nozzle - Dispersant experiments

Low		Medium		High	
200 L/min		300 L/min		400 L/min	
Exp#	d_{50}	Exp#	d_{50}	Exp#	d_{50}
3	680	3	240		
				5	230
		7	230	7	230
9	210	9	230	9	240
		1	320		

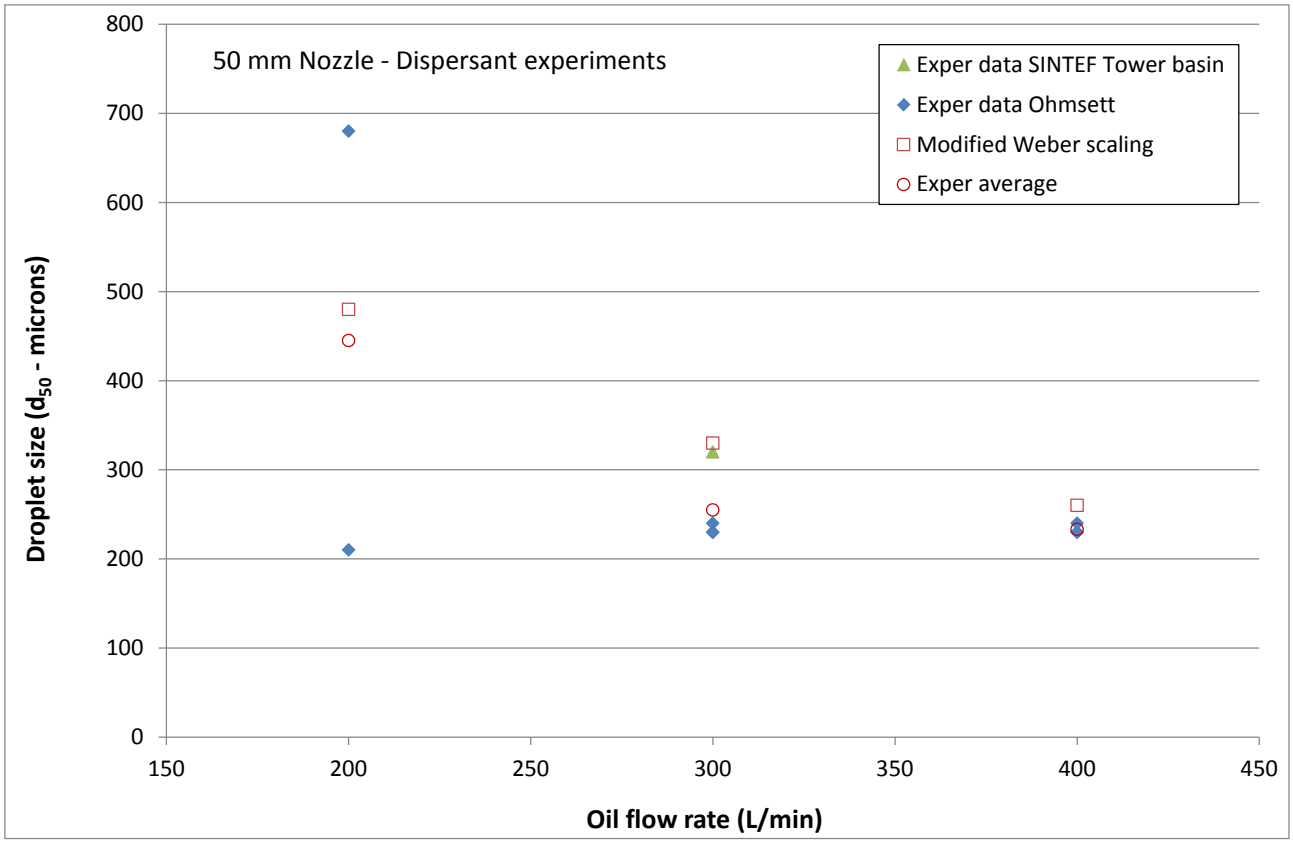

Figure 5.19: 50 mm Nozzle and dispersants: Droplet sizes (d_{50}) as a function of flow rates for all experiments (Ohmsett/Tower Basin). Dosage experiments (2, 1 and 0.5% dispersants) are also included. Predicted values (Modified Weber scaling- open squares) and average values for experimental data (open circles) are also included in the figure.

5.4 Experimental versus predicted values (modified Weber scaling)

One of the main objectives of this study is to generate droplet size data from up-scaled releases to improve or verify existing models for predicting initial droplet size distribution from subsea releases.

Modified Weber scaling (Johansen et al., 2013) is one of the alternatives for predicting initial droplet sizes from subsea releases. Measured droplet sizes (d_{50}/D) for the experiments performed in this study are plotted against the predicted values using modified Weber scaling. The experimental data are presented in Table C.1. Figure 5.20 shows the comparison of measured versus modified Weber number predicted droplet sizes for treated and untreated oil. Figure 5.21 shows these data identified by oil flow rate. Figure 5.22 shows the comparisons by treated and untreated cases for the data collected in this study along with data collected in the smaller scale tests conducted at SINTEF.

Only data of sufficient quality (**Green** or **Yellow** coding, see chapter 5.3, or Table C.1 are included in Figure 5.20 and Figure 5.21.

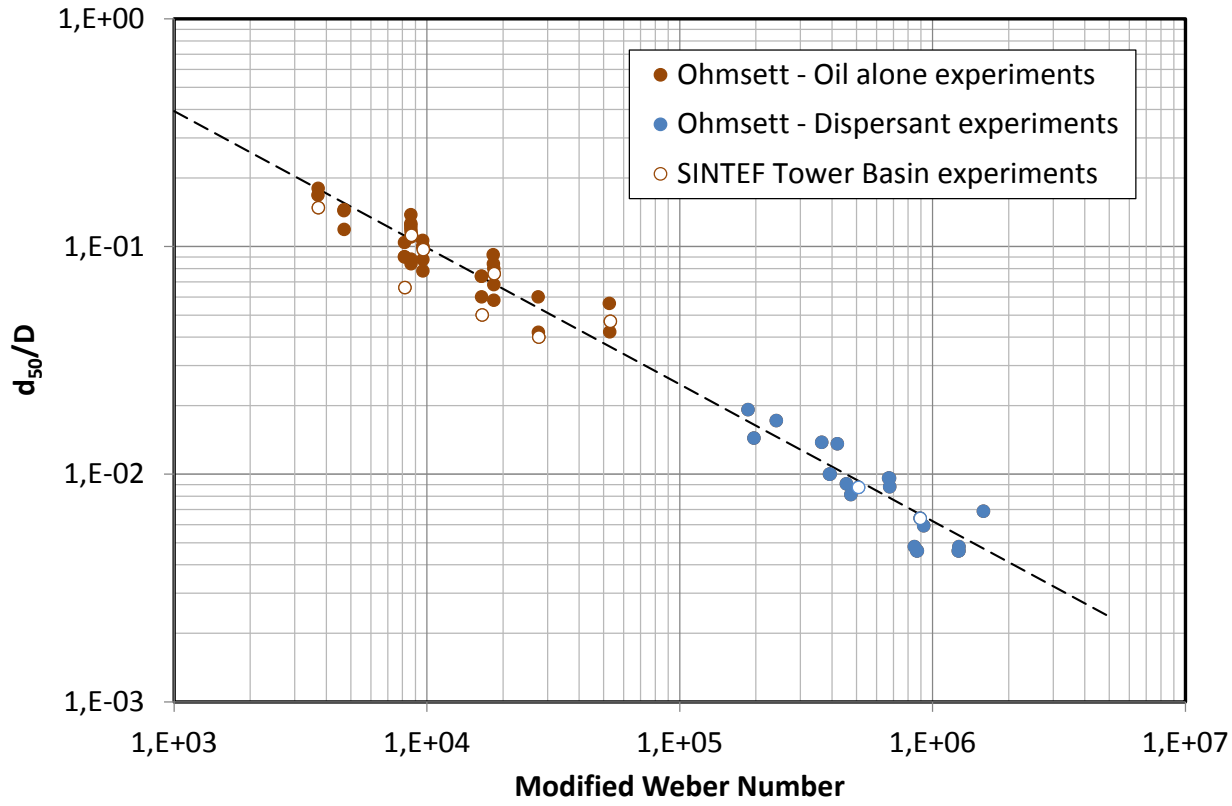

Figure 5.20: d_{50} from SINTEF Tower Basin experiments (open circles) and from Ohmsett (closed circles) plotted against the modified Weber number. Results with no treatment (brown markers) and with dispersants (blue markers). The dashed line represents the predicted line with coefficients A = 25 and B = 0.08, from the API D3 Phase-I report (Brandvik et al., 2014). Experimental data are presented in Table C.1

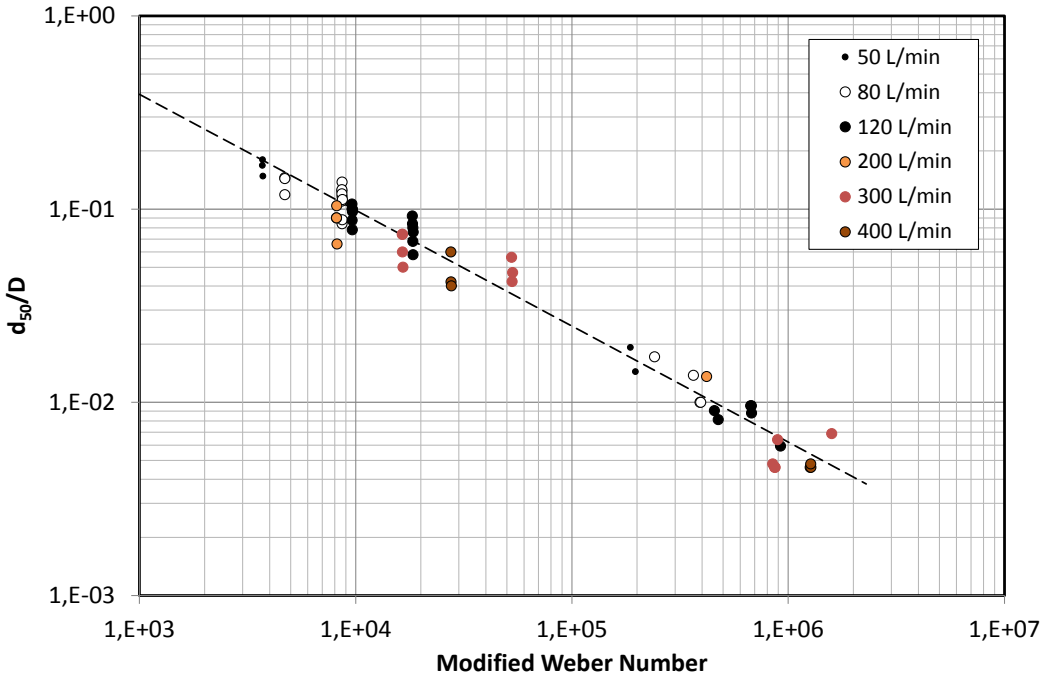

Figure 5.21: d_{50} from experimental data (Tower Basin & Ohmsett) plotted against the modified Weber number. Results are sorted after oil flow rate. The dashed line represents the predicted line with coefficients A = 25 and B = 0.08, from the API D3 Phase-I report (Brandvik et al., 2014).

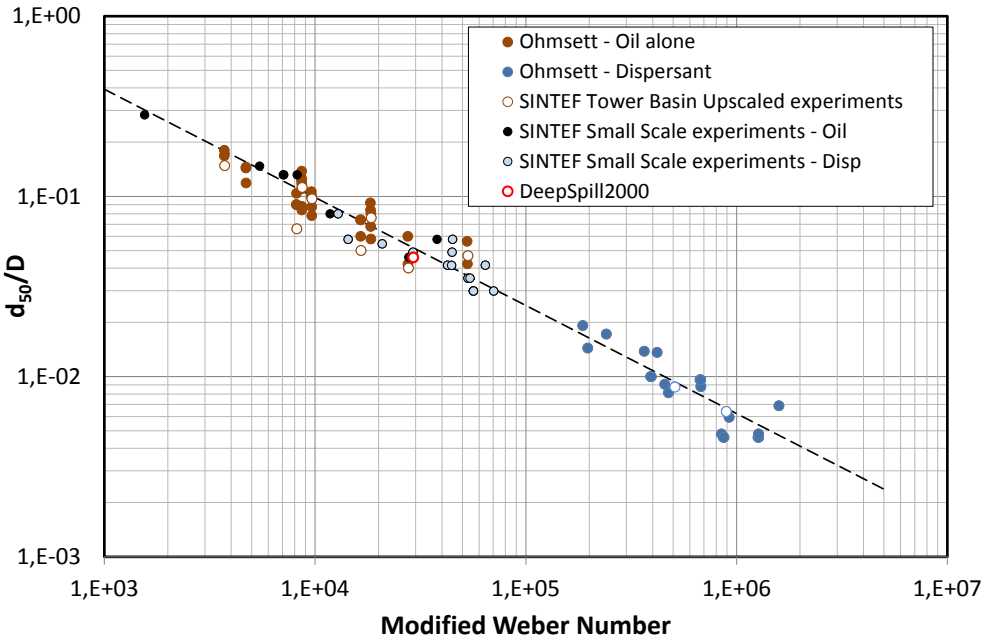

Figure 5.22: d_{50} from both large scale experiments (Tower Basin & Ohmsett), DeepSpil2000 and earlier small-scale experiments at SINTEF plotted against the modified Weber number. The dashed line represents the predicted line with coefficients A = 25 and B = 0.08, from the API D3 Phase-I report (Brandvik et al., 2014).

6 Discussions

The main objectives with this study have been to: Generate a dataset that can fill the gap between earlier laboratory experiments (1-8 mm nozzle) and the 2000 DeepSpill field experiment (120 mm nozzle) and use this data to improve or verify modified Weber scaling for predicting initial droplet formation for subsea releases.

However, to fulfil the main objectives listed above, the following objectives had to be met:

1. Identify suitable experimental facilities and develop experimental laboratory protocols to perform large scale subsea releases.
2. Predict plume behaviour for a wide range of release conditions and position instrumentation correctly in the plume.
3. Quantify oil droplets over a wide size range (50 – 12 000 microns) from experimental subsea releases.

The following sections discuss the individual topics listed above.

6.1 Generate data for improving and verifying modified Weber scaling

The classical approach to describe droplet splitting in stationary turbulence is to use Weber scaling to predict a maximum stable droplet size (Hinze, 1955). Based on BP funded experiments performed in the SINTEF Tower Basin in 2011-12 a modified Weber scaling was suggested (Johansen et al., 2013). The main advantage with the new approach is that it also includes contributions from;

1. Additional oil properties (includes oil viscosity)
2. Turbulence created by the buoyancy flux and
3. The gas void fraction

The obtained experimental data are compared with predicted values using the modified Weber scaling. The algorithm is used to predict d_{50}. The constants used (A & B) are described in the API Phase-I report (Brandvik et al., 2014).

Comparison of experimental and predicted data is presented in several figures in this report:

1. In the distributions for each nozzle size (25, 32 and 50 mm), for example Figure 5.8, are the predicted values (d_{50}) for each flow rate given as a table embedded in the figures.
2. For each nozzle size (25, 32 and 50 mm) all the acceptable replicates are plotted together with the predicted droplet sizes (d_{50}) as a function of flow rate, for example Figure 5.14. These figures illustrate the experimental uncertainty compared to the predicted values.
3. All the acceptable data generated in this study (green & yellow) are compiled and compared with predicted values in a common figure (Figure 5.20). Data from earlier small-scale studies at SINTEF for BP (Brandvik et al., 2013) and API D3 Phase-I and II (Brandvik et al., 2014 and Brandvik et al., 2015) are included in Figure 5.21 and Figure 5.22. Deviation from the expected predicted values are observed in some experiments with very large droplets, probably due too narrow measuring opening in the SilCams (Tower Basin experiments), see figure D1 (Appendix D). Deviations are also seen for the small dispersed droplets from the experiments with high flow rates where the droplets are quantified as smaller than predicted. This is probably due to the SilCam image processing algorithm which could reject large droplets due to higher probability of overlapping droplets.

Large droplets could also be lost due to plume fractionation, especially for the experiments with untreated oils and low flow rates (largest droplets).

The new experimental data generated in this study represent larger and more realistic oil droplet sizes than earlier experiments performed for API (Brandvik et al., 2014 and Brandvik et al., 2015). This was achieved by using larger nozzles and lower release velocities (2-5 m/s), than in the earlier experiments (5-20 m/s). These low velocities are more in line with real cases like Macondo (0.5 – 1 m/s).

The oil droplet sizes (d_{50}) from these experiments vary over a large range, from 1.2 mm (32 mm & 300 L/min) to 5.8 mm (50 mm & 200 L/min) for the untreated oils and in the 0.2 – 0.4 mm range for oil treated with dispersant (1%). These droplet sizes correspond well with predictions from modified Weber scaling and the earlier DeepSpill experiment in 2000 (see Figure 5.22). This finding contradicts the small oil droplets (0.05 – 0.150 mm) reported from modelling of from deep water releases by other authors (Paris et al., 2012 and Amman et al., 2015). However, the larger oil droplet sizes reported in this study corresponds well with predictions reported by Adams et al., 2013, Zhao et al., 2015 and Testa et al., 2016.

Predictions using modified Weber scaling are also verified at high pressure and with combined releases (live oil & natural gas) by experimental studies in hyperbaric chambers with pressure corresponding to 1750 meters depth (Brandvik et al., 2016 and Brandvik et al., 2017a)

6.2 Experimental facilities and protocols for up-scaled releases

Both the Ohmsett facility and the SINTEF Tower Basin have qualities which have been utilized in this up-scaling study. Ohmsett has a large water volume and physical dimensions (20 m x 200 m) which are very favourable for up-scaled experiments. However, the limited water depth (2.4 m) is a challenge. The SINTEF Tower Basin on the other hand, has a larger water depth (6 meter), but the limited water volume restricts both the duration and the number of parameters (e.g. nozzle size & flow rates) that can be explored per experiment or per day.

The experiments in the Tower Basin were used to test new and novel release arrangements (large nozzles, flow rates and realistic dispersant injection). All pumps, flow meters and pump controllers were tested and calibrated. Four new SilCams were also constructed and their main components and settings were varied to give optimum performance. The equipment built and used at SINTEF was shipped to the U.S. and used during the testing at Ohmsett.

The acquired data showed that the gap between the LED light source and camera (see Figure D1 in Appendix D) is critical and should be significantly larger than the largest droplets to be quantified to avoid discrimination of large droplets.

Possible discrimination of large droplets might be seen in Figure 5.2 (25 mm nozzle) and Figure 5.3 (32 mm nozzle) from the Tower Basin experiments, where the largest droplets, created by the lowest flow rates, are not very well described. For the 32 mm nozzle experiments the highest flow rates produce droplets as expected (modified Weber), while the measured droplets for the smallest flow rates (d_{50} = 3600 µm) are smaller than expected (d_{50} =5000 µm). This is not seen for the similar Ohmsett experiment, where the measured droplets for the 32 mm nozzle (Figure 5.10)

correspond well with prediction by modified Weber. A possible explanation for this could be the wider gap or path in the SilCams during the Ohmsett experiments (12 mm, Table 4.7), compared to the Tower Basin (10 mm, Table 4.2).

6.3 Plume behaviour and positioning of instruments

A standalone version of the near field model used in SINTEFs OSCAR model (DeepBlow or Plume 3D) was used to position the SilCam instruments in the plume (Figure 3.5 and Figure 3.2). The objective was to position one SilCam in the middle and one in the (upper) edge of the plume. The Silcam with the medium resolution was always the upper instrument, while the low resolution version was used as the lower instrument. In most cases one or both SilCams were in the plume for a sufficient length of time to generate representative data. In most cases a stable distribution was measured and quantified over a period of 30 seconds or more.

However, in some cases the instrumentation were not positioned along the centreline of the plume. The plume height could (in theory) be adjusting during the experiment by changing the towing speed. However, with short experimental time (60-90 seconds), difficulties in visually observing the plume position in the basin and two simultaneous releases, the towing speed was kept constant. Only in a few cases, where the plume surfaced before the instrumentations, the towing speed was increased to reduce the plume height in the basin.

6.4 Quantification of droplet sizes from different nozzle sizes and release rates

A limited number of experiments were done in the Tower Basin covering the three nozzle sizes and all flow rates (see Figure 5.2, Figure 5.4 and Figure 5.6). Selected images are provided from tests using each of the three nozzles for oil alone and with dispersant injection (see Figure 5.1, Figure 5.3 and Figure 5.5). However, these examples are only single images and cannot fully represent the difference in droplet sizes between the experiments. The droplet size distributions are usually based on images from a 30 second period (450 images) which represents 5 000 – 30 000 quantified droplets for untreated oil and from 300 000 to over a million of quantified droplets for treated oil. With the exception of possible discrimination of large droplets during the initial experiments in the Tower Basin, as discussed above, droplets were quantified and representative distributions were obtained for all experiments. The droplet size distributions for each flow rate & nozzle size show generally a good fit to a lognormal distribution (see examples in Figure 5.13). A possible improved fit to the skewed Rosin Rambler (RR) can be seen for experiments with the largest droplets (lowest flow rates), where the largest bins represent very large and unstable droplets. The low stability of the droplets in the 10-12 mm range could distort the upper tail of the distribution. We are also approaching the upper size range for the configuration of the SilCams used during these experiments (see Table 4.7).

Several replicate experiments were performed for each combination of nozzle size and flow rate. For the 25 mm nozzle, 3 to 9 replicates were performed for the oil alone experiments and 3 to 4 replicates for the treated oil experiments (see Table 5.1 and Figure 5.14). For the two larger nozzle sizes the numbers of replicates are;

- 32 mm: 3 to 6 (untreated) and 1 to 2 (dispersant)
- 50 mm: 4 to 6 (untreated) and 2 to 4 (dispersant)

The data quality of these replicates is evaluated based on several factors (see page 46, Section 5.3) and given a colour code; green, yellow and red (excellent, acceptable and not acceptable). The data quality is generally very good and most of the data are classified as green or yellow, and less than 20% are classified as "Not acceptable".

7 Conclusions

Conclusions based on the analysis of the presented data are summarised in the following list:

1. The large-scale experimental data generated in this study show a very high correlation with predicted values (d_{50}) from the modified Weber scaling algorithm.
2. This study represents a major leap forward in generating experimental data for models predicting initial droplet sizes from subsea oil & gas release and the effectiveness of subsea dispersant injection.
3. The generated data are produced at more realistic release conditions (e.g. low release velocities) and the droplet sizes produced for both treated oils (d_{50} of 200-400 µm) and for untreated oils (d_{50} of 1200 - 6000 µm) are representative for realistic droplet sizes for a deep water oil release.
4. The experiments show that SSDI will reduce the droplet size by an order of magnitude using a dispersant dosage of 1%. Since the untreated droplets formed in these experiments were similar in size to those expected in a real-world blowout like Macondo, the Study results strongly suggest that SSDI would provide similar performance in the real world.
5. This new large-scale data set fills in the gap between the earlier SINTEF studies in the Tower Basin and Mini Tower and the DeepSpill field release in 2000, both with respect to release diameters, oil flow rates and droplet sizes. The data set is also unique with respect to its high number of replicate measurements (3 – 4 replicates for most settings).
6. The large oil droplets formed under these more realistic release conditions, the good fit with the DeepSpill2000 field experiment and the high correlation with modified Weber scaling contradicts the very small oil droplet sizes reported from deep water releases by other authors (Paris et al., 2012 and Amman et al., 2015). However, other scientists report droplet sizes that correspond well with those reported in this study (Adams et al., 2013, Zhao et al., 2015 and Testa et al., 2016).
7. A new and unique concept for large-scale laboratory subsea releases has been developed and tested (towed nozzles, dispersant injection systems and oil flow monitoring)
8. New and novel sensors for quantifying oil droplets over a wide size range (20 – 12 000 microns) have been developed and verified (SINTEF Silhouette camera). The instrument exists in several versions (concentration & particle size ranges), also a high pressure version operating down to 2000 meters depth.
9. Modified Weber scaling has also been verified to accurately predict droplet sizes of combined releases of live oil & natural gas at deep water pressures (Brandvik et al., 2015 and Brandvik et al., 2017a).

8 Recommendations and further work

The following recommendations are given based on the conclusions from this study:

1. Data from even larger scaled experiments would be useful to further improve and document the scalability of prediction from models like the modified Weber scaling. This should be performed as controlled scientific field trials with release of both oil & gas using SSDI, similar to the DeepSpill experiment in 2000.
2. The new dataset from this study should also be used to calibrate, verify and further develop other models for predicting oil droplet sizes for subsea releases of oil & gas.
3. This study focused on releases of oil alone, similar experiments including combined releases of oil & gas are needed to study the influence of varying gas void fractions. Such studies have been performed at smaller scales (0.5 – 3 mm nozzles), but large-scale experiments at Ohmsett (25 – 50 mm nozzles), also including gas will generate valuable additional data.
4. Reliable estimates of how oil-water interfacial tension (IFT) is reduced by dispersant injection are important for modelling oil droplet sizes. The existing approach is to measure IFT on samples taken during basin or field experiment. IFT is measured with the spinning drop method after the oil droplets rise and form a surface layer. This may take more than 24 hours for the smallest droplets. This approach has several disadvantages, for example possible surfactant leakage out of the oil phase. Developing methods for measuring IFT in-situ during experiments or directly in the field (based on droplet geometry and oil properties) are needed to obtain more relevant IFT data. Such data will improve our understanding of the relationship between dispersant dosage, reduction in IFT and oil droplet sizes.

In such future studies it will be crucial to use sensor technology that can distinguish between gas bubbles, oil droplets and plankton/sediment particles (50 – 12 000 µm range) and quantify them individually. This is possible with the new SINTEF SilCam technology.

9 Acknowledgement

Without the dedicated crew from MAR, led by Senior Test Engineer Allan Guarino, it wouldn't be possible to perform the high number of challenging experiments on the limited time available. The authors want to express their thanks to their creativity, dedication and willingness to work long hours when needed.

10 Literature

SINTEF API D3 JITF Subsea dispersant effectiveness reports

Finals versions are also available from API's web pages:
(http://www.oilspillprevention.org/oil-spill-research-and-development-cente)

Phase I: Brandvik, P.J., Johansen, Ø., Farooq, U., Angell G., and Leirvik, F. 2014: Sub-surface oil releases – Experimental study of droplet distributions and different dispersant injection techniques – version 2. A scaled experimental approach using the SINTEF Tower basin. SINTEF report no: A26122 (Unrestricted) Trondheim Norway 2014. ISBN: 9788214057393.

Phase-II: Brandvik, P.J., Johansen, Ø., Farooq, U., Davies E., Krause D. and Leirvik, F. 2015: Sub-surface oil releases – Subsurface oil releases – Experimental study of droplet size distributions Phase-II. A scaled experimental approach using the SINTEF Tower basin. SINTEF report no: A26866 (Unrestricted) Trondheim Norway 2015. ISBN: 9788214058406.

Phase-III: Brandvik, P.J., Emlyn Davies, Chris Storey, Cole Bradly and Frode Leirvik. 2016: Subsurface oil releases. Verification of dispersant effectiveness under high pressure - A scaled experimental approach using the SINTEF Tower Basin and SwRIs 90" high pressure chamber. SINTEF report no: A27469. Trondheim Norway 2016. ISBN: 978-821405857-4.

Phase IV: Davis J.E., Brandvik, P.J., Øistein Johansen, Ike Nagamine, Dorien Dunnebier, Stephen Masutani, Frode Leirvik, 2017: Fate of subsea dispersed oil droplets. An experimental study combining the SINTEF MiniTower and Univ. of Hawaii's inverted cone system. Phase-IV Report. SINTEF report - In preparation.

Phase V: Brandvik, P.J., Emlyn Davies, Chris Storey and Frode Leirvik. 2017a: Subsurface oil releases – Verification of dispersant effectiveness under high pressure with Live oil and combined with natural gas. Phase-V report. SINTEF report – In preparation.

Phase VI: Brandvik, P.J., Johansen, Ø., Davies, E. Leirvik, F., and Belore, R.. 2017b: Subsea Dispersant Injection – large-scale experiments to verify algorithms for initial droplet formation (modified Weber scaling). An approach using the Ohmsett facility, NJ, USA and SINTEF Tower Basin in Norway. Phase-VI report. SINTEF report no: OC2017 A-087 (Unrestricted) Trondheim Norway 2017. ISBN: 978-82-7174-280-5.

Other references used in this report:

Adams, E. E.; Socolofsky, S. A.; Boufadel, M. 2013. Comment on “Evolution of the Macondo Well Blowout: Simulating the Effects of the Circulation and Synthetic Dispersants on the Subsea Oil Transport. Environ. Sci. Technol. 2013.

Aman, Zachary M., Paris, Claire B., May, Eric F., Johns, Michael L., & Lindo-Atichati, Davidi, High-pressure visual experimental studies of oil-in-water dispersion droplet size, Chemical Engineering Science, Volume 127, 4 May 2015, pp. 392–400.

Agrawal, Y.C., Pottsmith, H.C., 2000. Instruments for particle size and settling velocity observations in sediment transport. Marine Geology 168, 89-114.

Andrews, S., Nover, D., Schladow, S.G., 2010. Using laser diffraction data to obtain accurate particle size distributions: the role of particle composition. Limnology and Oceanography: Methods 8.

Belore, R., 2014. Subsea Chemical Dispersant Research. In proceedings of the 37th AMOP Technical Seminar on Environmental Contamination and Response. Pp. 618-650 Canmore, Alberta.

Brandvik, P.J., Johansen, Ø., Leirvik,F., Farooq, U., and Daling, P.S. 2013. Droplet breakup in sub-surface oil releases – Part 1: Experimental study of droplet breakup and effectiveness of dispersant injection. Mar. Pollut. Bull. 2013 Volume 73, Issue 1, 15 2013, pp. 319-326.

Brandvik et al., 2017c: Subsea injection of dispersants, effectiveness of different dispersant injection techniques – An experimental approach (In preparation).

Brandvik et al., 2017d: Subsea Dispersant Injection (SSDI) effectiveness as a function of dispersant dosage, dispersant type and oil properties - an down-scaled laboratory approach (In preparation).

Chen, F. and Yapa P.D., 2007. Estimating the oil droplet size distribution in deepwater oil spills. Journal of Hydraulic Engineering, February 2007, 197-206.

Daling, P.S., Leirvik, F., Reed, M., Almås, I.K., P.J. Brandvik, B.H. Hansen, A. Lewis, M. Reed. 2014: "Surface Weathering and Dispersibility of Macondo MC252 Crude Oil. Mar. Pollut. Bull. 2014. Volume 87, Issues 1–2, pp. 300–310.

Davies, E.J., Nimmo-Smith, W.A.M., Agrawal, Y.C., Souza, A.J., 2011, Scattering signatures of suspended particles: an integrated system for combining digital holography and laser diffraction, Optics Express, 19, 25488-25499.

Davies, E.J., Nimmo-Smith, W.A.M., Agrawal, Y.C., Souza, A.J., 2012, LISST-100 response to large particles, Marine Geology, 307-310.

Davies, Brandvik and Leirvik 2017: The use of spectral transmittance imaging to size and classify suspended particulate matter in seawater. Mar. Pollut. Bull. 2017, vol. 115 Issue 1-2 pp. 402 - 410.

Graham, G., Nimmo-Smith, W.A.M., 2010. The application of holography to the analysis of size and settling velocity of suspended cohesive sediments. Limnology and Oceanography: Methods 8, 1-15.

Hinze, J.O., 1955: Fundamentals of the hydrodynamic mechanism of splitting in dispersion processes. A.I.Ch.E. Journal, Vol. 1, pp. 289-295

Johansen, Ø., 2003. Development and verification of deep-water blowout models. Marine Pollution Bulletin, 47, 360-368.

Johansen, Ø., Rye H. and Cooper C., 2003. Deep Spill – Field Study of a simulated oil and gas blow-out in deep water. Spill Science & technology Bulletin, 8, 433-443.

Johansen, Ø., Brandvik, P.J., and Farooq, U. 2013. Droplet breakup in sub-surface oil releases – Part 2: Predictions of droplet size distributions with and without injection of chemical dispersants. Mar. Pollut. Bull. 2013 Volume 73, Issue 1, 15 2013, pp. 327-335.

Mikkelsen, O.A., Hill, P.S., Milligan, T.G., Chant, R.J., 2005. In situ particle size distributions and volume concentrations from a LISST-100 laser particle sizer and a digital floc camera. Continental Shelf Research 25, 1959-1978.

Owen, R.B., Zozulya, A.A., 2000. In-line digital holographic sensor for monitoring and characterising marine particles. Optical Engineering 39, 2187-2197.

Paris, C.B., le Henaff, M., Aman, Z.M., Subramaniam, A., Helgers, J.,Wang, D.P., Kourafalou, V.H., Srinivasan, A., 2012. Evolution of the Macondo well blowout: Simulating the effects of the circulation and synthetic dispersants on the subsea oil transport. Environ. Sci. Technol. 46, 13293–13302.

Reynolds, R.A., Stramski, D., Wright, V.M., Wozniak, S.B., 2010. Measurements and characterization of particle size distributions in coastal waters. Journal of Geophysical Research 115.

Rye, H., Brandvik, P.J., and Reed, M. 1996. Subsurface oil release field experiment – Observations and modelling of subsurface plume behavior. In Proceedings of the 19th AMOP Technical Seminar, Environment Canada, Ottawa, Ontario, pp. 1417-1436.

Rye, H., Strøm, T., and Brandvik, P.J. 1997. Subsurface blowouts: Results from field experiments. Spill Science & Technology Bulletin, 4: pp. 239-256.

Testa, J.M., Adams, E., North, E.W., He, R., 2016. Modeling the influence of deep water application of dispersants on the surface expression of oil: A sensitivity study. J. Geophys. Res. Ocean. 121, 5995–6008.

Thorne, P.D., Agrawal, Y.C., Cacchione, D.A., 2007. A comparison of Near-Bed Acoustic Backscatter and Laser Diffraction Measurements of Suspended Sediments. IEEE Journal of Oceanic Engineering 32.

Thorne, P.D., Hanes, D.M., 2002. A review of acoustic measurement of small-scale sediment processes. Continental Shelf Research 22, 603-632.

Zhao, L., Boufadel M.C., Adams E., Socolofsky S.A., King K., Lee K., Nedwed T. 2015: Simulation of scenarios of oil droplet formation from the Deepwater Horizon blowout. Mar. Pollut. Bull. (2015),

A Description of SINTEF Tower Basin

A.1 Basic facilities

The basic parts of the SINTEF Tower Basin were constructed and built in 2005 as a part of SINTEFs research activity within deep water releases. This was a follow-up activity of the DeepSpill field experiment in 2000. This basic infrastructure was financed by STATOIL ASA. Due to reduced focus on deep water releases and since our main ice basin at SeaLab was heavily booked for other project, the Tower Basin was not mounted and tested until January 2011. The ice basin without the Tower Basin and the mounted Tower Basin during the first filling are seen in Figure A.1.A drawing showing the scaffolding/railing around the Tower Basin together with the ventilated hood and oil collecting system is shown in Figure A.2. The main components of the basin before the first experiment in March 2012 are shown in Figure A.3 and the principles of the experimental set-up for the Tower Basin are shown in Figure A.4.

The main specifications of the Tower Basin are:

1. The tank is 6 meters high, 3 meters wide and holds 40 m^3 of natural sea water.
2. The sea water is rinsed through high capacity sand filters and holds a stable and high purity.
3. All release rates of oil and gas are remotely controlled and both set points and real values are logged on a central control system.
4. The tank has three remotely operated and programmable instrument platforms. The positions of these are logged during operation (depth and axial position).
5. To insure proper HSE working conditions a scaffolding/railing around the tower and a staircase to reach the top section is installed for inspection and sampling
6. A ventilated hood prevents light hydrocarbons to enter the laboratory hall. It is not necessary for the operators to wear any breathing protection.
7. A overflow system to skim off surfacing oil from the top of the tower ensure safe and efficient removal of surface oil.
8. A disposal system approved by the local environmental authorities is in place to take care of the surface oil and the large volume of oil containing water. Especially the chemical enhanced dispersion experiments will create very small droplets with very long settling times.

The principal overview of the experimental set-up (Figure A.4) shows the main features of the Tower Basin. Oil, gas and dispersants can be delivered over a wide range of flow rates and internal ratios. Both oil and gas are delivered through mass controllers and both the set points and the obtained values are logged during an experiment. We have two pressurized tanks (30 bar) for delivering the oil (25 and 100 Liters). The system is operated and monitored from a central computer through a program written in NI LabView©. A screen dump of the settings and obtained values for flow rate (oil) is also given in Figure A.4. The log of the actual values obtained during the experiments is important for further analysis of the data.

NB! *This is a general text describing the capabilities of SINTEF Basin Tower and MiniTower. The resources allocated to a specific project (type of equipment, sampling frequency etc.) are scope dependent and described in the experimental plan of each project.*

Figure A.1: Ice basin without propellers and other equipment used for circulation showing the fundament for the Tower Basin (left) and the initial mounting of the Tower Basin in January 2011 (right).

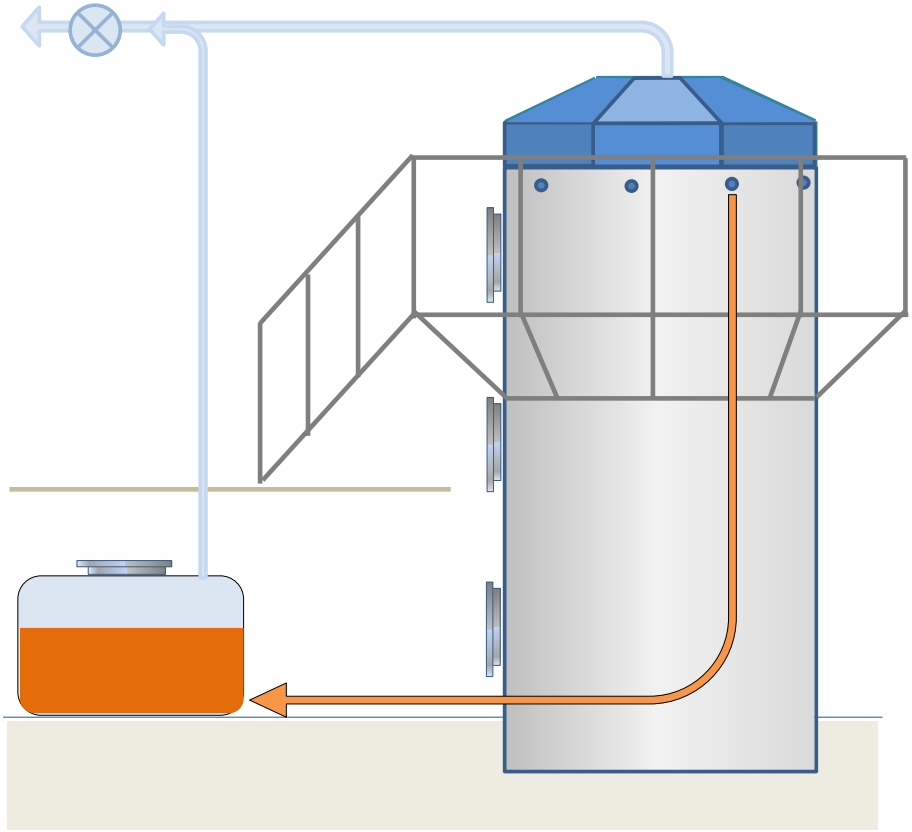

Figure A.2: Principles for the scaffolding/railing around the tower, ventilated hood and overflow system to collect surface oil from the top of the tower.

Figure A.3: The Tower Basin per March 2012 showing the scaffolding, staircase and the railings to ensure safe working conditions and the ventilated hood.

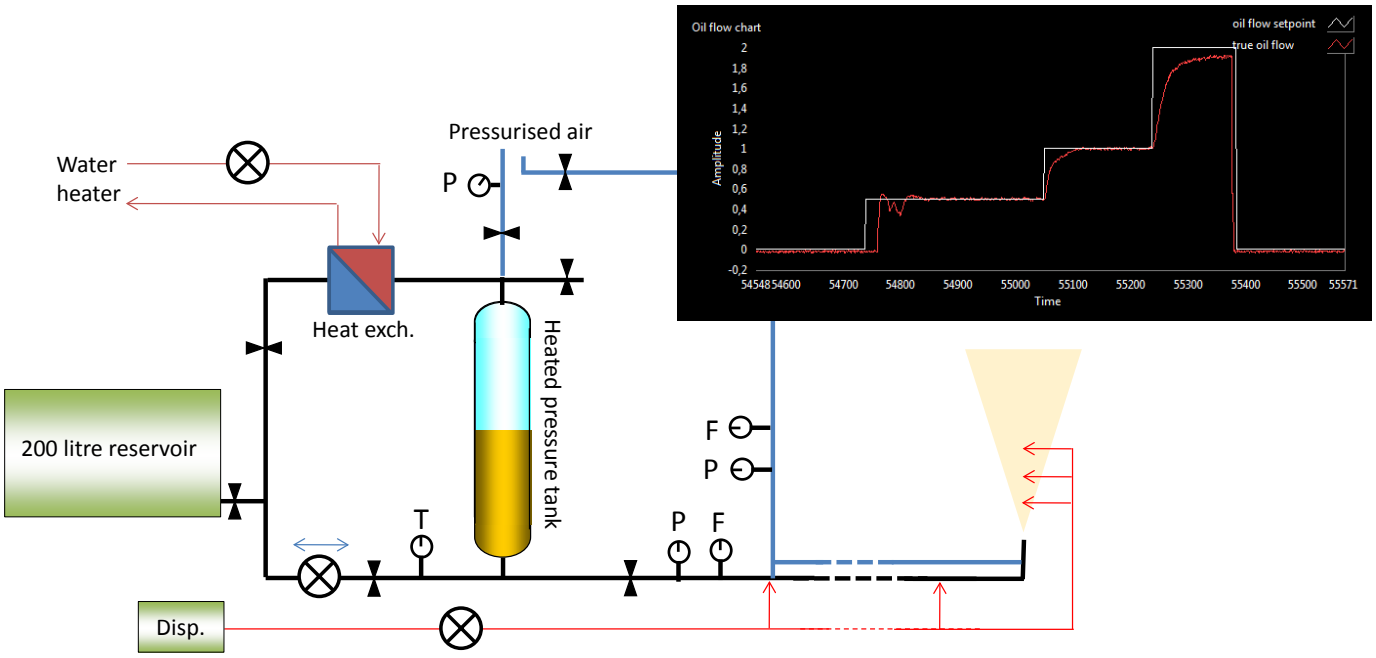

Figure A.4: Principle overview of the experimental set-up showing how oil, gas (air) and dispersant will be released during a Tower Basin experiments (P: Pressure gauge, F: Flow controller). An example of the set point for oil flow rate (L/min) and the obtained values are also given. This is a screen dump from the operator's computer during an experiment.

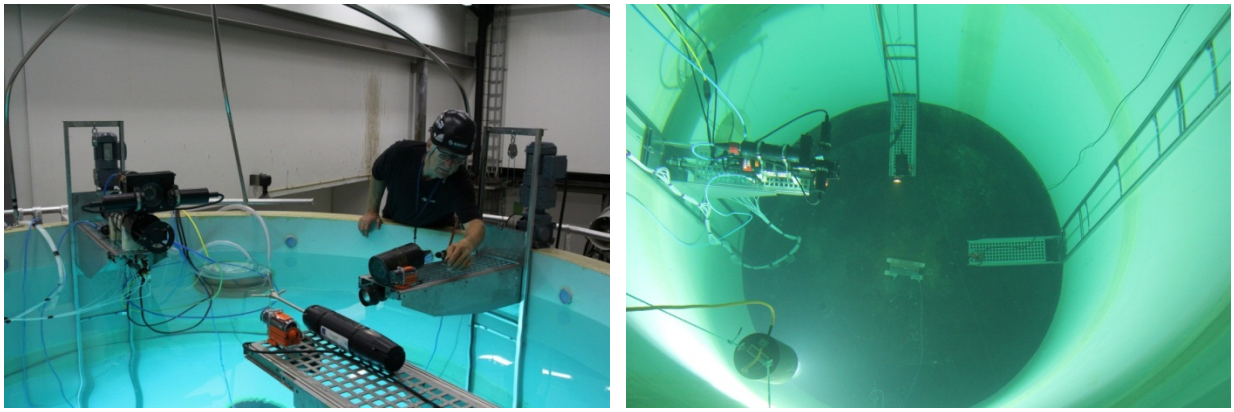

Figur A.5: Left: Adjustment of camera equipment and the Vitrino 3D current profiler with all three instrument platforms in surface position. Right: All three instrument platforms lowered into the tank and ready to initiate an experiment. The squared release platform can be seen in the middle on the bottom of the tank.

A.1.1 Monitoring during the experiments

This chapter contains the description of the different monitoring techniques used during the blow-out simulation experiments. The main monitoring is performed in the centre of the plume approximately 3 metres above the release point. A suit of instruments is mounted on a piston operated platform which is inserted into the plume. The platform is mounted on a slide on the inner wall of the basin and its vertical and radial position can be continuously adjusted, see Figure A.6. The instrument platform can continuously be lifted or lowered in the tank during an experiment to study variations in droplet size as a function of height. However, monitoring too close to the release could be difficult due to saturation of our instrumentation, especially the LISST instrument.

A.1.2 Droplet size distribution

Since documentation of oil droplet size distribution is central in many projects, three different approaches can be used to measure droplet size distribution of the rising oil droplets (see Figure A.6). How many and which methods used depends on the scope of the specific projects.

1. LIST 100X Particle size analyzer (2 - 500 µm)
2. In-situ macro camera with a green laser focusing plane (5 - 2500 µm)
3. External particle Visual Microscope, Mettler Toledo PVM V819 (5 -1200 µm)

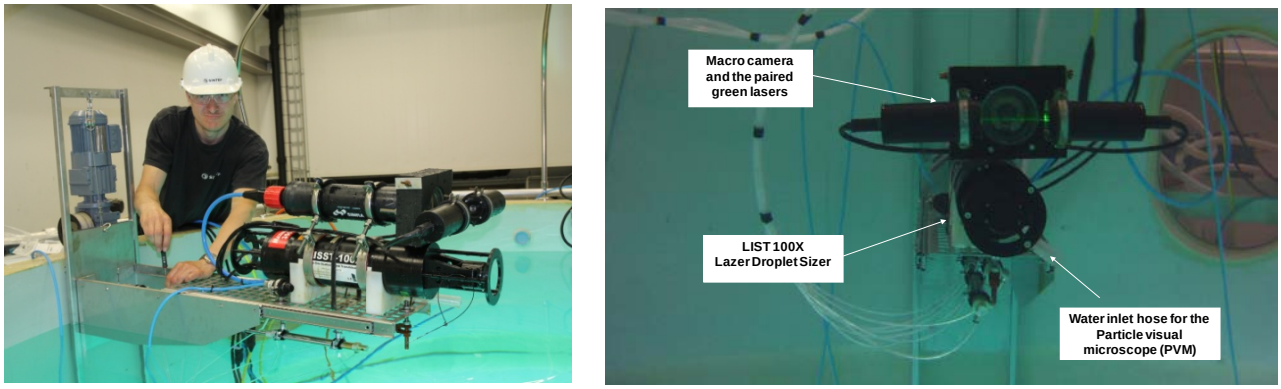

Figure A.6: The three systems for monitoring droplet size distribution shown during adjustment over the water surface and submerged.

The LISST-100X and the in-situ macro camera is operated inside the Tower Basin (Figure A.6) and can do measurement at different locations with respect to the oil plume. The external camera (PVM) is located outside the tank, but the water is collected from a hose located together with the LIST 100X (Figure A.6). Images from PVM and In-situ camera are used to generate droplet size distributions that are complementary to distributions from the LISST-100X, since they can detect larger droplets.

A.1.2.1 Water sampling

Water samples can be taken in the same position in the tank as droplets sizes are measured. The water is sampled through a short flexible hose located on the moving sampling platform. The water samples can be analysed for (dependent on the scope of the projects):

a. Oil content (Total hydrocarbons – THC)
b. Dispersant content (For dispersant experiments)

A.1.2.2 In-situ measurement of oil in water

The overflow hose (no pumping) used for water sampling above can also be used for monitoring of oil-in-water content (droplets and dissolved components). This is done by ultraviolet fluorescence (UVF) with an UviLux flow-through cell. The water flows through this cell before being sampled.

A.1.2.3 Oil sampling

The oil in the water samples taken from the plume can be analyzed for the following parameters:

a. Interfacial tension (when dispersants are applied).
b. Surfactant content (a part of the C9500 solvent package a glycol ether (DPnB) is used as reference, GC-MS analysis).

A.1.2.4 Video documentation

Several video cameras are used to control and document the operation of the Tower Basin during an experiment (operational cameras). These cameras are used to monitor the following locations:

a. The release nozzle
b. The use of injection tools for dispersant (wand, dispersant ring etc.)

The video footage from the operational cameras is stored as a part of the operational documentation, but is usually not used for further analysis.

The video recordings used for documenting and analysing the droplet sizes are taken by four HD cameras (1280 x 960 pixels) at four different adjustable heights over the release point (for example 0, 0.5, 1 and 1.5 meters). An example of such video is given in Figure A.7. Close-up or macro still or video cameras are also used to study details regarding injection of dispersants, turbulence around release nozzle etc. (Figure A.8).

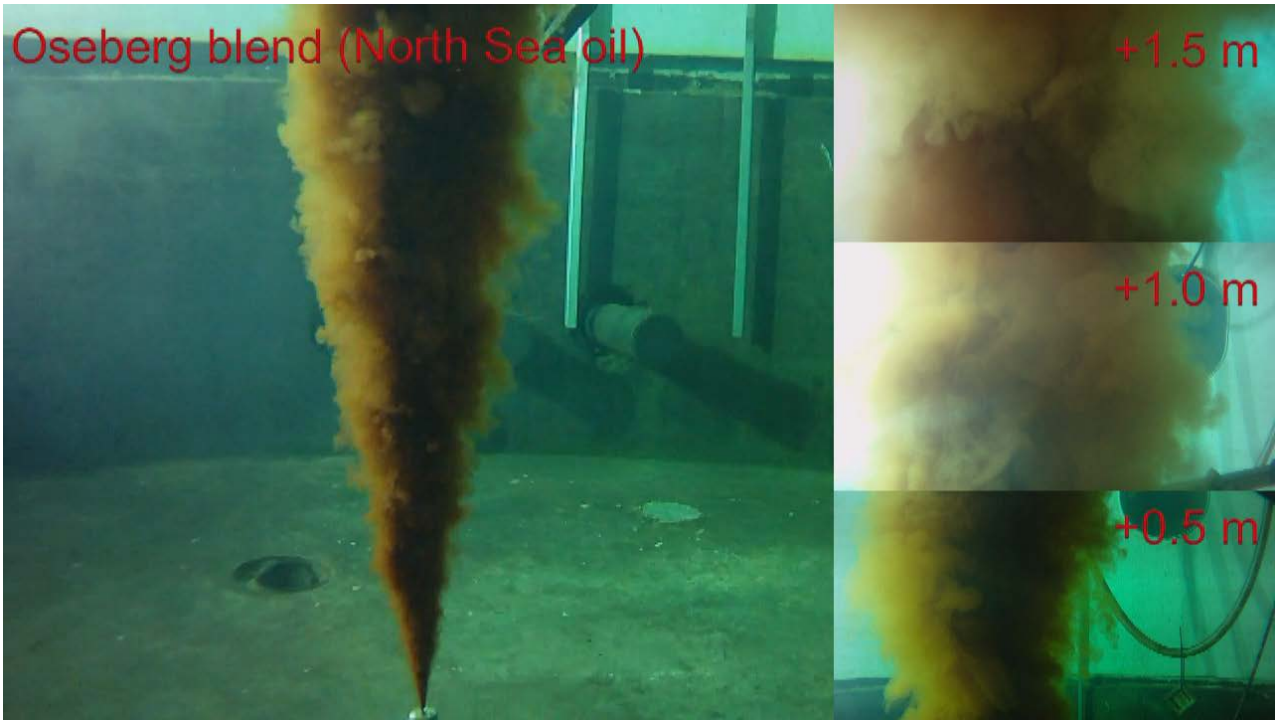

Figure A.7: An example of a composite video showing the four HD cameras covering the rising oil flume at 0.5 m intervals over the release point. This is from earlier experiments with a North Sea crude (Oseberg blend).

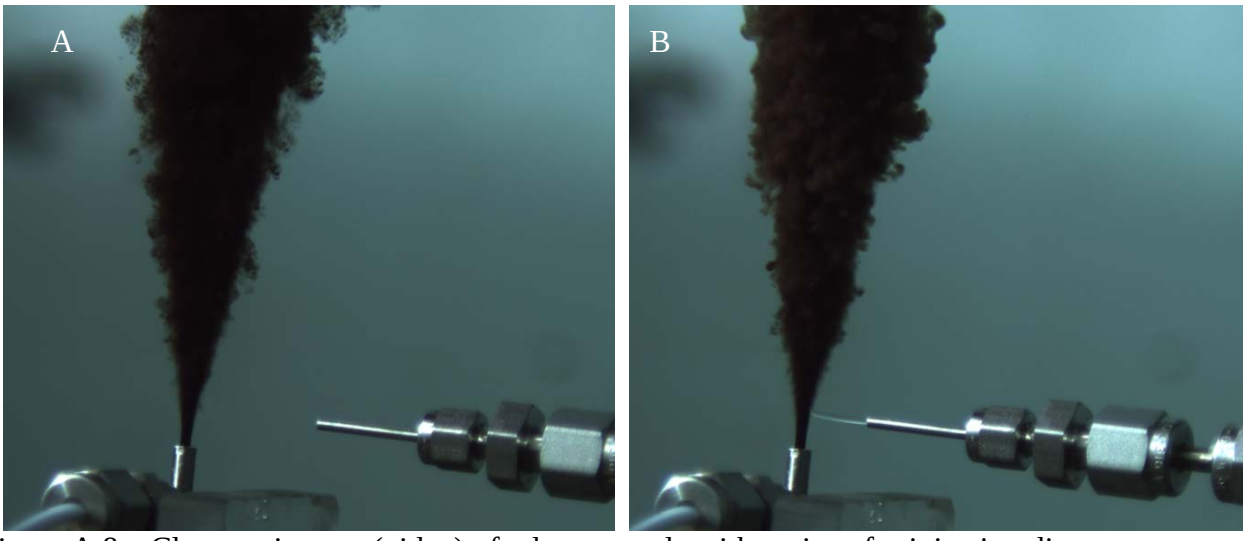

Figure A.8: Close-up images (video) of release nozzle with options for injection dispersant horizontally into the oil. A: Oil released alone, no dispersant, B: Dispersant injected.

A.1.3 General description of a Tower Basin experiment

This section gives a general description of a Tower Basin experiment. A more specific procedure for operating the Tower Basin is found in our internal operational procedures (Laboratory procedure no: 507). This procedure is a part of SINTEF general QA system for laboratory activities.

A short version of this procedure for a blow-out experiment in the Tower Basin is given below:

a. Test filling, release and control equipment.
b. Fill Tower Basin with sea water and check for leaks.
c. Check background values (particle/oil concentration, droplet size distribution, temperature).
d. Determine and program test conditions (oil type and rates of gas/oil).
e. Check and confirm status on monitoring equipment.
f. Prepare for experiment, perform background monitoring (approximately 3 meters above release nozzle)
g. Initiate experiment, start release of oil/gas/dispersant (dependent of experiment type)
h. Monitoring of oil/gas/dispersant plume (0.5 - 3 min)
    - Video cameras (4 cameras at three different heights)
    - Oil droplet size distribution (LISST-100X, particle visual microscope (PVM) and in-situ macro camera/lasers).
    - UVF monitoring of oil content/dissolved components
    - Water and oil sampling, dependant on type of experiment.
i. Stop release
j. Collection, initial quality control of monitoring data and storage of data.
k. Settling of oil droplets and removal/skimming of surface oil
l. Emptying/disposal of used water containing small oil droplet and dissolved oil components according to lab. Procedure.
m. Cleaning and control of equipment.

A typical Tower Basin experiment consist of two days of preparation (filling of water, filling of oil in the pressurized tank, testing of release and monitoring equipment etc.), one day for the actual experiment and two days for settling of oil droplets and cleaning of the tank and monitoring equipment, QA, storage and initial treatment of data, chemical analysis etc.

B Description of the Ohmsett facility

Ohmsett is the National Oil Spill Response Research & Renewable Energy Test Facility in U.S. and provides performance testing of full-scale oil spill response equipment and marine renewable energy systems (wave energy conversion devices), and helps improve technologies through research and development (see Figure B.1).

It is the largest outdoor saltwater wave/tow tank facility in North America and is the only facility where full-scale oil spill response equipment testing, research, and training can be conducted in a marine environment with oil under controlled environmental conditions (waves and oil types). With recent emphasis on developing renewable energy sources, Ohmsett's mission has expanded to offer a research and testing venue for wave energy conversion devices.

The facility, located an hour south of New York City, in Leonardo, New Jersey, is maintained and operated by the U.S. Department of Interior's Bureau of Safety and Environmental Enforcement (BSEE) through a contract with MAR, Incorporated of Rockville, Maryland.

During the three week testing on this project a crew from MAR, covering a broad range of crafts, was responsible for operating the facility. This MAR crew was led by Senior Test Engineer Allan Guarino, and their dedicated effort during the complete project period was a key factor to the success of this project.

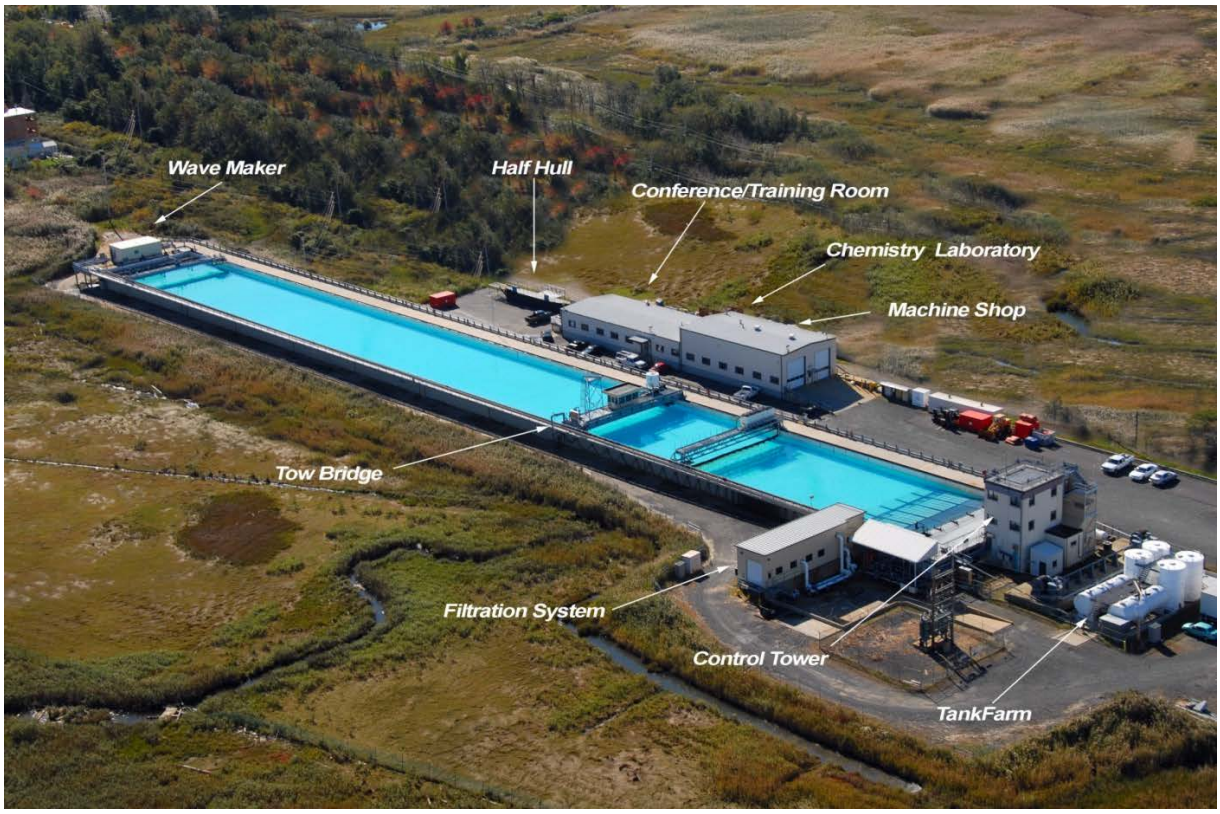

Figure B.1: Overview of the Ohmsett facility showing the main test basin and the surrounding facilities (Photo: Ohmsett).

The Ohmsett facility has the following general capabilities:

- A main towing bridge capable of towing test equipment at speeds up to 6.5 knots
- An auxiliary bridge oil recovery system to quantify skimmer recovery rates
- A wave generator capable of simulating regular waves up to one meter in height, as well as a simulated harbor chop, FM Slides with selectable: slue rates, start and stop
- Pierson-Moskowitz & JONSWAP spectra parameterized by wind speed & scale
- An oil distribution and recovery system that can handle heavy, viscous oils and emulsions
- A control tower with a fully-computerized 32-channel data collection system as well as above-and below-water video
- A movable, wave-damping artificial beach
- A centrifuge system to recover and recycle test oil
- Blending tanks with a water and oil distribution system to produce custom oil/water emulsions for testing
- A filtration and oil/water separator system
- An electrolytic chlorinator to control biological activity
- Permanent and mobile storage tanks that can hold over 227,000 litres of test fluids
- A vacuum bridge to clean the bottom of the tank
- Staging and shop area for special fabrication
- On-site chemistry laboratory
- 15,000 lb forklift
- A fully equipped machine shop, chemistry laboratory and a 50-seat training facility

C Droplet size data from the Tower Basin and Ohmsett experiments

Table C.1: Droplet sizes from subsea experiments at SINTEF and Ohmsett with varying nozzle size (25 – 50 mm), oil flow rates (80 - 300 L/min), dispersant C9500 (1%) and Oseberg blend. Dispersant experiments performed with simulated injection tool (SIT). Modified Weber scaling (MWS) is used to predict oil droplet sizes.

Exp no	Nozzle (mm)	Flow rate (L/min)	Oil Temp (°C)	Water Temp (°C)	Oil visc (cP)	IFT (mN/m)	d_{50} (µm) Measured	d_{50} (µm) Predicted MWS	Comment
1	25	50	13	5.1	4,6	20	4500	4507	
4	25	50	4,7	3.8	5,0	20	4200	4511	
0	25	50	15	12	4,2	20	3700	4502	SINTEF Tower Basin
1	25	80	13	5.1	4,6	20	3450	2711	
1	25	80	13	5.1	4,6	20	2900	2711	
2	25	80	3,8	4.5	5,1	20	2750	2716	
2	25	80	3,8	4.5	5,1	20	2100	2716	
4	25	80	4,7	3.8	5,0	20	3100	2715	
4	25	80	4,7	3.8	5,0	20	3150	2715	
6	25	80	6	6.0	4,9	20	3000	2714	
6	25	80	6	6.0	4,9	20	2200	2714	
0	25	80	15	12	4,2	20	2800	2707	SINTEF Tower Basin
1	25	120	13	5.1	4,6	20	2000	1724	
2	25	120	3,8	4.5	5,1	20	2300	1728	
4	25	120	4,7	3.8	5,0	20			SilCam out of oil plume
4	25	120	4,7	3.8	5,0	20	2100	1727	
6	25	120	6	5.6	4,9	20	1450	1726	
6	25	120	6	5.6	4,9	20	1700	1726	
0	25	120	15	12	4,2	20	1900	1721	SINTEF Tower Basin
3	25	50	4,6	5.7	5,0	0,2			Low/uneven dispersant dosage
5	25	50	4,6	5.7	5,0	0,2	480	424	
7	25	50	5,8	5.6	5,0	0,2	360	424	
3	25	80	3,2	4.8	5,1	0,2	345	281	
0	25	80	15	12	4,2	0,2			Saturation of SilCam
5	25	80	4,6	5.7	5,0	0,2	250	278	
7	25	80	5,8	5.6	5,0	0,2	250	278	
3	25	120	3,2	4.8	5,1	0,2	220	195	
5	25	120	4,6	5.6	5,0	0,2	240	194	
7	25	120	5,8	5.6	5,0	0,2	240	194	
1	32	80	13	5.1	4,6	20	4650	5006	
4	32	80	7	5.3	4,9	20			SilCam out of oil plume
8	32	80	7	5.3	4,9	20	4600	5010	
8	32	80	7	5.3	4,9	20	3800	5010	

Exp no	Nozzle (mm)	Flow rate (L/min)	Oil Temp (°C)	Water Temp (°C)	Oil visc (cP)	IFT (mN/m)	d_{50} (µm) Measured	d_{50} (µm) Predicted MWS	Comment
0	32	80	7	5.3	4,9	20			Discr of large droplets due to narrow sensor path (initial exp)
1	32	120	13	5.1	4,6	20	3200	3254	
2	32	120	3,8	4.5	5,1	20	3400	3259	
4	32	120	4,7	5.7	5,0	20	2800	3258	
6	32	120	6	5.6	4,9	20	2500	3257	
8	32	120	7	5.3	4,9	20	3200	3257	
0	32	120	15	12	4,2	20	3100	3250	SINTEF Tower Basin
2	32	300	6	5.6	4,9	20	1350		Optics smeared with oil
6	32	300	6	5.6	4,9	20	1350	1171	
8	32	300	7	5.3	4,9	20	1800	1171	
0	32	300	15	12	4,2	20	1500	1167	SINTEF Tower Basin
5	32	80	4,6	5.7	5,0	0,2	550	463	
7	32	80	5,8	5.6	5,0	0,2	220	463	
3	32	120	3,2	5.7	5,1	0,2	290	326	
9	32	120	7	5.6	4,9	0,02	190	215	
9	32	120	7	5.6	4,9	0,2	260	321	
9	32	120	7	5.6	4,9	1	320	619	
5	32	300	4,6	5.7	5,0	0,2	220	143	
0	32	120	15	12	4,2	0,2	280	304	SINTEF Tower Basin
1	50	200	13	5.1	4,6	20	5200	5620	
4	50	200	4,7	5.7	5,0	20	4500	5600	
8	50	200	7	5.3	4,9	20	4500	5623	
0	50	200	15	12	4,2	20			Transparent oil used for initial 50 mm experiments at SINTEF. SilCam underestimate sizes.
1	50	300	13	5.1	4,6	20	3700	3689	
2	50	300	4,7	5.7					SilCam out of oil plume
4	50	300	4,7	5.7	5,0	20	3000	3698	
6	50	300	7	5.3		20			SilCam out of plume
8	50	300	7	5.3	4,9	20	3700	3692	
0	50	300	15	12	4,2	20			Transparent oil used for initial 50 mm experiments at SINTEF. SilCam underestimate sizes.
2	50	400	6	5.7		20			SilCam out of oil plume
6	50	400	6	5.7	4,9	20	2100	2708	
8	50	400	7	5.3	4,9	20	3000	2708	
0	50	380	15	12	4,2	20			Transparent oil used for initial 50 mm experiments at SINTEF. SilCam underestimate sizes.
3	50	200	3,2	5.7	5,1	0,2	680	514	
9	50	200	7	5.6	4,9	0,2	210	508	
3	50	300	3,2	5.7	5,1	0,2	240	361	
7	50	300	5,8	4.8	5,0	0,2	230	359	

Exp no	Nozzle (mm)	Flow rate (L/min)	Oil Temp (°C)	Water Temp (°C)	Oil visc (cP)	IFT (mN/m)	d_{50} (µm) Measured	d_{50} (µm) Predicted MWS	Comment
9	50	300	7	5.6	4,9	0,2	230	356	
0	50	300	15	12	4,2	0,2	320	338	SINTEF Tower Basin
5	50	400	4,6	5.7	5,0	0,2	230	278	
7	50	400	5,8	5.6	5,0	0,2	230	278	
9	50	400	7	5.6	4,9	0,2			SilCam saturated

The experiments labelled "0" are the experiments at SINTEF Tower basin (see Table 3.1 and Table 4.1). Experiments labelled "1-9" are from the testing at Ohmsett (see Table 4.4 and Table 4.6). Data from some experiments are not included in the table due to not sufficient data quality (see section 5.3). The IFT values are taken from earlier studies with Oseberg blend and C9500 (Brandvik et al., 2015). Viscosities are measured at SINTEF lab as a function of temperature at high shear rates (1000 s^{-1}) relevant for such experimental subsea releases (2-5 m/s release velocity).

Sea water salinity at SINTEF Tower Basin experiments was 3.5%. For the Ohmsett experiment the salinity was measured to 2.8%. The reduced salinity was mainly due to fresh water input (rain & snow). The salinity was increased or adjusted regularly by adding salt.

D Possible platforms for quantifying oil droplet distributions

This appendix contains a description of different available options for quantifying oil droplets. This text gives a review of the existing technology and was a part of the preparation for this project and the development of the Silhouette Camera.

With up-scaled release conditions (larger nozzle diameter and high release fluxes) it was necessary to modify the droplet measurement strategy. In doing this it was important for droplet size and concentration to be measured within the release plume. To maximise the experimental output it was beneficial to modify the measurement technology to exploit the state of the art in particle measurement. With the modifications required to maintain reliable droplet size and concentration measurements, an appropriate imaging system will not only capture the information currently measured in standard Tower Basin experiments, but will also enable additional measurements of droplet shape and rise speed from the same system and with minimal extra set-up time and resources.

Droplet size and concentration measurements at SINTEF and SL Ross were earlier obtained using LISST-100 and a laser-sheet imaging systems that enable measurements of droplet size and concentration from an undisturbed sample from within the release plume. Alternatives measurement techniques, such as the Coulter Counter, exist but these rely on the extraction of samples from the experiment. The fragile nature of oil droplets leads to complications with extraction techniques because of an increased likelihood for coalescence and/or droplet breakup prior to the determination of their size, which results from the extraction process. *In-situ* measurements are therefore a key component in ensuring accurate droplet sizes and concentrations.

The increase in nozzle diameters required for up-scaling will result in droplet diameters and concentrations that will exceed the measurement constraints of the LISST-100 and laser-sheet imaging system. This section outlines existing technologies that have the potential to provide useful information on droplet characteristics within a Tower Basin system. The advantages and disadvantages of each are summarised and a proposed solution is presented.

D.1 Laser diffraction (e.g. LISST-100)

Laser particle sizing is a commonly used method for determining an *in-situ* droplet size distribution and concentration. This is because of its ability to measure particle characteristics *in-situ*, at a relatively high sample rate and with minimal computational processing requirements.

The LISST-100 is able to estimate the particle size distribution by inverting measurements of forward-angle scattering (Agrawal and Pottsmith, 2000). Within the instrument collimated laser light passes through the sample volume onto a receiving lens. A specially made array of 32 detectors, positioned at the focal plane of the receiving lens, receives an intensity distribution of scattered light from the particles within the sample volume. The angle at which light is scattered is proportional to the size of the scattering particle. As such, the optical power distribution on the ring detector gives the essential information on the particle size distribution within the sample volume. The total volume concentration in the sample can then be obtained by summing the volume of particles within each size class.

An evaluation of the effect of particle composition on the reliability of inverting LISST-100 scattering into a size distribution was made by Andrews et al. (2010). They concluded that the instrument was sensitive to refractive effects, but performed well when measuring mineral grains, as these were close to the refractive indices used for data processing (n'=1,55 rel. to air). Davies et al., (2012) demonstrated that the role of refractive index (and hence particle composition) in biasing the LISST-100 response was only important for larger particles. Typical refractive indices for oil are approximately n'=1,44 (rel. to air) indicating that the use of laser diffraction technology for measuring large oil droplets could be problematic, even if the upper size limit for the LISST-100 was increased beyond the current limit of 500 µm (e.g. as per the LISST-Floc, which is no longer in production).

D.2 Electrical impedance (e.g. Coulter Counter)

Coulter Counter instruments adopt a particle sizing technique that is reliant on changes in the levels of electrical resistivity caused by particles passing through a narrow aperture. The change in resistivity is proportional to the particle volume. Wider apertures allow for measurements of larger particles (up to about 600µm) and narrower apertures enable measurements of less than 1µm. Unfortunately, this method is restricted to *ex-situ* use and the size range is heavily dependent on the aperture width used. In addition to concerns of particle break-up due to shear forces generated through the aperture, measurements informed through multiple aperture configurations also encounter difficulties when splicing multiple distributions (Reynolds et al., 2010).

D.3 Multiphase flow probes

Multiphase flow probes measure particles rising through the flow tips and the high sampling rates enable particle size information to be obtained from the high frequency temporal changes in the signal. However, multiphase flow probes are reliant on a sufficiently different refractive index of the particle in relation to the surrounding medium. This difference in refractive index represents the change in the propagation speed of light through the two mediums.

The refractive index of the particle relative to a medium is expressed as a complex number:

$$n = n' \, i + n''$$

where n' is the real part (ratio of the speed of light in a vacuum and the particle) and n'' is the imaginary part (which represents absorption).

Advice from RBI-Instruments was that the multiphase flow probes require the real part of the refractive index of the particle and medium to differ by more than 10%. For water n'=1,33 (in a vacuum) and for oil n'=1,45; creating a difference in real refractive index of 8.2% for oil in water, and subsequently rendering the technology problematic for oil experiments within the Tower Basin.

D.4 Acoustic scanners

Some commercially available sonar scanners have the potential to provide information on droplet concentrations and plume dimensions, although the ability to obtain accurate size estimates by way of acoustics remains in a primitive state, with no suitable system currently available commercially. Acoustic scanning systems may therefore not provide suitable information to be worthwhile investing in an up-scaled Tower Basin measurement platform.

D.5 Acoustic backscatter sensors

Multi-frequency acoustic backscattering may be used to retrieve information on mean particle size and concentration (Thorne and Hanes, 2002). However, for a comprehensive assessment of droplet characteristics it is important for an accurate droplet size distribution to be recorded, and currently this is not possible using acoustic technology, which is limited to estimations of only an average size for a population. An advantage of acoustic measurements of droplets is that a near-instantaneous profile of a water column or plume cross-section is possible - a result that is not achievable using optics due to the higher attenuation of light through water in relation to sound. A comparison of acoustic backscatter and laser diffraction measurements was investigated in the work of Thorne et al. (2007), who showed that measurements of mean grain size were consistent between the instruments, but that there were some discrepancies when measuring particle concentration.

D.6 Optical backscatter sensors

Optical backscatter sensors are often used for turbidity measurements in marine environments. Similarly to the acoustic backscatter sensors, very recent research in to the possibility of obtaining size information remains in a primitive state, and as such can only be used for droplet concentration measurements following careful calibration. Optical backscatter sensors, on the other hand, are relatively inexpensive and could be deployed as a vertical array within the Tower Basin. The optical backscattering signal is proportional to the total concentration of all particles (oil + mineral + biological). As the only 'particles' within the Tower Basin experiments are oil droplets, the optical backscatter signal would provide estimates of total droplet concentration throughout the height of the plume and would be less susceptible to differences in fluorescence between oil types (which would be the case if using a flourometer).

D.7 Imaging systems

A comprehensive comparison of marine particle size measurements from a Coulter Counter, LISST-100 and imaging was conducted by Reynolds et al. (2010). They found all three techniques reported generally good estimates of average particle size when known spherical standards were used. The performance of the LISST-100, when subjected to size distributions with features such as narrow peaks, was noted as less accurate than that of the Coulter Counter. This is as expected, given the angular resolution of the LISST-100 scattering detectors, which results in relatively broad size bins in comparison to a Coulter Counter. Despite this, the typical size distribution widths of oil droplets are not within the 'narrow' region that was shown to be problematic. Mikkelsen et al. (2005) conducted a comparison of the LISST-100 in relation to standard imaging methods and concluded that the imaging technique used in their study had a tendency to report particle sizes larger than that of the LISST-100, but that a generally good agreement was apparent over the size ranges in which both instruments overlap. This lead to the suggestion that particle size distributions from both instruments could be 'spliced', providing information over a size range spanning 2.5μm (the lower limit of the LISST-100 type-c) to several millimetres. This 'splicing' of droplet size distributions could form a potential method for obtaining a very broad range of droplet size measurements within an up-scaled Tower Basin experiment, provided that concentrations were not in excess of the maximum limit using the 90% path reduction modules for the LISST-100 and that contamination from droplets outside the LISST-100 size range (Davies et al., 2012) was accounted for.

D.8 Digital in-line holography (e.g. LISST-Holo)

The application of in-line holography has recently become a topic of interest for the measurement of marine suspended particles, such as sediments and phytoplankton, and a commercial system (LISST-Holo) is now produced by Sequoia Scientific Inc. to complement their LISST-100 series of instruments. Owen and Zozulya (2000) and Graham and Nimmo-Smith (2010) describe how digital in-line holography can be used to measure marine particle size, shape and settling velocity. One of the main advantages of digital holography is that the hologram of the sample volume can be reconstructed at any depth through the imaging volume (substantially increasing the effective depth-of-field), allowing for an accurate measurement of any particle within the sample without errors due to focussing which are problematic in standard imaging techniques and microscopy. A study by Davies et al (2011) compared the responses of in-line holography and laser diffraction and reported very good agreement between the two techniques. The LISST-Holo has also been recently been evaluated alongside the LISST-100 in the SINTEF Mini-Tower and produced promising results for oil droplet size, shape and concentration measurements. Despite its ability to measure droplets of mm-scales, however, the maximum working concentrations for the LISST-Holo are lower than that of the LISST-100, most probably making it unusable in the high concentration conditions expected in an up-scaled Tower Basin experiment.

D.9 Measurement assessment summary

A summary of the different measurement techniques are given in table D1 below.

Table D1: Summary of pros et cons of possible methods

System/Technology	Pros.	Cons.
Laser diffraction	- Measurements of droplet size distribution and concentration - Undisturbed, *in-situ* measurement - Reliable for droplets <500µm	- Limited to droplets <500µm - Limited in concentration
Electrical impedance	- Can resolve fine peaks in the droplet size distribution - Can measure smaller droplets than the LISST-100	- Limited to droplet <~600µm - Ex-situ sampling - High shear rates through sampling aperture could cause incorrect size estimates
Multiphase flow probes	- Fast sampling rates	- Problematic for resolving oil in water
Acoustic scanners	- Provide concentration estimates through the plume cross-section	- No droplet size information
Acoustic backscatter sensors	- Provide instantaneous concentration profile	- No droplet size information
Optical backscatter sensors	- Provide concentration estimates at a high sample rate	- No droplet size information - One sample point (unlike acoustic backscatter)

Imaging systems	- Wide size range (0.02 – 12 mm) - Measure droplet shape - Measure concentration - Measure droplet rise speed	- Path length must be optimized to reduce 'overlapping' droplets - More data processing than the LISST-100
Holography	- Measure droplet size - Measure droplet shape - Measure concentration - No depth of field errors	- Upper concentrations are relatively low - More data processing than standard imagery - Standard software offer low image update and/or slow processing (Sequoia/Wet lab)

D.10 Proposed measurement system for this project

We propose to design and build a new measurement platform to acquire droplet size information from within the up-scaled plume. This will involve the introduction of a new imaging system, specifically designed to handle the high concentrations and larger droplet sizes.

A simple silhouette-based approach (similar to that adopted by Mikkelsen et al., 2005) will allow flexibility in controlling the imaging volume, which will reduce the likelihood of contamination for multiple overlapping particles. A schematic illustration of the system is outlined in Figure D1.

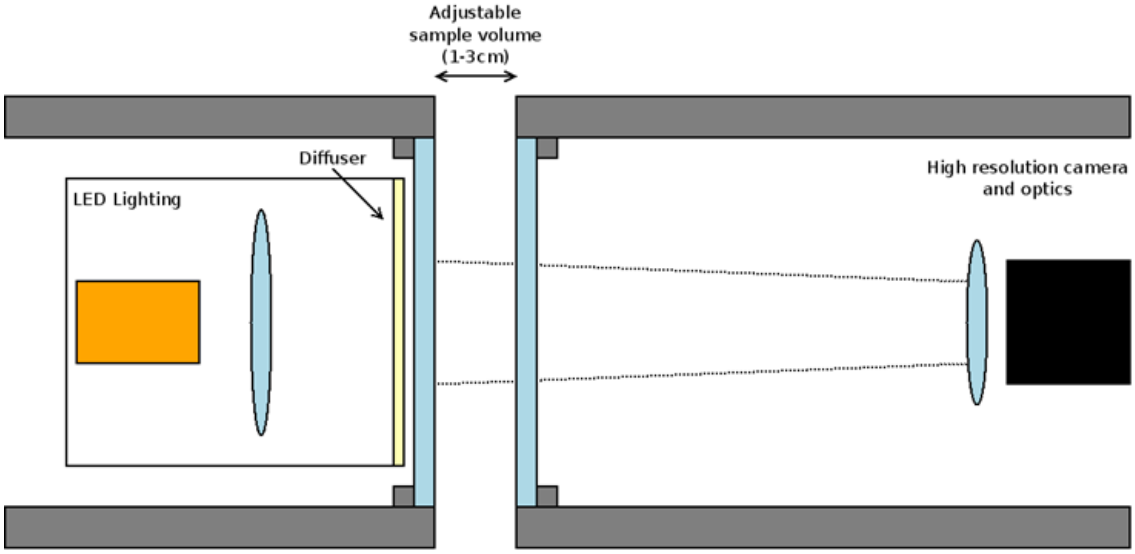

Figure D1: Schematic overview of the basic silhouette camera configuration, consisting of diffuse LED lighting on the far side of the sample volume and a high resolution camera and associated optics on the near side.

The silhouette camera (Figure D1) will consist of an LED light source on the far side to illuminate particles from behind, and a high-resolution digital camera and telecentric lens on the near side of the sample volume. The width of the sample volume (i.e. distance between the window of the light source housing and the window of the camera housing) will be adjustable (within the range of 1-5 cm) to enable flexibility for varying concentrations. A large path length will reduce under-sampling of large particles while reducing the width will reduce multiple overlapping particles within the

image frame. Figure D2 shows computer generated images which simulate a 'best case scenario' for expected droplet concentration and size distribution, as measured using the silhouette camera proposed, for a given path length and oil concentration (15 mm and 4000 ppm). The first part of the figure simulates measurements of droplets from untreated oil (Figure D2 a-b) assuming a 30 mm release nozzle and 200 L/min flow rate (d_{50} = 1500 µm). The simulated droplet size distributions of treated oil (1% dispersant) are shown in Figure D2 c-d and it can be seen that the droplet distribution is shifted to smaller droplets (d_{50} = 490 µm).

However, it is important that the path length remains adjustable between experiments in order to maintain the ability to capture image good quality images over a range of experimental release conditions, as a path length too short will expose the imaging system to under sampling errors if concentrations are reduced or if the droplet size distribution is significantly altered.

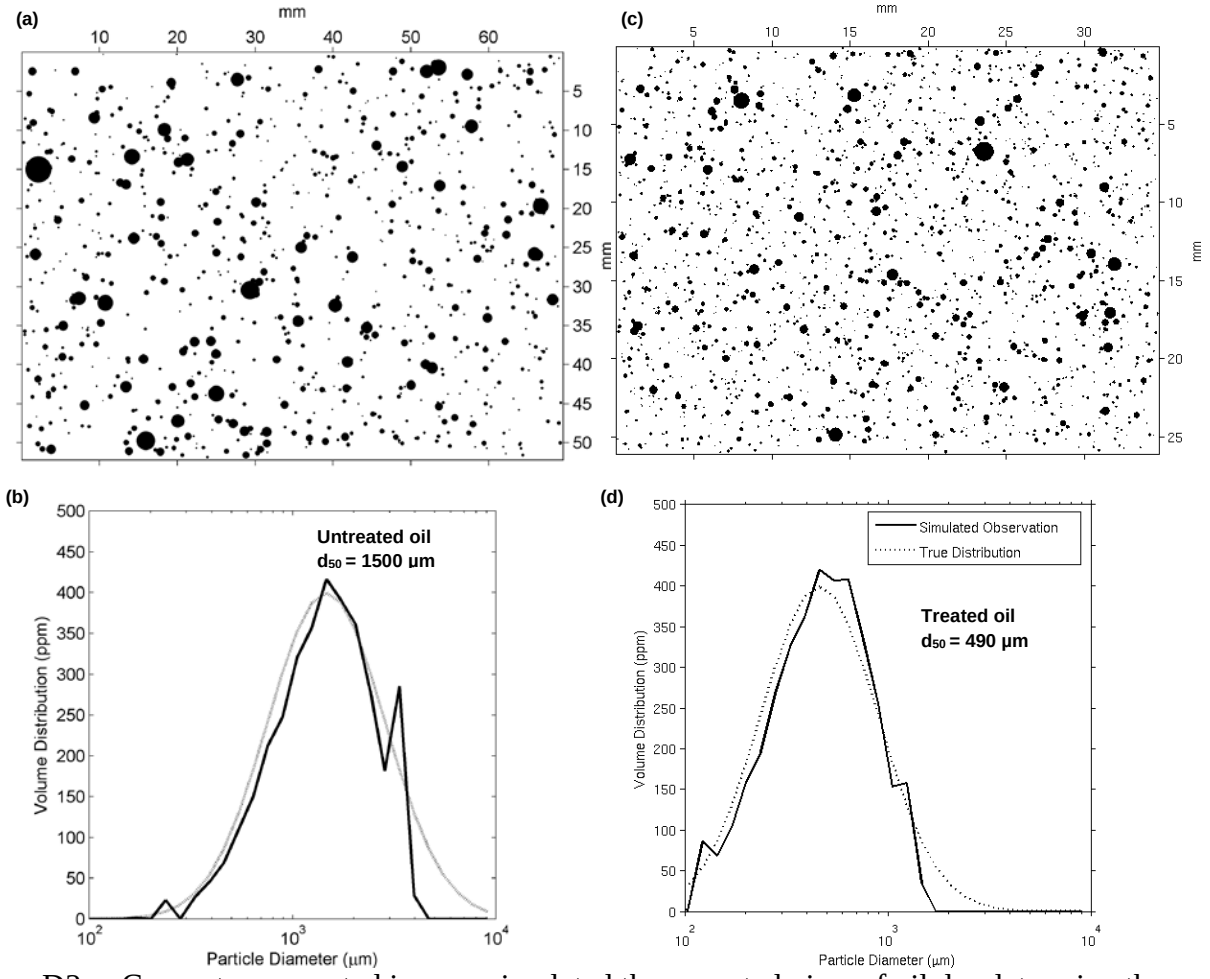

Figure D2*:* Computer generated images simulated the expected view of oil droplets using the system outlined in Figure D1 with a focus length of 15 mm. Associated volume distributions from an average of 62 images (1 second of measurements). Oil concentration simulated in both images is 4000 ppm, with a d50 of 1500 µm and 500 µm from a log-normal size distribution. These concentrations and droplet sizes are expected using a 30 mm nozzle, 130 L/min flow rate (a-b) and similar treated with 1% dispersant (c-d) predicted using the Modified Weber scaling (Johansen et al., 2013).

Errors due to out-of-focus particles will be minimised by use of a bright background light source and telecentric lens. Standard imaging lenses cause changes to the magnification of objects outside of the focal plane exposing droplet size estimates to substantial errors. It is therefore important to use a telecentric lens, which removes errors due to magnification so that particles appear the same size regardless of their position within the sample volume.

It is unlikely that any optical or imaging system will be capable of resolving accurate droplet size distributions if d_{50} exceed 5 mm when combined with the high concentrations, as this will produce multiple overlapping or obscured droplets, even for very narrow path lengths. Selected release conditions (nozzle diameter and release rate) will therefore need to be carefully planned to constrain the droplet sizes and concentrations to within the measurable range of this system.

Technology for a better society
www.sintef.no